"Catalytic Reactions on Iron/Cobalt and Iron/Nickel Alloys"

by

Peter John Smith

Thesis submitted for the degree of

Doctor of Philosophy

University of Edinburgh

January 1980

Declaration

The work described in this thesis was carried out while the author was a member of a research team in the Department of Chemistry, University of Edinburgh, between 1/10/76 and 1/10/79. The results concerning nitrogen chemisorption and ammonia synthesis were obtained by Dr. David W. Taylor and all other results were obtained by the author unless acknowledged otherwise in the text. This thesis was composed personally

[redacted]

During the period of this research I attended the following postgraduate lectures, Catalytic Club Seminars (1976-1979), Chemistry at its most colourful, The encouragement and exploitation of inventiveness in the oil industry, Modern techniques for surface science (conference at Cambridge), Use of computer facilities in the chemistry department, and Catalysis in industry.

Acknowledgements

During the period of this research the author was privileged to be a member of an I.C.I. Ltd. sponsored research team investigating catalytic reactions on alloy catalysts. The members of this group, Professor C. Kemball, F.R.S., Mr. D.A. Dowden, Dr. D.A. Whan, Dr. D. Taylor, Dr. D.W. Taylor, Dr. A.J. Pearman and Mrs. L. Watson, helped to make the time in Edinburgh both enjoyable and interesting and I wish to express my thanks to all of them.

I am especially grateful to Dr. David W. Taylor for allowing me to freely use results obtained by him (i.e. all measurements of ammonia synthesis rates and nitrogen chemisorption rates) and for help in the design of the carbon monoxide hydrogenation experiments. I am also deeply indebted to many other people, without whose assistance the research described in this thesis would have been impossible: Mr. E.G. Clingly, I.C.I. Ltd. for making some of the catalysts and instructing the author in the art of catalyst preparation; Mr. D.T. Lye, I.C.I. Ltd. for measuring X-ray parameters and explaining the intricacies of X-ray diffraction; and all the other people at I.C.I. Ltd., Agricultural Division who made my time there useful and very enjoyable.

Special thanks are also due to my academic supervisors, Professor C. Kemball, F.R.S. and Dr. Duncan Taylor, both of whom had occasional trying times with a rather awkward student. I should also like to express my gratitude to my industrial supervisors i.e. Dr. S.A. Topham and Mr. J.D. Rankin both of whom made many useful suggestions and contributed immensely to making my stay at Billingham pleasant.

I also thank the Science Research Council for the provision of a research studentship. Finally, I thank Mrs. M. Manson for typing my difficult to read script and so transforming it into what it is now.

To Suzanne

(without whose financial support I would have been

very poor for three years!)

Contents

Chapter Nine Hydrogenation of Carbon Monoxide Over Group VIII Base Metal Alloys

Preface

The catalytic synthesis of ammonia is a subject of immense interest due to its industrial importance. While the mechanism of the reaction is still unclear, results have tended to show that the slow step in the synthesis of ammonia is the chemisorption of nitrogen. Transition metals to the left of Group $VIII_1$ chemisorb nitrogen very strongly and form stable nitrides. To the right of Group $VIII_1$ nitrogen is not readily chemisorbed to any appreciable extent and in this way the acknowledged maximal activity for elements of Group $VIII_1$ can be rationalised.

The activity of a metal for the reversible dissociation of the nitrogen molecule (the slow step of which is also probably nitrogen adsorption) can be determined by measuring the velocity with which nitrogen isotopes undergo the equilibration reaction,

$$N_2^{28} + N_2^{30} \rightleftharpoons 2N_2^{29} \qquad 1$$

As has been found for ammonia synthesis, catalysts showing maximal efficiency for reaction 1 are also the elements of Group $VIII_1$.

Although the largest activity for dissociative nitrogen chemisorption and ammonia synthesis catalysis has so far been found for the Group $VIII_1$ metals it does not mean that these elements represent the optimum average electron/atom ratio requirement for dissociative nitrogen chemisorption. The possibility exists that alloying with an adjacent transition metal may result in the formation of a more active catalyst. Iron-cobalt and iron-nickel alloys provide a good system for examining this possibility since they are readily prepared in

high area and the phase diagrams are reasonably well known.

The first part of this thesis is concerned with an investigation of the ability of iron-cobalt and iron-nickel alloys to bring about the reversible dissociation of the nitrogen molecule as shown by studying reaction 1. The results of this investigation are then compared with the ammonia synthesis activities and nitrogen chemisorption characteristics of the alloys.

There are several similarities between the ammonia synthesis reaction and the methanation reaction (i.e. $CO + 3H_2 \rightarrow CH_4 + H_2O$). Both reactions involve the hydrogenation of isoelectronic molecules and both occur on Group VIII metal catalysts. There is also some similarity in the behaviour towards alkali promoter and in the nature of their respective rate limiting steps.

In view of the similarities between ammonia synthesis and methanation, the research was extended to include an investigation of the hydrogenation of carbon monoxide on iron-cobalt and iron-nickel alloys. In the second part of this thesis the results of this investigation are presented and a comparison made between methanation and ammonia synthesis.

Chapter One

Alloys and Catalysis

During the last half century, binary alloys were extensively used to investigate catalytic phenomenon e.g. in studying the role of order/disorder effects[1] and in probing the relationship between electronic structure and catalytic activity[2]. Moreover, with the advent of techniques which provide surface compositions, alloys have now become a fertile ground for the investigation of configurational or geometrical influences. This widespread use of alloy catalysts has generated a wealth of experimental information and the present chapter summarises some of the main features of alloy catalysts and more specifically iron/cobalt and iron/nickel alloy catalysts.

1:1 Structure of alloy catalysts

1:1:1 Geometric structure of alloys

It is possible to distinguish two structural categories of solid solution, namely interstitial solid solutions, where atoms occupy interstices in the host structure and substitutional solid solutions, where dissolved atoms replace atoms in the host structure. Some metals, which are similar in size and electronic structure, have unlimited mutual solubility and form a continuous series of solid solutions without change of phase whereas others which have only limited mutual solubility form multi phase solid solutions.

The usual method of characterising substitutional solid solutions (substitutional alloys) is by determining lattice spacing by X-ray diffractometry. Alloy lattice spacings invariably lie

between the values of the two component metals and in some situations lattice spacing is a linear function of composition (Vegard's Law). X-ray diffractometry also provides bulk phase composition.

It is now known, that the surface composition of an alloy may not necessarily be identical to that of the bulk. Bulk composition can be routinely found e.g. by X-ray fluorescence spectroscopy whereas surface composition must be determined by more difficult investigations. During the last decade several new techniques for determining surface composition have emerged e.g. selective chemisorption[3], electron excited Auger emission spectroscopy[4] and photon excited electron emission[5] (E.S.C.A.).

When the chemisorptive properties of alloy constituents are markedly different e.g. Pt/Au, selective chemisorption can be used to estimate surface composition. In essence, the method relies on comparing total surface area i.e. e.g. Pt and Au with the area (platinum area) involved in chemisorbing gases such as carbon monoxide.

The estimation of surface composition from spectroscopic measurements such as Auger and E.S.C.A. is more straightforward. However, these techniques probe the surface to a depth of several atomic layers and because of this they may not give a wholly accurate description of the surface. Nevertheless, such measurements have found widespread application.

Although the investigation of surface composition of alloys is fairly novel several generalisations have emerged from the experimental material e.g. (i) the surface tends to be enriched by the component with the lower sublimation heat (lower surface energy) and (ii) surface composition is a function of the

gases in contact with the alloy and that the component with the higher heat of adsorption of gases in the atmosphere tends to accumulate in the surface.

1:1:2 Electronic structure of alloys

Two different, though not contradictory, approaches have been used to explain the electronic structure of metals and alloys. Electron Band Theory[6], envisages a metal as a collection of fixed nuclei surrounded by a "moving sea" of valency electrons. The application of quantum statistics to the "electron sea" allows the calculation of cohesive properties and other electronic characteristics. Valence Bond Theory[7], considers the metal lattice to be a large covalent molecule in which each atom is bonded to its neighbours by resonating covalent bonds. Electronic properties are then described in terms of localised electron orbitals. Valence Bond Theory, although conceptually simple is too empirical to have much application in explaining catalytic reactions and has now been superceded.

Application of Fermi-Dirac statistics to the "electron sea" of Electron Band Theory showed that valency electrons could be envisaged as being distributed in a definite number of discreet energy levels or bands. In the case of transition metals these bands (called s and d bands) were shown to overlap and catalytic activity was considered to be associated with the degree of occupancy of the highest used d band.

Considerable effort has been expended in trying to correlate catalytic activity with d band occupancy but major successes have not always been achieved. In fact, recent photo-electron spectroscopy studies have cast doubt on the validity of

such an approach[8]. A more advanced quantum mechanical interpretation, coherent potential approximation theory, may provide a fuller description of electronic properties[9].

1:1:3 Surface ensembles

The geometric principle, often called the ensemble effect when applied to binary alloys, originates in the pioneering work of Kobozev[10]. In the late 1930's Kobozev suggested that the surface of a promoted iron ammonia synthesis catalyst consisted of small islands of iron (ensembles of iron) isolated from each other by promoter atoms. Reaction was postulated to occur only on ensembles of particular size and orientation. The concept has been extended to alloys[11].

When an active metal (A) is dissolved (alloyed) in an inactive metal (B) surface clusters (or ensembles) of differing composition e.g. A+2B, 5A+B are generated. Alloying may also form isolated groupings of active metal A. The number and type of all such ensembles are a function of alloy composition and ensemble theory attempts to correlate catalytic activity with variation in size and number of surface ensembles.

The probability of different surface ensembles (e.g. 5A's) occurring has been calculated by Dowden and these probabilities along with ideas on d band filling have been used to predict heats of adsorption of simple gases on alloy surfaces[12]. Ensemble theory has also been successful in explaining a number of catalytic observations e.g. the decline in methanation activity of ruthenium/copper alloys with added copper[13] and the fall in hydrogenolysis activity of nickel/copper alloys with added copper[14].

1:2 Iron, cobalt and nickel alloys

Structural and electronic properties of alloy catalysts used in the present investigation are reviewed in subsequent sections.

1:2:1 Iron-cobalt alloys

Cobalt exhibits two stable polymorphs, α cobalt (hexagonal) and β cobalt (face centred cubic) with α→β transition temperature at 633 K. Above this temperature there are no other structural changes but a magnetic transition does occur at 1388 K. Dissolved nitrogen and hydrogen stabilise the β phase e.g. dissolved hydrogen can lower the transition temperature by circa 20 K. A phase diagram[15] for the iron/cobalt system is shown in Figure 1:1.

At temperatures below 1500 K iron has two stable polymorphs, α iron (body centred cubic) and γ iron (face centred cubic) with α→γ transition temperature at 1183 K. The temperature of the iron α→γ transition increases slightly with added cobalt reaching a maximum value of 1258 K with 45% cobalt. With cobalt concentrations greater than 75% the transition temperature is sharply lowered to ambient temperatures and with cobalt concentrations between 70-90%, a two phase region based on α and γ iron solid solutions is formed.

Iron/cobalt alloys exhibit ordering[16] and the α phase which contains 50% cobalt, is always ordered below temperatures of 823 K. Examination of Figure 1:1 shows the existence of an "upper structure" of FeCo of the type CsCl. The presence of other intermetallics e.g. Fe_2Co, $FeCo_2$, Fe_3Co and $FeCo_3$ has been suggested on the basis of indirect evidence but no direct proof of their formation has been given.

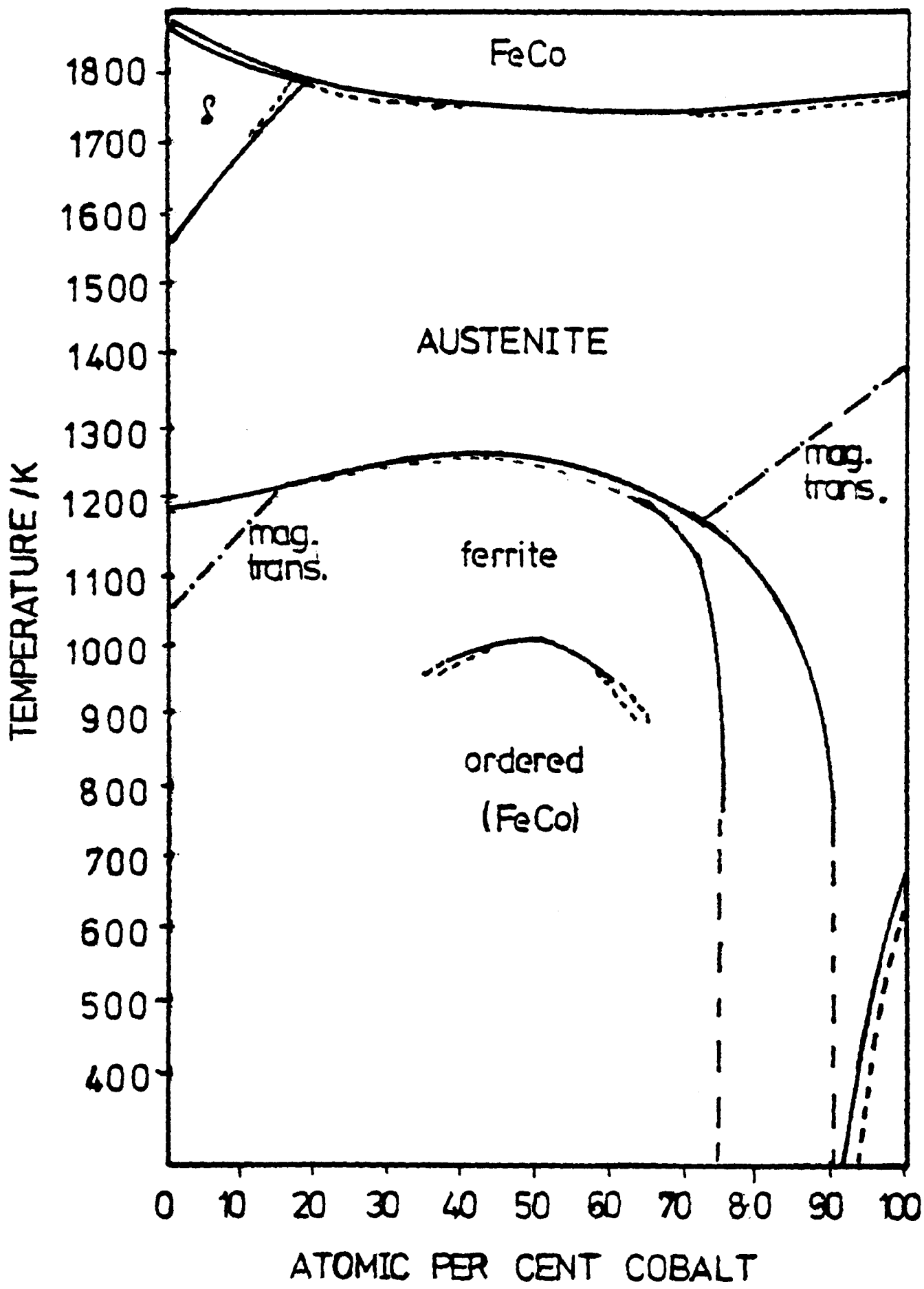

Figure 1:1 The iron-cobalt phase diagram.

The number of d holes in iron/cobalt alloys passes through a maximum at 35% cobalt but according to available literature there is no effect on the magnetic properties between 20-70% cobalt.

1:2:2 Iron-nickel alloys

Nickel, like γ iron, has a face centred cubic lattice. The atomic radius of nickel is approximately 2% less than that of iron and nickel and γ iron possess unlimited mutual solubility. Addition of nickel to iron widens the γ range of the latter. A phase diagram[17] for the iron/nickel system is shown in Figure 1:2.

Despite a large number of investigations, data concerning the iron/nickel phase diagram usually only show good agreement at temperatures above 873 K. This has been associated with the rate of attainment of equilibrium conditions which are retarded at lower temperatures by a sharp reduction in the rate of diffusion of metal atoms which make up the crystalline lattice of the alloys. Consequently, Figure 1:2 may not be a true equilibrium diagram below 873 K.

Nickel is known to form a series of intermetallic compounds with iron and at least seven separate compounds are known. There is general agreement, that at 673 K and within the composition range 60-83% nickel, a compound of formula $FeNi_3$ exists.

With an increase in the nickel content of the alloy the degree of filling of d levels in iron/nickel alloys increases and the number of unpaired d electrons is reduced. The atomic magnetic moment of iron/nickel alloys, characterising the number of unpaired electrons and equal for pure iron to 2.2 μB shows no change within the range 0-20% nickel but after 20% nickel the magnetic moment falls linearly to a value of 0.61 μB for pure nickel.

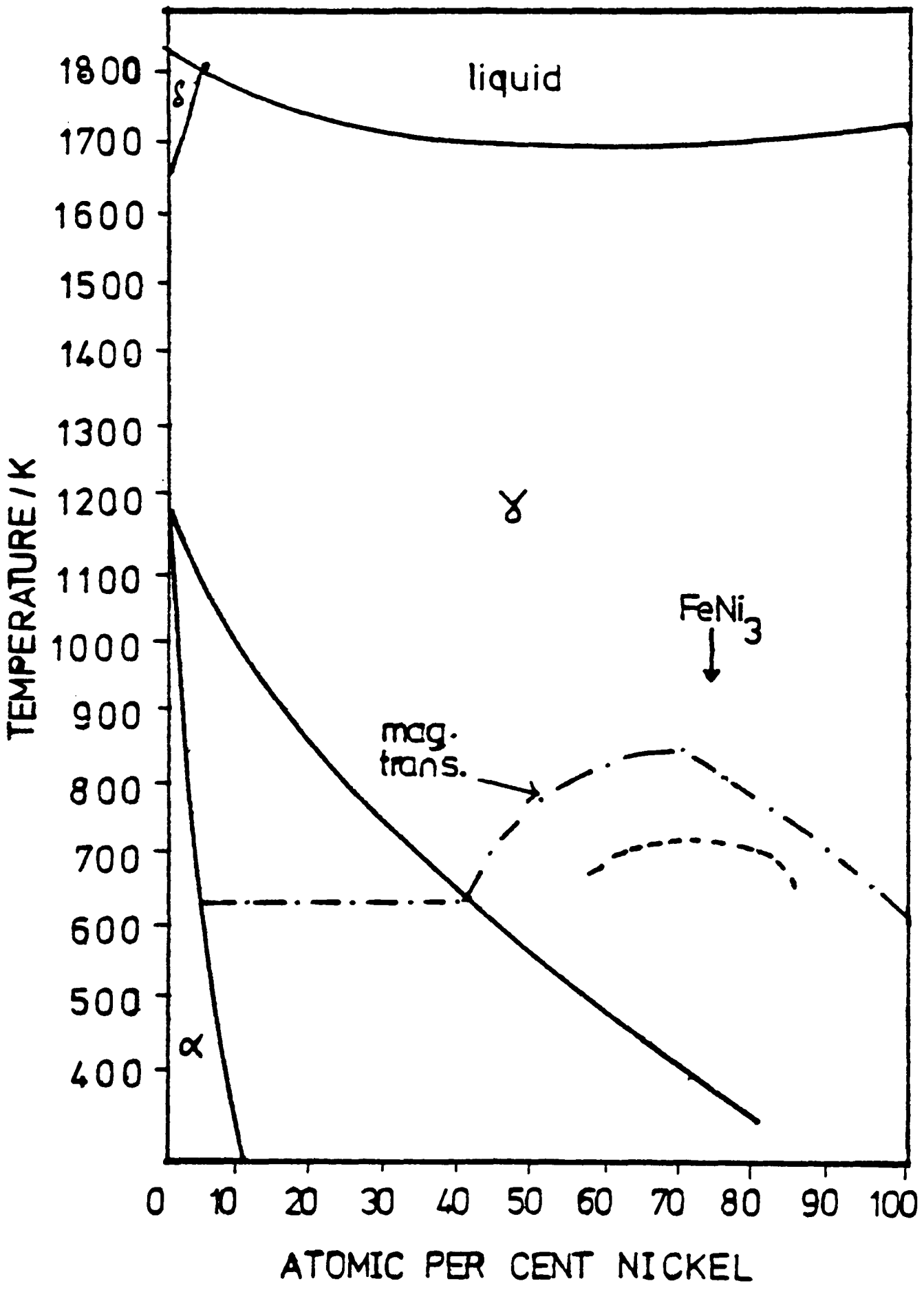

Figure 1:2 The iron-nickel phase diagram.

Chapter Two

Nitrogen Adsorption on Group VIII Metals

The interaction of nitrogen with metal surfaces has been extensively studied over the last fifty years to try and elucidate the part played by adsorbed nitrogen during the catalytic synthesis of ammonia. Adsorption studies relevant to the present investigation (concerning base metal alloys) are reviewed in the following chapter.

2:1 Low temperature adsorption studies

Adsorption isotherms for nitrogen on doubly promoted (1.59% K_2O, 1.3% Al_2O_3) iron ammonia synthesis catalyst[18], nickel[19,20] and cobalt[21] powders have been measured at low temperatures. Early workers interpreted such isotherms as being associated with Van der Waals adsorption but later investigators considered the existence of low temperature chemisorbed nitrogen species. Kokes[22] has suggested that at 77 K as much as 28% of a nickel surface may be covered with chemisorbed nitrogen. Other authors[23] have suggested the presence of several undissociated chemisorbed states of nitrogen, on iron films, at 77-90 K. Numerous measurements of the heat of adsorption of nitrogen, at low temperatures, have been made and values for the heat of adsorption on iron[24], manganese[25], cobalt[25] and nickel[25] have been reported.

The preferential adsorption of nitrogen by specific crystal planes has been suggested[26,27]. Brill[28] considers that

adsorption (at 77 K) occurs preferentially on the (111) plane of iron and accounts for this by a theoretical model for the nitrogen/metal bonding.

Although inherently interesting, low temperature chemisorption studies have proved difficult to relate to conditions of ammonia synthesis and consequently they have been of little assistance in elucidating the role of absorbed nitrogen during the synthesis reaction.

2:2 Adsorption of nitrogen on iron and promoted iron

The first study of the adsorption of nitrogen by doubly promoted (K_2O, Al_2O_3) iron, between 623-723 K, was undertaken by Emmett and Brunauer when they measured both the rate of adsorption (at one atmosphere pressure) and the volume of nitrogen adsorbed with pressure and temperature[29]. From measured adsorption isotherms a value for the heat of adsorption of nitrogen, on promoted iron, (147 kJ mol^{-1}) was estimated and the measured rate of adsorption was of the right magnitude to be associated with the slow step in the catalytic synthesis of ammonia. However, the available evidence did not allow a decision to be made on whether the nitrogen was adsorbed associatively or dissociatively but it was considered likely that at least some of the surface nitrogen was present as atoms.

Several years later, general equations for the rate of adsorption and desorption of nitrogen on iron and for the variation of amount adsorbed with pressure were derived by Brunauer, Love and Keenan[30]. These equations, which were based on the dissociative chemisorption model, permitted the calculation of adsorption isotherms which were subsequently shown to be in good agreement with experimental isotherms.

The experimental determination of nitrogen adsorption isotherms is complicated by the fact that nitrogen does not readily chemisorb on iron or promoted iron. The adsorption is usually highly activated and surface coverages greater than $\theta=0.5$ are rarely attained. The slow chemisorption of nitrogen and the consequent difficulty in obtaining thermodynamic equilibrium coverages is discussed later.

An adsorption equation, which varies discontinuously with surface coverage, has been reported[31]. When applied to adsorption at 673 K on promoted iron it was found that three different forms of nitrogen were involved in the adsorption. Evidence for three forms of adsorbed nitrogen, on doubly promoted iron at high pressures, has been furnished by other investigators[32].

The rate of chemisorption of nitrogen on singly promoted iron, measured with a high vacuum balance, has been shown to be proportional to the nitrogen pressure[33]. The rate measurements were described by an Elovich equation and thus measured activation energies for adsorption and desorption varied linearly with coverage. A similar investigation, involving adsorption on pure iron, gave results which were consistent with a rate equation based on a modified Elovich treatment[34].

Several workers have tried to identify the influence of promoters e.g. alkali and alumina, on the velocity of nitrogen adsorption. The adsorption of hydrogen and of nitrogen on iron supported on alumina with added alkali (K_2O) has been investigated between 77 and 613 K[35]. Introduction of alkali caused an increase in hydrogen adsorption without effecting the magnetic properties of the iron. The quantity of adsorbed nitrogen also increased in the presence of alkali.

Another investigation, using variously promoted iron catalysts, which studied nitrogen adsorption at 723 K and hydrogen adsorption at 473 K found different results[36]. A series of iron catalysts containing, Al_2O_3, $Al_2O_3 + K_2O$ and $Al_2O_3 + K_2O + CaO + SiO_2$, was found to behave analogously with respect to the chemisorption of nitrogen and hydrogen over a wide range of temperature and pressure. This parallelism was attributed to the similar nature of the chemical bonds involved in the surface compounds of nitrogen and of hydrogen.

Study of the simultaneous adsorption of nitrogen and hydrogen by iron and promoted iron has attracted interest. The influence of hydrogen and nitrogen on the adsorption characteristics of each other has been investigated by Sastri who found that adsorption of hydrogen was greater from a nitrogen/hydrogen mixture than from pure hydrogen[37]. Similarly, except at 476 K and 573 K, nitrogen chemisorption was enhanced in the presence of hydrogen. These observations were explained by proposing the existence of surface intermediates of the form, -NH-, $-NH_2$, $-NH_3$.

A similar investigation by Tamaru, has shown that the chemisorption of nitrogen is accelerated by hydrogen corresponding to the amount of hydrogen simultaneously chemisorbed[38]. Mixed adsorptions of equal pressures of hydrogen and nitrogen revealed mutual enhancement at low coverages and the author makes the general point that the behaviour of nitrogen towards a metal surface, in the absence of hydrogen, should not be correlated with that during ammonia synthesis conditions since the two gases have a mutual influence on each other.

The rate of chemisorption of nitrogen on a surface covered with chemisorbed hydrogen has been reported to be an order of magnitude greater than the rate of adsorption on a hydrogen free surface[39]. Correspondingly, the isosteric heat of adsorption of nitrogen is quoted as 54.6 kJ mol^{-1} on a hydrogen free surface (θ=0.01) and as 101 kJ mol^{-1} on a hydrogen covered surface (θ=0.02). The preliminary adsorption of hydrogen also decreases the activation energy for adsorption.

The chemisorption of nitrogen, hydrogen and nitrogen/hydrogen mixtures by commercial ammonia synthesis catalyst and a catalyst prepared by reduction of ferrocyanide have been compared[40]. Nitrogen chemisorption proceeded much faster on the ferrocyanide catalyst (residual potassium salt?) and the mutual enhancement of nitrogen and hydrogen (from nitrogen/hydrogen mixtures) was similar on both catalysts. In contrast to nitrogen adsorption on iron/K_2O and iron/Al_2O_3/K_2O catalysts, the presence of presorbed hydrogen on iron/Al_2O_3 catalysts did not effect the chemisorption of nitrogen.

Adsorption of various mixtures of nitrogen/hydrogen (3/1, 2/1, 1/1, and 1/3) on well reduced magnetite at 323 K and 400 torr total pressure has been investigated and it was found, disregarding the initial period, that more than one quarter of the adsorbed gas was desorbable as a mixture of equal proportions hydrogen and nitrogen[41]. The observation was independent of the nitrogen/hydrogen mixture used initially for the adsorption. The result is explained by proposing the formation of a weakly chemisorbed stoichiometric complex which decomposes on desorption.

The nature of surface nitrogen intermediates, during ammonia synthesis on iron, has been investigated, by measuring calorimetrically the heat of decomposition of NH radicals[42]. The

major surface intermediate, during the synthesis reaction at 773 K and 200 atmospheres, is suggested to be molecular nitrogen. However, as temperature is decreased the surface coverage of NH radicals increases and at 600 K the surface is suggested to be covered with equal proportions of NH radicals and molecular nitrogen. The heat of decomposition of NH radicals i.e.

$NH \rightarrow \frac{1}{2}H_{2(g)} + N_{(adsorbed)}$ is quoted as 52 kJ mol^{-1}.

The rates of nitrogen chemisorption and ammonia synthesis, on singly promoted iron, have been compared under conditions of similar surface nitrogen coverage[43]. Rates of reaction were found to be comparable and on the basis of this observation it was suggested that the rate determining step in ammonia synthesis is adsorption of nitrogen.

The adsorption of nitrogen by promoted iron, during ammonia synthesis conditions, has been investigated by Tamaru[44]. By examining the rate of nitrogen chemisorption and the reaction between adsorbed nitrogen and hydrogen he found that the overall rate determining step in ammonia synthesis depended on reaction conditions. Nitrogen chemisorption was suggested to be rate determining at low temperature and high pressure while hydrogenation of chemisorbed nitrogen was considered to be rate limiting at high temperature and low hydrogen partial pressure.

With the advent of modern surface techniques, the interaction of nitrogen with specific crystal planes has been widely investigated. The adsorption of nitrogen on iron (100) surfaces has been studied by Auger electron spectroscopy and by L.E.E.D.[45]. Activation energies for adsorption (21 kJ mol^{-1}) and desorption (252 kJ mol^{-1}) were determined and found to be consistent

with a dissociative adsorption resulting in the formation of a surface nitride layer. Although surface atomic nitrogen constituted the major phase some of the nitrogen did dissolve into the bulk.

The chemisorption of nitrogen and hydrogen on iron (111) has also been investigated by L.E.E.D. and low energy photoelectric spectroscopy[46]. It was shown that nitrogen was dissociatively chemisorbed with a sticking probability of about 10^{-7} at 473 K and that the chemisorbed nitrogen formed a nitride layer which showed no reaction with hydrogen at pressures up to 10^{-5} torr and temperatures of 650 K. No evidence was found for any reconstruction of the iron surface and the authors report that the adsorption of nitrogen on iron is not structure sensitive.

In contrast to this, Boudart has suggested that nitrogen adsorption (on iron) is structure sensitive and that preferential chemisorption occurs on the (111) plane[47]. The active site for chemisorption is considered to be one where surface atoms have seven nearest neighbours (C_7 centres) and the concentration of such sites can be increased by a nitrogen induced surface reconstruction.

Support for this suggestion concerning C_7 sites is given by a recent Chinese study of nitrogen adsorption on potassium promoted polycrystalline iron. The Chinese workers agree that the active site for chemisorbing nitrogen is a cluster of seven iron atoms arranged in the form of an "open pot". The realisation that such a site may be responsible for nitrogen chemisorption helps to explain why the most active iron ammonia synthesis catalysts are often formed by reduction of magnetite.

When magnetite (Fe_3O_4), which has a spinel structure is reduced a pseudomorph is formed[48]. The resulting α iron has the

same dimensions and external form (with (111) planes - C_7 sites parallel to the surfaces) as the magnetite spinel had before the oxygen ions were removed. High ammonia synthesis activity may then be accounted for in terms of the large numbers of exposed C_7 centres.

Dumisec also agrees that surface iron atoms with a co-ordination number greater than seven are the most active in dissociating molecular nitrogen and accounts for this in terms of molecular orbital symmetry and reaction mechanism[49]. Iron C_7 centres are considered the most suited for bonding nitrogen molecules in a π fashion and the poorest for σ bonding.

The adsorption of nitrogen by clean iron (100) and iron (111) has been studied under U.H.V. conditions by a variety of physical techniques[50]. Above room temperature only dissociative chemisorption occurred and measured initial adsorption activation energies were 21 and 0 kJ mol^{-1} on iron (100) and iron (111) respectively. Activation energies for desorption were 244 (100) and 209 kJ mol^{-1} (111) so nearly equal values for the strength of the metal/nitrogen bond result.

Nitrogen chemisorption on iron (100) gave rise to an ordered structure which could be explained in terms of nitrogen atoms located in four-fold sites on the unreconstructed iron (100) surface, leading to a configuration similar to that in the (002) plane of (f.c.c.) Fe_4N. The situation as regards the iron (111) plane is slightly more complex.

Several independent observations strongly suggested that the (111) plane had undergone a nitrogen induced surface reconstruction. It is thought that nitrogen chemisorption is accompanied by the formation of hexagonal layers of "surface nitride" which have a thickness of about two atomic layers and are related to the (111)

plane of Fe_4N. At 500 K the initial rate of nitrogen adsorption is faster by about a factor of twenty on the (111) plane. The dissociative chemisorption of nitrogen on iron (110) has also been examined and at 683 K, the initial rates of nitrogen adsorption have a ratio of 60:30:1 for iron (111):iron(100):iron(110)[51].

In addition to single crystal studies, the interaction of hydrogen and nitrogen on polycrystalline iron has been examined[52]. An investigation, carried out between 77-400 K and pressures less than 10^{-4} torr, showed that hydrogen was able to displace nitrogen from an iron surface whereas nitrogen could not displace hydrogen (it was physically adsorbed on a layer of chemisorbed hydrogen). Co-adsorption of nitrogen and hydrogen indicated that hydrogen was distributed over the entire surface whereas nitrogen was restricted to specific areas or crystal planes.

2:3 Adsorption of nitrogen on cobalt and nickel

Madden searched for a chemisorbed nitrogen species on the (100) plane of nickel, by L.E.E.D. and photoelectric work function measurements but after exposing the surface to 10^{-3} torr nitrogen at 623 K he found no evidence for chemisorbed nitrogen[53]. However, higher pressure adsorption studies have revealed the existence of chemisorbed molecular species[54]. Russian workers have published infrared stretching frequencies corresponding to nitrogen chemisorbed on the (111), (110) and (100) crystal planes of nickel. When such chemisorbed nitrogen was treated with hydrogen, infrared bands corresponding to nitrogen adsorbed on the (111) and (110) planes were displaced whereas nitrogen chemisorbed on the (100) plane remained static[55]. This implied that not all chemisorbed nitrogen was capable of participating in the synthesis of ammonia and that nitrogen chemisorbed on (111) and (110) planes was especially active.

The chemisorption of nitrogen by polycrystalline nickel films at 473 K has been studied[56]. The adsorption was slow and had an activation energy of 33.6 - 58.8 kJ mol^{-1} depending on the degree of coverage. Chemisorbed nitrogen was found to react with hydrogen to form ammonia and the reaction was independent of the temperature of nitrogen chemisorption. The latter observation is in contrast to previous work[54] and the investigators conclude that the most likely surface nitrogen species are N=N (with two bonds to the surface) :N-N and N (with three bonds to the surface). It is also suggested that the rate of hydrogenation of adsorbed nitrogen is faster on nickel than iron and that the most probable rate determining step in ammonia synthesis (on nickel) is the chemisorption of nitrogen.

The adsorption of nitrogen on cobalt (formed by reduction of Co_3O_4) with and without alkali has been studied[57,58,59]. Alkali (K_2O) promoted cobalt was found to chemisorb nitrogen at a rate proportional to the one half power of nitrogen between 303-493 K whereas unpromoted cobalt chemisorbed nitrogen much slower and at a rate proportional to the first power of nitrogen. On promoted cobalt there are at least two different surface nitrogen species, one being irreversibly adsorbed (dissociative ?) and the other reversibly adsorbed (associative ?). The amount of the former relative to the latter increased with increasing temperature.

The co-adsorption of nitrogen and hydrogen by cobalt and alkali promoted cobalt has also been investigated . Below 473 K adsorption of nitrogen is inhibited by preadsorbed hydrogen and when preadsorbed nitrogen is contacted with hydrogen, even at 323 K, ammonia is rapidly formed.

The chemisorption of nitrogen by ruthenium and alkali promoted ruthenium has been the subject of an intensive investigation

by Japanese workers[60,61]. By studying the adsorption by a variety of methods e.g. infrared spectroscopy[62,63], reactivity of adsorbed nitrogen to hydrogen[64] and isotope exchange of adsorbed nitrogen with gaseous nitrogen they have come to a conclusion on the nature of the adsorbed nitrogen species. It is thought that there can be several types of sorbed nitrogen: (i) adsorbed atomic and molecular nitrogen and (ii) corrosively chemisorbed nitrogen in the bulk of the ruthenium.

2:4 Summary of main features of nitrogen adsorption on group VIII metals

Nitrogen adsorption on group VIII metals, which is often characterised by Elovich kinetics, is a difficult process and at moderate temperatures thermodynamic equilibrium coverages are never rapidly established. The rate of nitrogen chemisorption and the volume of nitrogen adsorbed is increased by alkali and by hydrogen. Comparison of the rate of nitrogen chemisorption and the rate of ammonia synthesis on iron and cobalt, under conditions of similar surface nitrogen coverage, indicates that nitrogen chemisorption is most probably the rate determining step in ammonia synthesis. Adsorbed nitrogen may be either molecular or atomic or a mixture of both depending on experimental conditions.

The velocity of nitrogen chemisorption on iron depends on crystal geometry. The iron (111) plane, which has iron atoms with seven nearest neighbours arranged in the form of an "open pot", chemisorbs nitrogen faster than other crystal planes. The number of iron (111) planes can be increased by a nitrogen induced surface reconstruction and it seems likely that catalytic activity for ammonia synthesis is associated with this crystal plane.

Chapter Three

Nitrogen Isotope Equilibration

Many metals, especially those of group VIII, are capable of catalytically dissociating molecular nitrogen. Direct evidence for molecular nitrogen dissociation can be obtained by measuring the velocity with which nitrogen isotopes undergo the equilibration reaction:

$$N_2^{28} + N_2^{30} \rightleftharpoons 2N_2^{29} \qquad (A)$$

Observations of reaction A have been widely used to try to elucidate the part played by adsorbed nitrogen during the ammonia synthesis reaction.

3:1 Nitrogen isotope equilibration on iron and promoted iron

The first observation of nitrogen isotope equilibration used a doubly promoted (K_2O, Al_2O_3) iron ammonia synthesis catalyst[65]. Preparation of catalyst samples involved a four day reduction, with temperatures as high as 773 K, using hydrogen which had been purified by passage through heated copper and a liquid air trap. The velocity of the equilibration reaction was very slow, being first measurable at temperatures above 723 K. The rate of the equilibration process was markedly increased by hydrogen and an apparent activation energy of 210 kJ mol^{-1}, for nitrogen isotope equilibration occurring in a three to one nitrogen/hydrogen mixture, was determined. These observations were rationalised by suggesting

that the rate determining step in nitrogen isotope equilibration (on iron ammonia synthesis catalyst) was either the rupture of valence bonds of adsorbed molecular nitrogen or migration of nitrogen atoms over the surface and that hydrogen accelerates such processes.

The observation that nitrogen isotope equilibration did not proceed on ammonia synthesis catalyst below 723 K was difficult to reconcile with the fact that both ammonia synthesis and ammonia decomposition occurred, on similar catalysts, at much lower temperature. To account for this discrepancy Kobozev suggested that the surface of the promoted iron catalyst consisted of ensembles of iron surrounded by and isolated from other ensembles by promoter atoms[66]. Ammonia synthesis and ammonia decomposition were envisaged to proceed on an isolated ensemble whereas nitrogen isotope equilibration involved the interaction of nitrogen adsorbed on different ensembles. The higher temperature for nitrogen isotope equilibration was needed to bring about surface migration of nitrogen. The validity of this hypothesis was tested by Kummer and Emmett when they re-examined the nitrogen isotope equilibration reaction on a very carefully reduced iron ammonia synthesis catalyst[67].

Unlike previous workers they found that isotope mixing occurred in the temperature range 673-723 K. In addition, the rate of equilibration was of the right order to be accounted for by assuming that all nitrogen evaporating from the catalyst surface was completely equilibrated with respect to nitrogen isotope exchange. Accordingly, no special assumption as to the nature of the iron surface (such as, the ensemble theory of Kobozev) was required to explain the behaviour of promoted iron surfaces towards mixtures of nitrogen isotopes. Rates of equilibration were increased by

added hydrogen and severely retarded by small quantities of oxygen and this suggested that the failure of previous workers to observe measurable rates, below 723 K, was probably due to traces of oxygen poison which may not have been completely removed from their catalysts during reduction.

The influence of catalyst reduction procedure on the velocity of nitrogen isotope equilibration on iron ammonia synthesis catalyst has been studied by other workers. Promoted iron (4.7% Al_2O_3, 0.3% K_2O) was reduced in a stream of hydrogen, purified by passage through a palladium/silver thimble, over a four day period at temperatures as high as 873 K[68]. The measured rate of equilibration was proportional to the one half power of the nitrogen pressure and the apparent activation energy was 138.6 kJ mol^{-1}. Hydrogen was found to exert no influence on the rate of the equilibration reaction above 673 K whereas it accelerated the rate at 624 K. The anomolous effect of hydrogen was explained by reference to possible surface intermediates. At lower temperatures (ca. 473 K) nitrogen is predominantly held as molecular (N≡N) or undissociated (-N=N- or -N=N-) nitrogen whereas at higher temperature (ca. 723 K) it is held in a dissociated form (N≡). The accelerating influence of hydrogen at 623 K is suggested to be concerned with the hydrogenation of adsorbed nitrogen molecules with the formation of imino (NH) and amino (NH_2) radicals by splitting N≡N, -N=N- or =N-N= bonds. When measured rates of nitrogen equilibration were compared with those given in the literature for similar catalysts it was shown that the present catalyst was much more active towards the equilibration reaction and this was explained by reference to the initial reduction which was carried out by use of hydrogen in the pure form. From this work, the general point is made that very pure

hydrogen must be used for reducing active nitrogen equilibration catalysts.

Krylova and Roginskii studied nitrogen isotope equilibration on several different catalyst formulations: iron (I) - unpromoted; iron (II) - added K_2O; iron (III) - added K_2O and Al_2O_3; iron (IV) - added K_2O, Al_2O_3 and CaO to try to resolve the part played by promoter atoms in dissociating molecular nitrogen[69]. They found that the most active catalyst (activity per unit mass) was the unpromoted iron and based on this observation proposed that nitrogen was held on the iron surface in a non-dissociated molecular form.

Gorbunov et al conclude that both K_2O and alumina increase the specific activity (activity per unit area) of iron for nitrogen isotope equilibration and that the promotional effect of K_2O is greater than that of alumina[70]. They also found that the true order of reaction (i.e. the dependence of equilibration rate on total nitrogen pressure) was lower on promoted iron and that the apparent activation energy for the process increased with promoter content.

The influence of promoter content on the form of adsorbed nitrogen on iron catalysts has been investigated. Well reduced iron (prepared by precipitation from ferric nitrate solution) and promoted iron (5% Al_2O_3, 1% K_2O) catalysts were obtained by oxide reduction in flowing pure hydrogen at 773 K for periods of sixty days[71]. Equilibration experiments were carried out in a circulating system which could be divided into two parts. Nitrogen-15 was introduced to the part which involved the reactor and was adsorbed by the catalyst until an equilibrium (no evidence for this is given) was established at the reaction temperature. Nitrogen-14 was then introduced to the other part of the circulatory system to the amount of a pressure exactly equal to the equilibrium pressure of the enriched gas. Thereafter

the parts containing the two gases were connected and the gas circulated through the reactor. This rapid mixing could not affect the adsorption equilibrium in addition to the isotopic displacement because the pressures of gas were equalised in advance.

The displacement process of adsorbed nitrogen was isotopically traced by measuring the time course of the isotopic concentration of the gas phase. The rate of displacement of adsorbed nitrogen was compared with the rate of isotope equilibration and the influence of hydrogen on the latter process investigated.

On pure iron the observed rate of displacement of nitrogen (at 375 torr pressure) was not constant for all adsorbed nitrogen. During the initial stages of reaction the rate of displacement was approximately five times faster than that of equilibration but after this initial period the rates of displacement and isotope equilibration became comparable. The relationship between the displacement process and the isotope mixing reaction is illustrated in the following mechanism:

$$N_{2(g)} \underset{I}{\rightleftharpoons} N_{2(a)} \underset{II}{\rightleftharpoons} 2N_{(a)}$$

where it is assumed that isotope mixing is caused by the dissociative chemisorption of nitrogen.

The rate of isotope equilibration is measured by the rate of process II while the rate of displacement is associated with the rates of processes I and II, depending on the relative rates. When rate I is larger than rate II, the rate of displacement is faster than isotope equilibration in the initial stages. In the later stages of the displacement, where the larger part of the adsorbed nitrogen is isotopically equilibrated with the gas phase, the

displacement is controlled by process II and thus the rates of isotope equilibration and displacement coincide.

As the experimentally observed rates of displacement and equilibration were similar, this work strongly suggests the existence of an undissociated state of nitrogen being rapidly displaced with gaseous nitrogen. It was calculated that about 80% of the adsorbed nitrogen was in some undissociated form. Hydrogen exerted no influence on the observed rate of equilibration.

Promoted iron behaves differently from pure iron. Although the rate of displacement of nitrogen from promoted iron is not uniform with respect to adsorbed nitrogen, the highest rate of displacement is in agreement with the rate of isotope equilibration and there is good evidence for dissociatively adsorbed nitrogen. The amounts of nitrogen adsorbed (per unit area) by iron and promoted iron are similar and this implies that the observed difference in the features of displacement are associated with a transformation of the adsorbed state.

Hydrogen increased the rate of isotope equilibration on promoted iron and a slight hydrogen isotope effect was observed. The hydrogen isotope effect was not large, but enough to indicate that hydrogen was chemically involved in dissociating nitrogen. It is suggested that nitrogen dissociation occurs in the following manner:

$$N_2 + 2H \longrightarrow 2NH$$

If equilibration proceeds in this way the promotional effect of hydrogen is easily understood.

A comparison of the rates of nitrogen displacement and isotope equilibration on unpromoted iron has also been undertaken

by Soviet workers[72]. Catalysts (prepared by precipitation of ferric nitrate solution) were reduced in flowing hydrogen at 673 K for eight days and rates of isotope equilibration and displacement were measured using an apparatus similar to that used by Japanese workers. Nitrogen equilibration results were in good agreement with theoretical curves calculated by assuming that the equilibration was affected through adsorption/desorption with the desorbed gas in equilibrium during the reaction. The general conclusion is formulated as: nitrogen adsorbed on iron, under the investigated conditions, forms a homogeneous adsorption layer in which equilibration occurs far more rapidly than adsorption and desorption of nitrogen molecules.

The suggestion by Soviet workers that dissociated nitrogen is the predominant surface species on unpromoted iron is in contrast to the Japanese workers who consider that the most likely surface intermediate, at such temperatures, is associatively adsorbed nitrogen. The discrepancy is thought to be due to the different pressures of nitrogen used by the different workers (Japanese 375 torr, Soviet 20 torr).

Rates of ammonia synthesis and nitrogen isotope equilibration on iron, promoted (4% Al_2O_3, 2% K_2O) iron and cobalt have been compared[73]. In the case of iron and cobalt the rates of reaction were comparable and a common rate determining step viz. dissociative chemisorption of nitrogen is suggested. On promoted iron the equilibration proceeded at only one tenth the rate of synthesis and this was explained in terms of insufficient mobility of chemisorbed nitrogen atoms.

However, another study which involved a quantitive comparison of the rates of nitrogen isotope equilibration and

ammonia synthesis, on promoted iron, taking account of different surface coverages of nitrogen, showed the rates to be equal[74]. In addition, the activation energies for both processes, calculated at constant fugacity of adsorbed nitrogen, were in satisfactory agreement and it is suggested that nitrogen isotope equilibration and ammonia synthesis have a common rate determining step.

A recent study by Boreskov et al investigated the relationship between dissociative adsorption of nitrogen (measured by nitrogen isotope equilibration) and ammonia synthesis over iron and molybdenum nitride catalysts[75]. Rates of homomolecular isotope equilibration and equilibration of adsorbed nitrogen with gaseous nitrogen were found to be comparable and it was concluded that isotope equilibration proceeded by an adsorption/desorption mechanism. The apparent activation energy and pressure dependence of homomolecular isotope equilibration were approximately 138.6 kJ mol^{-1} and 0.5 respectively on both iron and molybdenum nitride. The rates of ammonia synthesis and nitrogen isotope equilibration, when compared under conditions of similar nitrogen surface coverage, were found to be equal and this was interpreted as both reactions having a common rate determining step i.e. the dissociative chemisorption of nitrogen.

Nitrogen isotope equilibration, at reduced pressures, has been investigated and it was shown that the isotopic equilibrium for nitrogen adsorbed on a clean polycrystalline iron was not established at temperatures less than 400 K and at nitrogen pressure of 10^{-4} torr[76]. This was also the case when a red glowing iron wire was used as catalyst. As no change in the isotopic composition of the nitrogen gas was observed over an eleven hour period it was concluded that, under the experimental conditions, nitrogen did not dissociatively adsorb on iron.

The possibility that the equilibrium could be established in the presence of hydrogen - perhaps via. N_2---H adducts was also investigated. Experiments showed that in a nitrogen 14/15 mixture with a partial pressure of 6×10^{-4} torr in the presence of hydrogen with partial pressure 4×10^{-4} torr the formation of $N^{14}N^{15}$ could not be detected over a clean iron film at 373 K even after fifteen hours. A similar result was found for a glowing red iron wire.

When the same investigation was carried out with a tungsten filament, of comparable area to the iron catalyst, the formation of $N^{14}N^{15}$ was detected within several minutes. Thus, the lack of equilibration with the iron sample could not be associated with poor experimental conditions. The experimental results do not support the theory that the isotopic equilibration of nitrogen can be established by hydrogen as far as the low pressure range is concerned.

However, in another study of the interaction of nitrogen isotopes on iron (100) and iron (111) crystal planes isotope equilibration was observed at 373 K[77]. The rate of equilibration was faster on the (111) plane and the study favours the existence of atomically bound nitrogen.

3:2 Nitrogen isotope equilibration on ruthenium

The activation of molecular nitrogen by alkali metal promoted ruthenium has been the subject of an extensive investigation by Japanese workers. Potassium promoted ruthenium on active carbon catalysts were prepared by the impregnation method from aqueous chloride solutions, reduced by circulating hydrogen at 673 K for sixty five hours and subjected to adsorption of potassium vapour at 673 K. Equilibration experiments were carried out in a

circulating system and reaction was monitored by means of a quadrupole mass spectrometer[78].

The isotope equilibration reaction readily takes place in the temperature range 473-573 K with rate given by,

$$R = A \exp(-92{,}000 \sim 93{,}000/RT)P^{\frac{1}{2}}$$

where P is the total nitrogen pressure (50 torr<P<250 torr) and the activation energy is expressed in joules per mole.

N^{15} tracer experiments proved that all adsorbed nitrogen was displaceable by gas phase nitrogen i.e. all the adsorbed nitrogen was capable of participating in equilibration reactions[79]. Rates of ammonia synthesis and of nitrogen isotope equilibration are comparable and this is consistent with the rate determining step for both processes being the dissociation of a nitrogen molecule on a surface of low coverage.

The kinetics of nitrogen isotope equilibration have been studied on ruthenium catalysts with and without added potassium at 553-753 K and 40-200 torr nitrogen pressure[80]. The first order kinetics observed on ruthenium/alumina are changed by potassium addition into fractional order kinetics which approach first order as temperature increases. The change in kinetics was accompanied by an increase in apparent activation energy, whereas the equilibration activity increased by two or three orders of magnitude. The change in kinetics, as well as the estimated value for the heat of chemisorption (168 ± 25 kJ mol^{-1} on ruthenium/potassium) demonstrated that the addition of potassium intensified the adsorption strength of ruthenium towards nitrogen.

The effect of hydrogen on the velocity of nitrogen isotope equilibration, over ruthenium catalysts with and without potassium,

was then investigated. Addition of hydrogen increased the rate on pure ruthenium but decreased it on ruthenium/potassium i.e. the complete reverse from that observed on iron. The rate of ammonia synthesis is faster than isotope equilibration on pure ruthenium but the reverse is true on ruthenium/potassium catalysts.

Several possible reasons exist for the inhibition of isotope equilibration by added hydrogen on ruthenium/potassium catalysts. Firstly, adsorption sites are largely occupied by hydrogen owing to its larger adsorption strength ($K_H/K_N \approx 5$) so that the number of available sites for nitrogen decreases. Secondly, the adsorption constant for nitrogen decreases by about an order of magnitude in the presence of hydrogen.

The efficiency of potassium promoted ruthenium catalysts for nitrogen isotope equilibration has been associated with electron transfer from potassium to ruthenium. It is suggested that in the presence of nitrogen/hydrogen mixtures potassium metal is converted into potassium amide and this has a lower electron donating power than potassium metal and consequently catalytic efficiency for nitrogen equilibration is reduced. On unpromoted ruthenium catalysts the only possible surface products from mixtures of nitrogen/hydrogen are adducts of the form -NH, $-NH_2$ etc. and these would aid electron transfer to ruthenium (they are all electron donating) and this agrees with the observed increase in rate with added hydrogen.

A comparative study of potassium promoted active carbon/transition metal catalysts for nitrogen isotope equilibration has been published by Ozaki et al[81]. Catalysts were prepared by impregnation of active carbon prepared from Tsurumi coal (surface area $\approx$ 1000 $m^2\ g^{-1}$) by aqueous chloride solutions. Reduction and potassium addition were as detailed for ruthenium catalysts.

Figure 3:1 shows the equilibration rate (molecules per minute per gram catalyst) at 623 K as a function of the heat of formation of metal oxide, $-\Delta H_o$, (kJ mol^{-1}). The heat of formation of metal oxide has been shown to be a measure for the heat of chemisorption of gases[82].

Figure 3:1

Equilibration Rates at 623 K as a Function of $-\Delta H_o$

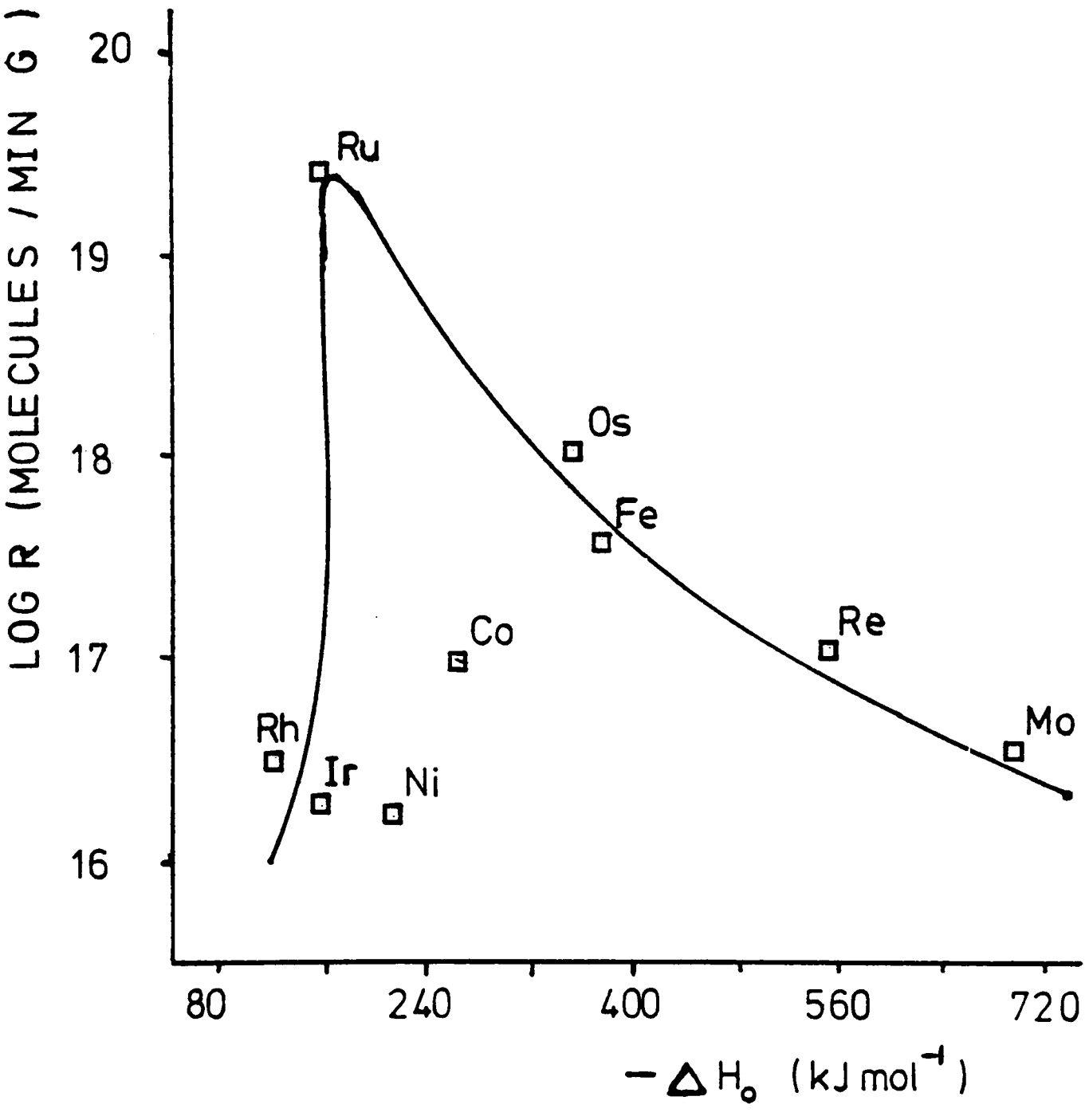

Figure 3:1, although having no particular meaning, illustrates the activity pattern at a glance.

The transition metals can be classified in terms of their experimentally determined apparent activation energies:

Class I	Ru (95)	Rh(105)	Os (93)	Ir(109)	
Class II	Re(168)	Fe(147)	Mo(160)	Co(160)	Ni(130)

all in kJ mol^{-1}.

This classification can be explained on the basis of metal affinity for nitrogen. Class I do not form nitrides and as such it is suggested that during nitrogen isotope equilibration there is a limited surface coverage and the observed activation energy relates to the activation energy for adsorption. Class II metals do form stable nitrides and their greater affinity for nitrogen implies that the measured activation energy is probably closer to that for desorption. No such classification is possible for ammonia synthesis, the rate of which is probably determined by chemisorption of nitrogen in all cases.

The activity of a ruthenium/iron alloy for nitrogen isotope equilibration and ammonia synthesis has been investigated[83]. The apparent activation energies for nitrogen isotope equilibration and ammonia synthesis over the ruthenium/iron catalyst are very similar to those found over iron but the observed activity is very much less than that of iron or ruthenium.

3:3 Nitrogen isotope equilibration on miscellaneous metals

Nitrogen isotope equilibration on metallic osmium catalysts, prepared by decomposition/reduction of ammonium osmium chloride in a stream of hydrogen at 573 K for eighteen hours, has been studied[84]. The equilibration reaction was measurable at 473 K and very rapid at 573 K with an apparent activation energy of 91.6 kJ mol^{-1}. Reaction was

inhibited by 3% hydrogen and with hydrogen concentrations greater than 50% there was no measurable equilibration at 573 K. Reaction rate was independent of nitrogen pressure (range 8-16 torr) and the authors suggest two possible mechanisms for isotope equilibration. Equilibration may proceed by either a slow migration of atomically bound nitrogen, on a surface on which active sites are few, or by repeated adsorption/desorption of nitrogen from configurationally more active centres. The available evidence did not allow a distinction to be made between the possible mechanisms.

Commercial rhenium powder, reduced in flowing hydrogen for ten hours at 1073 K, was found to be active in bringing about isotope equilibration at 773 K and the addition of hydrogen to the reaction mixture accelerated the equilibration[85]. Examination of the isotope equilibration on an oxygen poisoned surface indicated that the rhenium surface was heterogeneous and that only a small fraction of the surface was active in catalysing the equilibration reaction.

Initial investigation of the nitrogen isotope equilibration reaction on tungsten provided no evidence for equilibration activity below 1300 K[65] but more recent investigations have shown that dissociative chemisorption of nitrogen, on a tungsten filament, is possible at 1000 K[86,87]. The efficiency of a tungsten wire for catalysing isotope equilibration at 1000 K and 10^{-6} torr has been reported by Gasser. The very low measured efficiency was equated with a very low surface coverage of nitrogen and a mechanism consistent with atomically bound nitrogen was favoured.

The efficiency of molybdenum wire, as a catalyst for nitrogen isotope equilibration, was examined between temperatures of 1073-1273 K and nitrogen pressures of 10^{-7}-10^{-6} torr[88]. The efficiency, which was essentially independent of pressure, passed

through a maximum at 1200 K and the experimental data is consistent with equilibration proceeding by a Bonhoeffer-Farkas mechanism.

The absolute rate constants for nitrogen isotope equilibration on clean polycrystalline wires of molybdenum, rhenium and tungsten (at 1133-1623 K and pressure = 0.004 - 0.4 torr) have been determined[89]. An activated complex treatment in terms of partition functions gave reasonable agreement between theory and experiment for a mechanism for rhenium of molecular dissociation followed by atom recombination and for tungsten and molybdenum a reaction between atoms and molecules, possibly molecular radicals, competing for sites in the chemisorbed layer. The freedom of the activated complexes, relative to the respective adsorbed initial states, appeared to decrease in the order rhenium>molybdenum>tungsten.

Chapter Four

Hydrogenation of Carbon Monoxide

4:1 Nature of adsorbed carbon monoxide

It is now apparent that carbon monoxide is capable of both associative and dissociative adsorption on group VIII metals. Associative adsorption, which for sometime was accepted as being the case at all adsorption temperatures, is now thought likely to correspond only to the situation at lower temperature. Observations of associatively adsorbed carbon monoxide are presented in Table 4:1.

Table 4:1

Associative adsorption of carbon monoxide

Metal	Temperature/K	Technique used	Author
iron powder	195-433	isotope exchange	Webb and Eischens[90]
supported iron	298	i.r. spectroscopy	Eischens and Pliskin[91]
supported iron	293-473	i.r. spectroscopy	Blyholder and Neff[92]
cobalt film	170	i.r. spectroscopy	Baker et al[93]
nickel single crystal	<450	A.E.S. and L.E.E.D.	Madden et al[94]
iron, cobalt, nickel films	113-295	i.r. spectroscopy	Bradshaw and Pritchard[95]

Investigations which found evidence for dissociatively adsorbed carbon monoxide are shown in Table 4:2.

Table 4:2

Dissociative adsorption of carbon monoxide

Metal	Temperature/K	Technique used	Author
iron film	290	X.P.E.S. and U.P.E.S.	Kishi and Roberts[96]
nickel sheet	573-923	isotope exchange	Gregg and Leach[97]
nickel film	430	X.P.E.S. and U.P.E.S.	Joyner and Roberts[98]
molybdenum film	298	U.P.E.S. and X.P.E.S.	Atkinson et al[99]

From examination of Table 4:2 it is easily appreciated that during methanation and Fischer-Tropsch synthesis reactions carbon monoxide may be dissociated giving rise to surface carbon species.

4:2 Mechanism of interaction between carbon monoxide and hydrogen

Carbon monoxide, which is more strongly adsorbed than hydrogen (the maximum heat of carbon monoxide chemisorption is approximately 50% greater than that of hydrogen) on iron, cobalt and nickel readily displaces preadsorbed hydrogen at temperatures less than 350 K[100]. Above 250 K, carbon monoxide is capable of dissociating and interaction between carbon monoxide and hydrogen, in the adsorbed layer, becomes observable. Over the years several different theories have been proposed to describe the interaction of carbon monoxide and hydrogen on metal surfaces.

The earliest theory of carbon monoxide hydrogenation was that of Boudouard, which envisaged the involvement of elemental carbon and metal oxide[101]. This was followed, in 1926, by the "carbide theory" of Fischer and Tropsch which suggested the participation of bulk metal carbide[102]. In essence the carbide theory postulates that adsorbed carbon monoxide is reduced to carbide and water and that the metal carbide then reacts with adsorbed hydrogen to form methylene radicals which subsequently polymerise and desorb as olefinic and paraffic hydrocarbons. Later, Craxford and Rideal suggested the involvement of only surface carbide[103].

Support for the participation of carbides in hydrocarbon production came from the fact that many Fischer-Tropsch catalysts (e.g. iron, nickel and cobalt) readily formed carbides which on reaction with hydrogen produced hydrocarbons. However, as the carbide theory made no provision for explaining the production of oxygenated species the validity of its approach has been questioned.

The presence of oxygen containing intermediates was proposed in 1926, by Elvins and Nash, but attempts to detect such intermediates e.g. methanol or formaldehyde (on nickel) have proved unsuccessful[104]. Moreover, when methanol was used as a starting material, over a cobalt catalyst, the yield of hydrocarbon was less than when carbon monoxide and hydrogen were used[105]. The lack of direct evidence for oxygenated intermediates does not necessarily preclude their transitory existence and in fact two related mechanisms, for methanation and Fischer-Tropsch synthesis, involve the initial formation of an HCOH surface complex.

Vlasenko and Yuzefovich suggest that the most probable mechanism for the methanation reaction on nickel, cobalt and possibly iron is[106];

$$[\ ] + e + H_2 \rightarrow [H_2]^- \qquad 1$$

$$[\ ] + CO \rightarrow [CO]^+ + e \qquad 2$$

$$[CO]^+ + [H_2]^- \rightarrow [HCOH]^+ + e + [\ ] \qquad 3 \quad \text{(R.D.S.)}$$

$$[HCOH]^+ + [H_2]^- \rightarrow [CH_2] + H_2O + [\ ] \qquad 4$$

$$[CH_2] + [H_2]^- \rightarrow CH_4 + e + 2[\ ] \qquad 5$$

[ ] denotes a vacant active site on the catalyst surface and symbols in square brackets represent adsorbed species. Higher hydrocarbons are formed by polymerisation of methylene radicals.

Another mechanism, involving the oxygenated intermediate HCOH, has been proposed by Storch, Golumbic and Anderson[107]. In this treatment it is assumed that:

(i) hydrogen is adsorbed as atoms

(ii) chemisorption of carbon monoxide occurs on metal atoms with bonding similar to that in metal carbonyls

(iii) adsorbed carbon monoxide is partially hydrogenated as in equation A

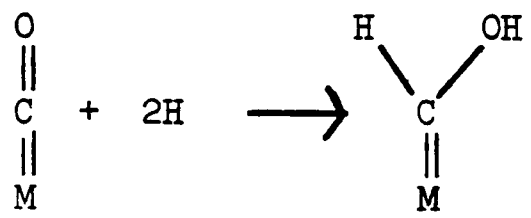

A

Chain initiation is as in equation A and chain growth is by condensation polymerisation of adsorbed hydroxylated species (equation B).

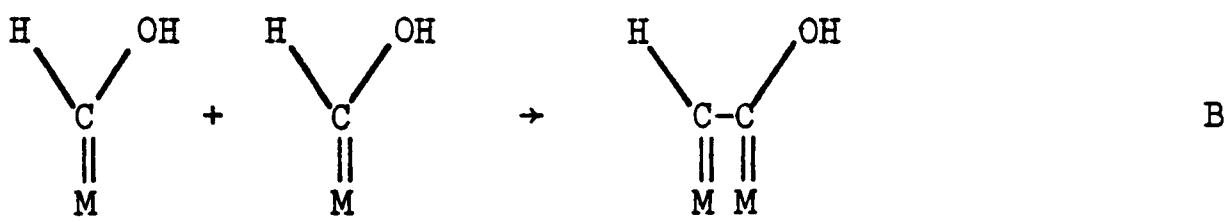

B

The reaction is terminated by hydrogenolysis of M-C bonds to yield alcohols, esters and hydrocarbons. Steps concerning chain growth are not applicable to methanation and a simplified reaction mechanism has been given:

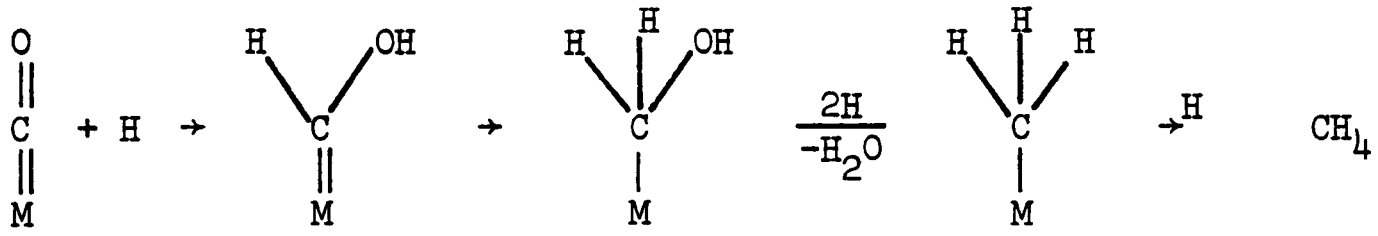

In an alternative model, that of Le Roux and Pichler, Fischer-Tropsch synthesis is viewed as being associated with a single surface site with carbon monoxide being inserted directly into a metal/carbon bond[108]. Carbon monoxide insertion increases the carbon number by one and water which is subsequently produced generates methylene and/or methyl groups as the predominant surface intermediate rather than oxygen containing groups. Auxiliary reactions are easily postulated to account for many of the observed synthesis products.

A reaction mechanism for Fischer-Tropsch synthesis, which involves only reaction steps which are well known in homogeneous systems, has been suggested by Olivé and Henrici-Olivé[109]. This

mechanism has some similarities to that of Le Roux in that both advocate the direct insertion of carbon monoxide into a metal/carbon bond.

Ponec and associates have recently proposed a mechanism for methanation, on nickel, which is a composite of previously postulated mechanisms[110]. There are three general features to this mechanism:

(i) carbon monoxide dissociates and adsorbed carbon (C_s) is partially hydrogenated (CH_x)

(ii) CH_x grows into a larger chain by repeated carbon monoxide insertion and partial hydrogenolysis (C_MH_N). It is not excluded that, after or during the insertion, oxygen is again split off from the $>C=O$ group

(iii) chain growth is terminated by hydrogenation.

The evidence on which this mechanism is based is presented in a recent review and it is sufficient to say that the observed reaction kinetics can be interpreted in terms of the rate determining step being the hydrogenation of adsorbed carbon[111].

4:3 Hydrogenation of carbon monoxide on alloy catalysts

Until the present time, there have been relatively few investigations concerning the methanation and Fischer-Tropsch synthesis activity of alloy catalysts. Iron present in platinum/iron clusters exhibited no Fischer-Tropsch synthesis activity and this was explained in terms of decreased iron electron density caused by electron withdrawal by platinum[112]. Electron donating species (e.g. K_2O) increased both methanation and synthesis activity and this is discussed in terms of $d\rightarrow\pi^*$ metal/carbon monoxide bonding.

The methanation activity of supported nickel/ruthenium catalysts has been reported by Bartholomew[113]. All catalysts exhibited similar characteristics to those of pure nickel but this is perhaps not surprising as only bimetallics up to 10% ruthenium were studied. No details are given with regard to extent of alloy formation or actual surface compositions.

Bond et al found that the activity of ruthenium/copper on silica catalysts for carbon monoxide hydrogenation between 530-670 K decreased with increasing copper content, while the activation energy remained constant at about 86 kJ mol^{-1}.[13] The activity (expressed as a turnover number) of an equimolar ruthenium/copper catalyst was estimated to be about fifty times less than that for pure ruthenium and selectivity towards higher hydrocarbons increased with added copper. The experimental results are interpreted in terms of copper segregating on the surface and reaction proceeding on an ensemble of about four ruthenium atoms.

The only other major study of carbon monoxide hydrogenation over alloy catalysts is that of Ponec and associates concerning nickel/copper alloys[114,115]. These workers found that the addition of small quantities of copper to nickel drastically reduced catalytic efficiency for carbon monoxide hydrogenation. The nature of adsorbed carbon monoxide and details of the interaction of adsorbed carbon monoxide with hydrogen were investigated by a variety of physical techniques (e.g. thermal desorption and infrared spectroscopy) and it was concluded that reaction was restricted to an ensemble of about four nickel atoms.

Chapter Five

Experimental and Treatment of Results

The experimental work described in this thesis may be divided into four main sections:

a) The preparation of a series of iron/cobalt, iron/nickel and ruthenium/rhodium catalysts.

b) The reduction and subsequent characterisation of catalysts, described in a), by differential thermal analysis, thermogravimetric analysis, X-ray diffractometry and selective chemisorption.

c) A study of the nitrogen isotope equilibration reaction on metal and mixed metal catalysts. This work was carried out in a static system using mass spectrometry as the means of analysis.

d) An investigation of carbon monoxide hydrogenation on catalysts used in c). This work involved the use of a static system with gas chromatography as the means of analysis.

5:1 Preparation of catalysts

5:1:1 Preparation of iron/cobalt and iron/nickel mixed metal catalysts

There are two methods of preparing substitutional alloys:

(i) Substitutional alloys of group VIII elements may be prepared by melting together the separate metals, followed by annealing or quenching, but this method

tends to form alloys of low area and as such it is of little use in catalyst preparation.

(ii) When excess base is added to a solution of iron/cobalt or iron/nickel nitrates a precipitate is formed. On calcination this precipitate forms a mixed metal oxide, which on reduction yields a high area substitutional alloy. This method was used to prepare the iron/cobalt, iron/nickel and nickel/cobalt alloy catalysts discussed in this thesis.

Experimental procedure

The desired quantities of metal nitrates were dissolved in water and the solution made up to three litres. The required quantity of ammonium bicarbonate (calculated to give an excess of ammonium bicarbonate) was dissolved in water to give ten litres. A quantity of aluminium nitrate, equivalent to 2.5% alumina (on a loss free basis) was then added to the mixed metal nitrate solution (alumina acts as a structure stabiliser and helps to maintain high surface area). Precipitation was carried out at ambient temperature over a twenty minute period by carefully adding the solution of the mixed metal nitrates to the ammonium bicarbonate solution. On completion of precipitation the slurry was filtered and washed with distilled water. After washing, the precipitate was dried overnight at 393 K, calcined in air at 723 K for four hours and then sieved with a 16 B.S. mesh sieve. The details of individual preparations and the analytical results on the final catalysts are shown in Table 5:1.

5:1:2 Preparation of alkalised catalysts

Alkali (K_2O) promoted metal catalysts were prepared by a technique similar to that outlined for the manufacture of iron/cobalt

Table 5:1

Catalyst Preparation Details

Sample	Weight of metal nitrates/g				Weight of ammonium bicarbonate/g
	Fe	Co	Ni	Al	
Fe	2,940	*	*	135	2,200
Fe95Co5	2,740	100	*	129	2,000
Fe90Co10	3,636	291	*	129	2,000
Fe80Co20	3,232	582	*	129	2,000
Fe60Co40	2,424	1,164	*	129	2,000
Fe40Co60	1,616	1,746	*	129	2,000
Fe20Co80	808	2,328	*	129	2,000
Co	*	2,910	*	176	2,000
Fe95Ni5	2,740	*	100	129	2,000
Fe90Ni10	2,596	*	196	129	2,000
Fe85Ni15	2,452	*	296	129	2,000
Fe80Ni20	3,232	*	582	129	2,000
Fe60Ni40	2,424	*	1,163	129	2,000
Fe30Ni70	1,212	*	2,036	128	2,000
Ni	*	*	2,908	165	2,000

Table 5:2

Preparation of alkalised iron, cobalt and nickel catalysts

Catalyst	Quantities of metal nitrates	Quantity of ammonium bicarbonate	Analytical report
Iron	688g $Fe(NO_3)_2$; 7.5g K_2CO_3; 14.7g $Al(NO_3)_3$	500 g	0.9% K_2O
Cobalt	471g $Co(NO_3)_2$; 7.5g K_2CO_3; 14.7g $Al(NO_3)_3$	500 g	0.6% K_2O
Nickel	471g $Ni(NO_3)_2$; 7.5g K_2CO_3; 14.7g $Al(NO_3)_3$	500 g	0.6% K_2O

All catalysts contained <0.02 wt. % sulphur and <0.02 wt. % chloride

and iron/nickel catalysts. The required quantities of metal nitrates and enough potassium carbonate to give approximately 4% K_2O were dissolved in three litres of water. This was then precipitated with ammonium bicarbonate and the precipitate washed, dried and calcined as described in section 5:1:1. The details of individual preparations and analytical results on final catalysts are shown in Table 5:2.

5:1:3 Preparation of supported ruthenium/rhodium mixed metal catalysts

When a metal is dispersed on an inert support its surface area per unit mass is increased. This provides, in the case where a metal is either very expensive or only available in a low area form, a convenient method for preparing high area metal catalysts. In studies of catalysis it is important that there should be little chemical interaction between metal and support as this may influence the catalytic properties of the metal. The support must also be free of any chemical promoters which might modify metal activity. The homogeneity of metal distribution is not critical in the case of single metals but it is essential when considering the preparation of alloy catalysts. If segregation occurs when two different metals are supported on a carrier alloy formation is impossible.

Catalyst support

The support used in the manufacture of impregnated catalysts, discussed in this thesis, was a high purity Condea ALC 169 alumina of sodium content less than 12 p.p.m.. The original powdered Condea ALC 169 (surface area $\sim 30\ m^2\ g^{-1}$) was mixed with 2% graphite (ex. Koch Light Analar) lubricant and pelleted. The resulting pellets were then calcined, in air at 1773 K, overnight to convert the alumina into

α alumina and burn off residual carbon. This procedure furnished $\frac{1}{8}$" diameter α alumina pellets of high purity.

Experimental procedure

The following generalised procedure was used to prepare all catalysts. Quantities of metal nitrates, calculated to contain 0.5 g total metal, were dissolved in that volume of water capable of being completely absorbed by 10 g of α alumina. This salt solution was then used to impregnate 10 g of alumina. The resulting impregnated pellet was dried at 393 K for one hour and then calcined (in air) at 723 K for four hours.

Ruthenium and rhodium nitrates are coloured and the homogeneity of their distribution on the α alumina carrier can be demonstrated by sectioning pellets and observing the colour distribution throughout the pellet. In all catalysts a homogeneous metal distribution was observed.

5:2 Characterisation of catalysts

5:2:1 Differential thermal analysis

Dynamic atmosphere differential thermal analysis experiments were conducted in a flow cell coupled to a Dupont 900A thermal analyser. In all experiments the following experimental conditions were employed:

sample mass	20 mg
sample particle size	70-120 B.S. sieve
reducing gas	hydrogen
gas flow rate	4 litres $hour^{-1}$
cell heating rate	20 K min^{-1}
gas pressure	one atmosphere
reference material	α alumina

5:2:2 Thermogravimetric analysis

Thermogravimetric experiments were performed in a dynamic hydrogen atmosphere using a Dupont 900A thermal analyser and mass changes of ±1 µg could be monitored with ease. Experimental conditions were similar to that described for Differential Thermal Analysis work (section 5:2:1).

5:2:3 X-ray diffractometry

A Philips MW 3100 instrument, using Co K_α radiation, was used to examine catalyst samples before and after reduction. Samples for X-ray examination were prepared in one of two ways.

Air stable samples

Samples of catalyst were ground into a fine powder with an agate mortar and pestle and then compressed into a sample holder and mounted on the spectrometer.

Air sensitive samples

Metal catalyst samples were prepared by reduction of metal oxides. After reduction, samples were sealed under nitrogen and transferred to a nitrogen dry box. Once in the dry box the metal was crushed and mixed with a small quantity of paraffin grease. The grease, which is invisible to X-ray radiation, acts as a binding agent and causes the sample to aggregate into a paste. A quantity of this paste was then placed in a sample holder, sealed under nitrogen, and mounted on the spectrometer.

Measured X-ray parameters

When determining lattice parameters, accurate X-ray

reflection angles were obtained by correcting experimentally measured reflection angles for instrumental variance using reflections from a small quantity of silicon incorporated into the test sample.

Average crystallite size was estimated by use of Scherrer's equation;

$$S = \frac{K\lambda}{B \cos \theta}$$

where λ is the X-ray wavelength (Å), K is a constant equal to 0.893, θ is the Bragg angle (radians), B is the line broadening (radians) and S is the mean crystallite size (Å).

5:2:4 Metal area determination

Metal areas of reduced catalyst samples were measured by room temperature carbon monoxide adsorption. Samples of catalyst (ca. 1 g) were reduced in flowing hydrogen according to a pre-determined schedule. Normally, this involved raising the temperature of the sample to 853 K over a four hour period then leaving overnight at 853 K. After reduction the sample was evacuated, usually at 773 K, for 18 hours then cooled to ambient temperature. Room temperature carbon monoxide adsorption isotherms were then measured by admitting successive known doses (via. a gas burette) of carbon monoxide into the sample volume and noting the decrease in pressure (measured by McLeod gauge) caused by adsorption. A schematic diagram, showing the construction of the apparatus used for measuring metal areas is shown in Figure 5:1.

A typical adsorption isotherm is illustrated in Figure 5:2.

Figure 5:2

Typical carbon monoxide adsorption isotherm for reduced catalyst

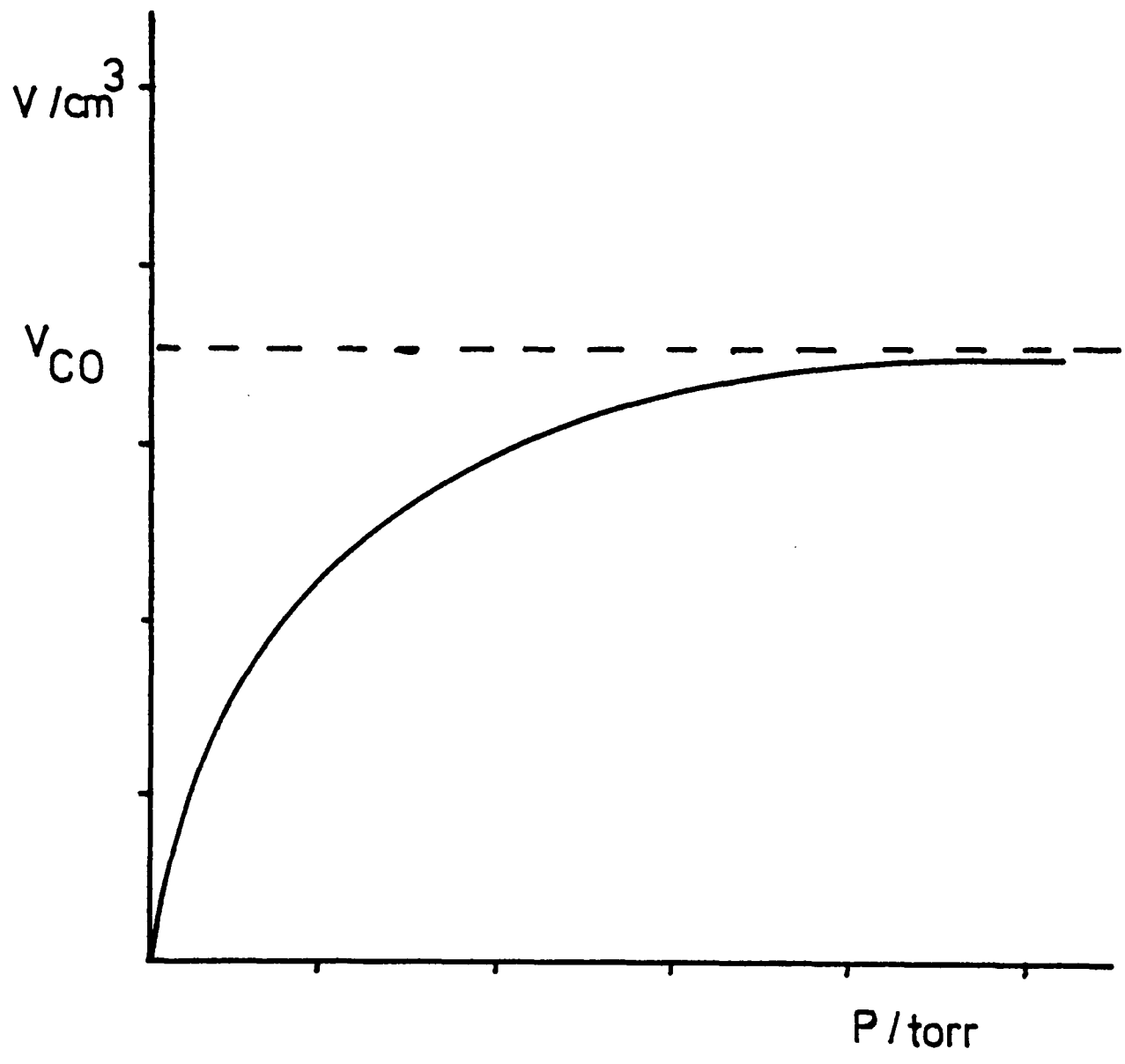

V is the volume of carbon monoxide adsorbed at room temperature, P is the pressure of carbon monoxide in the sample volume and V_{CO} is the critical volume of carbon monoxide needed to give a monolayer coverage from which the metal surface area is determined. In all calculations it was assumed that one carbon monoxide molecule occupied 1.3×10^{-19} m^2 of surface[116].

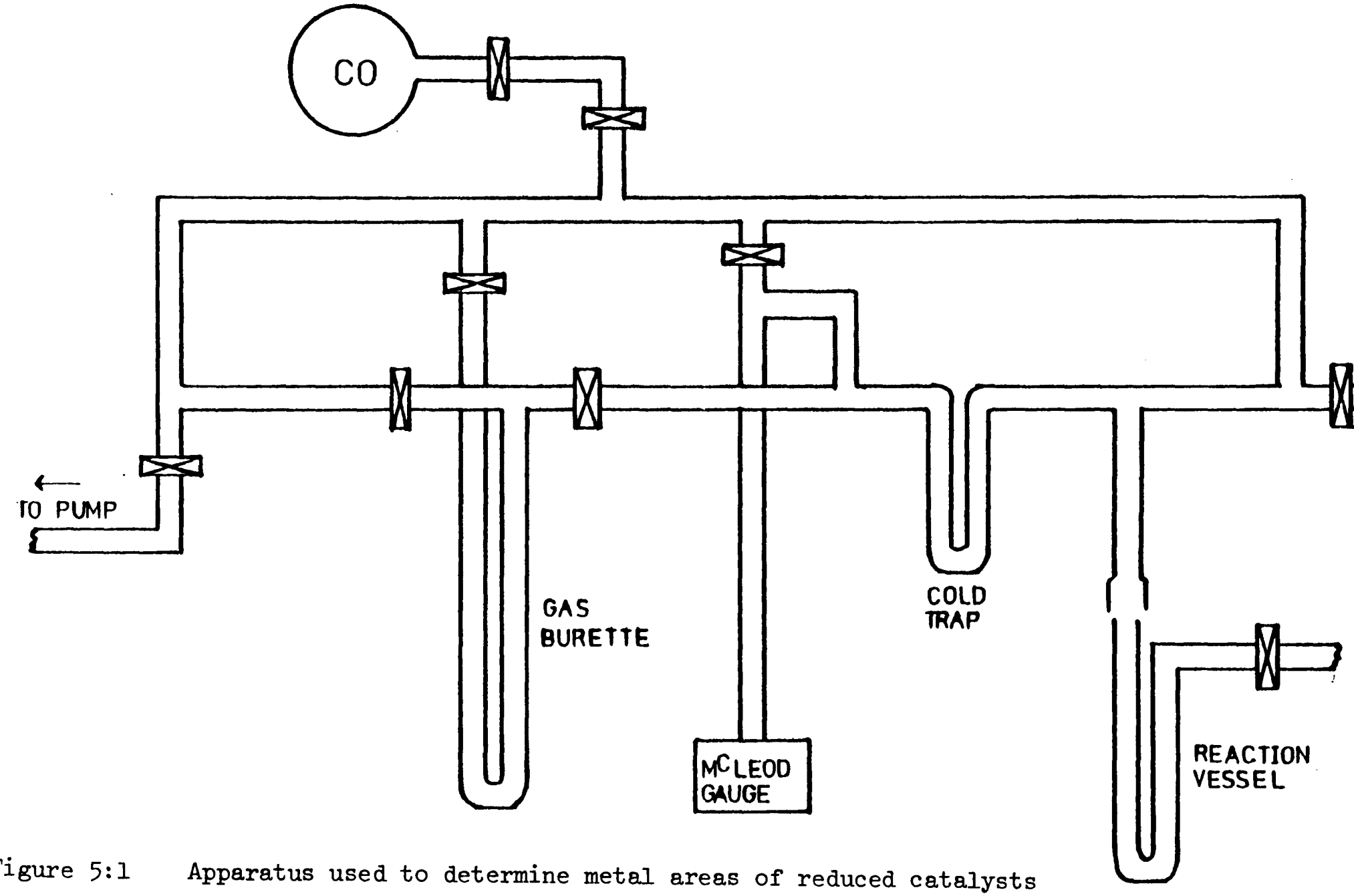

Figure 5:1 Apparatus used to determine metal areas of reduced catalysts and to study nitrogen adsorption.

5:3 Nitrogen isotope equilibration experiments

The apparatus used to study nitrogen isotope equilibration, on alloy catalysts, consisted of a high vacuum system and demountable silica reaction vessel connected to a mass spectrometer by a direct capillary leak.

5:3:1 High vacuum system

The design of the high vacuum system is shown diagramatically in Figure 5:3. The apparatus was constructed in pyrex glass with ground glass joints and taps lubricated by Apiezon L or T high vacuum grease. Evacuation of the system was obtained by a mercury diffusion pump, with cold trap, backed by a rotary pump (Edwards). Low pressures were measured by McLeod gauge and pressures between 1 and 150 torr were measured with a mercury manometer. Liquid nitrogen traps prevented mercury contamination of reactant and catalyst.

Gaseous volumes of sections of the line were calculated by use of a calibrated volume and the mercury manometer. The number of molecules admitted to the catalyst was estimated from a knowledge of the dosing volume, reaction vessel volume and total pressures before and after admission of reactant. Typically, 10^{20} molecules were admitted to the catalyst.

Catalyst samples were heated by a close fitting furnace, the temperature of which was measured by a chromel/alumel thermocouple connected to a Eurotherm controller. Accurate catalyst temperature was measured by a thermocouple attached to a Cormack 5000 digital thermometer. Temperature fluctuations of more than 1 K did not occur during catalytic experiments.

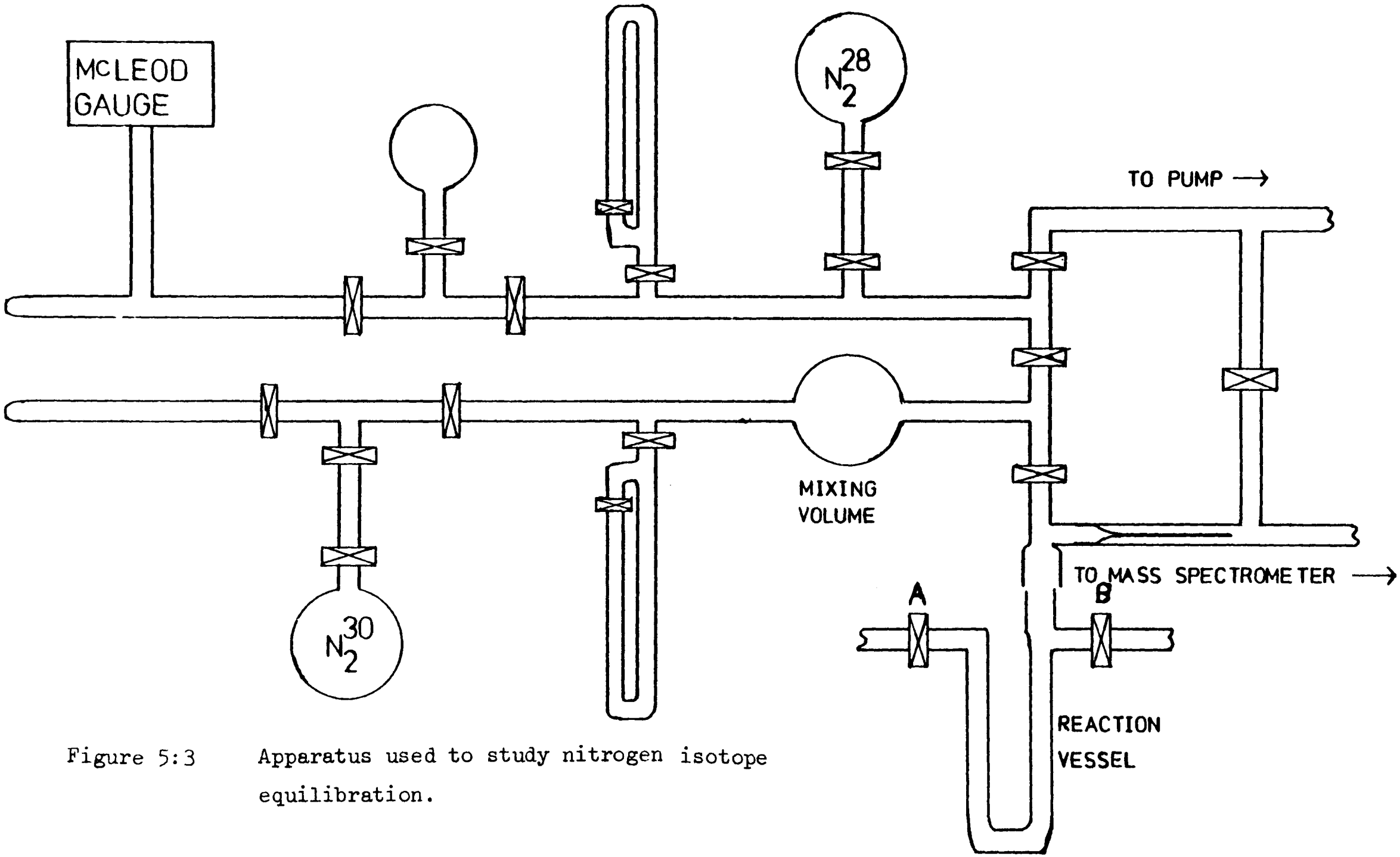

Figure 5:3 Apparatus used to study nitrogen isotope equilibration.

5:3:2 Reaction vessel and capillary leak

The reaction vessel used in all nitrogen isotope equilibration experiments is shown diagramatically in Figure 5:3. The lower portion of the vessel was constructed in silica and both taps were rotaflo taps. The vessel attaches to the high vacuum system via. a ground glass joint and hydrogen can flow through the vessel by means of taps A and B.

Reaction mixture was leaked into the mass spectrometer (see 5:3:3) by means of a long fine capillary. The capillary, which had a leak rate of about 2.7 kN m^{-2} of air into a volume of $2x10^{-5}$ m^3 in twenty minutes with a pressure differential of one atmosphere, allowed about 3% of the gas in the reaction vessel to flow into the mass spectrometer every hour. This gave ample gas for analysis without appreciably effecting the amount of gas in the reaction vessel.

5:3:3 The mass spectrometer

An A.E.I. M.S. 20 spectrometer was used to monitor all nitrogen isotope equilibration experiments. The source region was evacuated by means of an oil diffusion pump (A.E.I.) backed by rotary pump (Edwards). The tube unit was protected from contamination by a liquid nitrogen trap and pressure inside the ionisation chamber was measured with an ionisation gauge (A.E.I.) All mass spectra were recorded under the following conditions:

accelerator voltage	71 eV
electron current	10 μA
ion repeller	1.06 V
scan period	30 min^{-1}

5:3:4 Experimental procedure

An accurately weighed quantity of catalyst (ca. 1 g) was placed in the reaction vessel and the system evacuated. After evacuation a stream of hydrogen (purified by passage through a Deoxo catalytic purifier (Englehard Sales) and liquid nitrogen trap) was introduced into the vessel. The catalyst temperature was then raised in a similar manner to that described in 5:2:4. After reduction the catalyst was isolated from the hydrogen supply and evacuated for one hour at 853 K. The temperature was then lowered to the reaction temperature, usually somewhere in the region 773-843 K.

All reactions, except where otherwise stated, were conducted with a four to one mixture of nitrogen-14/nitrogen-15 at a total pressure of 50 torr. At the end of each experiment the nitrogen reactant was evacuated and the system purged with hydrogen for one hour at 843 K. After hydrogen treatment the catalyst was evacuated for one hour (at 843 K) and then cooled to the reaction temperature. This procedure enabled several experiments to be conducted on a single catalyst sample (see 6:2:1).

5:3:5 Treatment of nitrogen isotope equilibration results

The nitrogen isotope equilibration reaction:

$$N_2^{28} + N_2^{30} \rightleftharpoons 2N_2^{29}$$

was monitored mass spectrometrically. After correcting for background spectrum, peaks corresponding to masses 28, 29 and 30 were used to calculate the percentage composition of the reactant mixture. Percentage composition against time curves were then used to give an overall picture of the course of the reaction.

The nitrogen isotope equilibration reaction can be divided into six possible combinations between N_2^{28}, N_2^{29} and N_2^{30}:

$$N^{14}N^{14} + N^{15}N^{15} \rightleftharpoons N^{14}N^{15} + N^{15}N^{14} \qquad A$$

$$N^{14}N^{14} + N^{15}N^{15} \rightleftharpoons N^{14}N^{15} + N^{15}N^{14} \qquad B$$

$$N^{14}N^{15} + N^{14}N^{15} \rightleftharpoons N^{14}N^{14} + N^{15}N^{15} \qquad C$$

$$N^{14}N^{15} + N^{14}N^{15} \rightleftharpoons N^{14}N^{15} + N^{14}N^{15} \qquad D$$

$$N^{14}N^{14} + N^{14}N^{14} \rightleftharpoons N^{14}N^{14} + N^{14}N^{14} \qquad E$$

$$N^{15}N^{15} + N^{15}N^{15} \rightleftharpoons N^{15}N^{15} + N^{15}N^{15} \qquad F$$

The nitrogen-29 content increases as a result of reactions A and B but decreases due to reaction C. Therefore, the rate of formation of nitrogen-29 is a fraction of the total rate of exchange, R, and in general the observed rate of isotope equilibration is a mere fraction of the total rate, R.

The reaction between nitrogen-28 and nitrogen-30 is statistically twice as probable as that between nitrogen-29 isotopes and as half of the latter exchanges lead to disappearances of nitrogen-29, neglecting isotope effects, the rate of formation of nitrogen-29 is given by[117];

$$N\frac{dX_{N_2^{29}}}{dt} = R\left[2X_{N_2^{14}}X_{N_2^{15}} - \tfrac{1}{2}X^2_{N_2^{29}}\right] \qquad G$$

where N is the total number of nitrogen molecules (N_2^{28}, N_2^{29} and N_2^{30}) in the system and X's refer to the mole fractions of the isotope molecules indicated. As the total number of nitrogen-15 atoms in the reaction mixture is constant, the atomic fraction of nitrogen-15, f_{N^*}, is also constant,

$$X_{N_2}{}^{14} + X_{N_2}{}^{15} + X_{N_2}{}^{29} = 1; \quad f_N = 1 - f_{N^*}$$

$X_{N_2}{}^{14}$ and $X_{N_2}{}^{15}$ are given by

$$X_{N_2}{}^{14} = 1 - f_{N^*} - \tfrac{1}{2}X_{N_2}{}^{29}; \quad X_{N_2}{}^{15} = f_{N^*} - \tfrac{1}{2}X_{N_2}{}^{29}$$

Therefore, equation G can be written as,

$$N\frac{dX_{N_2}{}^{29}}{dt} = R\,[\,2f_{N^*}(1-f_{N^*}) - X_{N_2}{}^{29}\,]$$

$$\Rightarrow \quad N\frac{dX_{N_2}{}^{29}}{dt} = R\,[\,X^e{}_{N_2}{}^{29} - X_{N_2}{}^{29}\,] \qquad H$$

where $X^e{}_{N_2}{}^{29} = 2f_{N^*}(1-f_{N^*})$ is the equilibrium value of $X_{N_2}{}^{29}$.

Integration of equation H gives,

$$\frac{Rt}{N} = -\ln\,[(X^e{}_{N_2}{}^{29} - X_{N_2}{}^{29})/(X^e{}_{N_2}{}^{29} - X^o{}_{N_2}{}^{29})] \qquad I$$

where $X^o{}_{N_2}{}^{29}$ is the initial value of the mole fraction of nitrogen-29 in the reaction mixture.

Therefore, the rate of isotope equilibration is first order with respect to mole fraction of isotopic species and R/N is frequently referred to as the first order rate constant (k). Some comments are appropriate:

(i) The rate of exchange, R, is a function of the total nitrogen pressure ($N_2^{28} + N_2^{29} + N_2^{30}$) and as such the order of the equilibration has to be determined separately from the pressure dependence of R.

(ii) No mechanism for exchange is assumed in the derivation of equation I. The first order nature of the isotope

exchange arises from the probability of exchange and is independent of mechanism.

(iii) The first order rate constant, k, has the dimensions of moles S^{-1} and is independent of isotopic concentration but remains dependent on the reaction conditions, such as, total amount of nitrogen, amount of catalyst and temperature. Consequently, all catalytic activities are specified in terms of R as molecules exchanged per unit time for a given mass of catalyst.

The equilibrium mole fraction of nitrogen-29 ($X^e_{N_2 29}$) was found in two ways. The known value of the equilibrium constant for the reaction $N_2^{28} + N_2^{30} \rightleftharpoons 2N_2^{29}$ (statistical and experimental equilibrium constant equals 4) along with the initial partial pressures of nitrogen-28 and nitrogen-30 were used to calculate the equilibrium value, $X^e_{N_2 29}$, in the following manner.

$$N_2^{28} + N_2^{30} \rightleftharpoons 2N_2^{29}$$

At time = 0 40 10 0 (partial pressures in torr)

At time = t (40-x) (10-x) 2x where x is the partial pressure that has reacted.

Therefore, $\frac{4x^2}{(40-x)(10-x)} = K$ where K is the equilibrium constant. As K = 4, we can write -

$$\frac{4x^2}{(40-x)(10-x)} = 4$$

Solving the quadratic equation gives x = 8 and so the equilibrium mole fraction of nitrogen-29 ($X^e_{N_2 29}$) is 0.32.

As a check on the calculated equilibrium nitrogen-29 mole fraction, a reaction mixture containing four parts nitrogen-28 and one part nitrogen-30 was left over an iron catalyst for twenty four hours at 1073 K. After this time the reactant mixture was fully equilibrated and composition did not vary with time. The experimentally

determined nitrogen-29 mole fraction (0.32) agreed with the calculated value.

Values of the first order rate constant (k), determined at different temperatures, were plotted according to the Arrhenius equation,

$$k = A \exp (- E_A/RT)$$

where A is a frequency factor, E_A an apparent activation energy, R is the Universal Gas Constant and T is the absolute temperature.

5:4 Carbon monoxide hydrogenation experiments

The apparatus used to study hydrogenation of carbon monoxide consisted of a conventional high vacuum system, removable silica reaction vessel and a flame ionisation gas chromatograph.

5:4:1 High vacuum system

The apparatus, which is illustrated diagramatically in Figure 5:4, was constructed with pyrex glass. Evacuation was achieved by a mercury diffusion pump, with cold trap, backed by rotary pump (Edwards) and such a system allowed pressures less than 10^{-5} torr to be achieved. All ground glass joints and taps were lubricated by either Apiezon L or T high vacuum grease. Pressures below one torr were measured with a McLeod gauge and pressures between 1 - 760 torr were measured by Bourdon gauge.

Calibration of the various sections of the apparatus was performed by expanding hydrogen from a standard volume. Catalyst samples were heated by a closely fitting furnace, the temperature of which was controlled by a Eurotherm controller. Accurate catalyst temperature was measured by a chromel/alumel thermocouple attached to a digital (Cormack 5000) thermometer.

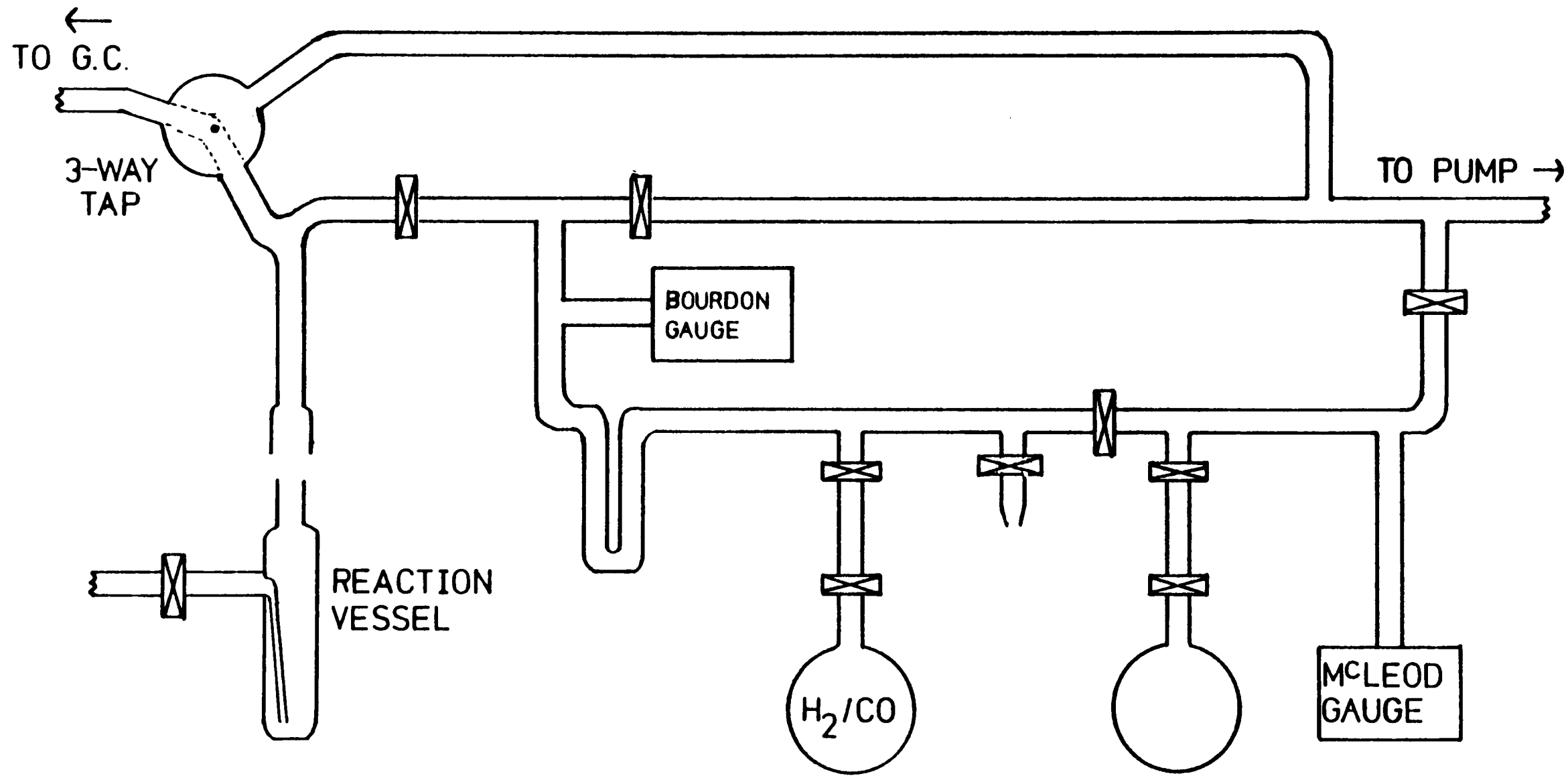

Figure 5:4 Apparatus used to study carbon monoxide hydrogenation.

5:4:2 Reaction vessel and chromatographic detection system

The silica reaction vessel used in all experiments is shown diagramatically in Figure 5:4. Catalyst reduction was brought about by a stream of hydrogen (purified by passage through a Deoxo catalytic purifier (Englehard Sales) and liquid nitrogen trap) which exited via. the gas handling line.

Samples for analysis were withdrawn from the reaction mixture by means of a three way tap. After withdrawal samples were introduced onto the column in a stream of helium carrier gas. The chromatographic column used, in this particular investigation, was a 4 m. $\frac{1}{4}$" o.d. stainless steel tube loaded with bis-2-methoxy-ethyladipate (13.5%) and di-2-ethylhexylsebacate (6.5%) on 60-80 mesh Chromosorb P and operated at room temperature with inlet helium carrier pressure 15 lb in^{-2}. Approximately 1% of the gas phase reaction mixture was removed with each sample taken. The resolved components were eluted to a hydrogen/air Perkin Elmer F11 flame ionisation detector. The resulting signals were amplified and parallel amplified signals supplied to a digital integrator (Smiths MK III) and servoscribe potentiometric recorder.

Chromatographic detector sensitivity values for different hydrocarbons were measured by analysing standard hydrocarbons and appropriate corrections made.

5:4:3 Experimental procedure

An accurately weighed quantity of catalyst (ca. 0.2 g) was placed in the reaction vessel and the system evacuated. After evacuation a stream of hydrogen (purified by passage through a Deoxo catalytic purifier (Englehard Sales) and liquid nitrogen trap) was introduced into the vessel. The catalyst temperature was then raised to 853 K as described in section 5:2:4. After reduction the

catalyst was isolated from the hydrogen supply and evacuated for one hour at 773 K. After evacuation the temperature was lowered to the desired reaction temperature, normally 473 K.

Pre-mixed reactant (a 3/1 mixture of H_2/CO at total pressure 80 torr) was admitted to the catalyst by means of a dosing volume and reactant analysis was as previously described (5:4:2).

5:4:4 Treatment of carbon monoxide hydrogenation results

Integrated peak areas, after correction for sampling loss and detector sensitivity, were used to estimate gas phase composition as a function of time. Plots of percentage composition against time were then drawn to illustrate the general character of the reaction. The initial rate of appearance of any particular product was estimated by drawing a tangent to the initial portion of the appropriate composition/time curve. Initial product distributions were inferred by expressing the individual product reaction rates as a percentage of the total reaction rate.

As carbon monoxide could not be detected by the flame ionisation detector a direct check on carbon balance was impossible. Consequently, unreacted carbon monoxide and/or carbon on the catalyst surface was estimated by expressing the existing gas phase carbon as a fraction of the total carbon present initially.

5:4:5 Ethane hydrogenolysis experiments

Ethane hydrogenolysis experiments (using a 3/1 mixture of H_2/C_2H_6 at 80 torr total pressure) were carried out in the apparatus used for carbon monoxide hydrogenation studies (5:4:1). The experimental procedure and treatment of results were as described for carbon monoxide hydrogenation experiments.

5:5 Materials used

Chemicals used in catalyst preparation work were supplied by British Drug Houses Ltd. and were of Analar purity. Nitrogen-14 and nitrogen-15 (Research Grade) were supplied by British Oxygen Company Ltd. and were used without further purification. Carbon monoxide (99.9% pure) and ethane (99.9% pure) were obtained from Cambrian Chemicals Ltd.. Carbon monoxide was used directly but ethane was purified by repeated freeze-pump-thaw cycles.

Chapter Six

Nitrogen Isotope Equilibration and Related Processes on Iron/Cobalt and Iron/Nickel Alloys: Catalysts Reduced at 853 K

The present chapter is divided into four parts:

a) Details of the physical and chemical properties of a series of iron/cobalt and iron/nickel catalysts.

b) The results of an investigation of the nitrogen isotope equilibration reaction on iron/cobalt and iron/nickel alloy catalysts.

c) A review of the results of a parallel study of the ammonia synthesis activity and nitrogen chemisorption properties of catalysts used in b).

d) A consideration of the relationship between nitrogen chemisorption, nitrogen isotope equilibration and ammonia synthesis on iron, cobalt and nickel and a detailed discussion of results reported in b) and c).

6:1 Characterisation of iron/cobalt and iron/nickel catalysts

6:1:1 Catalyst composition

Average atomic ratios (as measured by X-ray fluorescence spectroscopy) of iron/cobalt and iron/nickel catalysts are shown in Table 6:1.

Table 6:1

Average composition of iron/cobalt and iron/nickel catalysts

Sample	Actual Composition (a) / % Iron	Sample	Actual Composition (a) / % Iron
Fe	100	Fe	100
Fe(95)Co(5)	95.2	Fe(95)Ni(5)	97.6
Fe(90)Co(10)	91.5	Fe(90)Ni(10)	90.2
Fe(80)Co(20)	84.7	Fe(85)Ni(15)	85.5
Fe(60)Co(40)	63.8	Fe(80)Ni(20)	85.3
Fe(40)Co(60)	43.3	Fe(60)Ni(40)	63.0
Fe(20)Co(80)	21.6	Fe(30)Ni(70)	31.2
Co	0	Ni	0

(a) experimental values accurate to $\pm 0.1\%$.

The surface compositions of samples Fe(95)Co(5) and Fe(90)Ni(10), after reduction at 853 K, were estimated (by quantitative E.S.C.A.) to be Fe(75)Co(25) and Fe(60)Ni(40). However, due to problems associated with mounting reduced samples in the spectrometer these surface compositions may refer to a partially oxidised surface. The very low signal/noise ratio prevented quantitative analysis of surface alumina (present as a structure stabiliser).

6:1:2 Differential thermal analysis examination

Reduction characteristics of all catalysts were determined by reduction thermal analysis and experimental thermograms for iron/cobalt and iron/nickel catalysts are presented in Figures 6:1 and 6:2 respectively. Specific exotherms and endotherms were related to

particular reduction processes by examining catalyst samples by X-ray diffractometry prior to and after each exotherm and endotherm of interest.

The relevant processes in the reduction of these iron/cobalt and iron/nickel catalysts are as follows:

$$\alpha Fe_2O_3 \xrightarrow[A]{EXO} Fe_3O_4 \xrightarrow[FeO_{1+X} \quad B]{ENDO} \alpha Fe$$

$$Co_3O_4 \xrightarrow[C]{EXO} CoO \xrightarrow[D]{EXO} Co$$

$$NiO \xrightarrow[E]{EXO} Ni$$

Process A, the haematite to magnetite conversion, was observed to occur in both the iron/cobalt and iron/nickel catalysts at a temperature of about 483 K. As iron is progressively replaced by cobalt, in the iron/cobalt catalysts, the size of the endotherm associated with process B decreases and the maximum temperature of reduction falls from 753 K for pure iron to 602 K for Fe(20)Co(80). Increasing cobalt content results in the progressive appearance of exotherms corresponding to processes C and D. Process C was observed always about 573 K while process D occurred in the range 673-723 K.

Increasing nickel content causes a decrease in the size of the endotherm associated with process B and the maximum temperature of reduction falls from 753 K for pure iron to 573 K for Fe(30)Ni(70) while process E occurs at 593 K.

Addition of cobalt or nickel to the iron lattice progressively eases the reduction of the catalyst with nickel having the larger effect (753 K to 573 K).

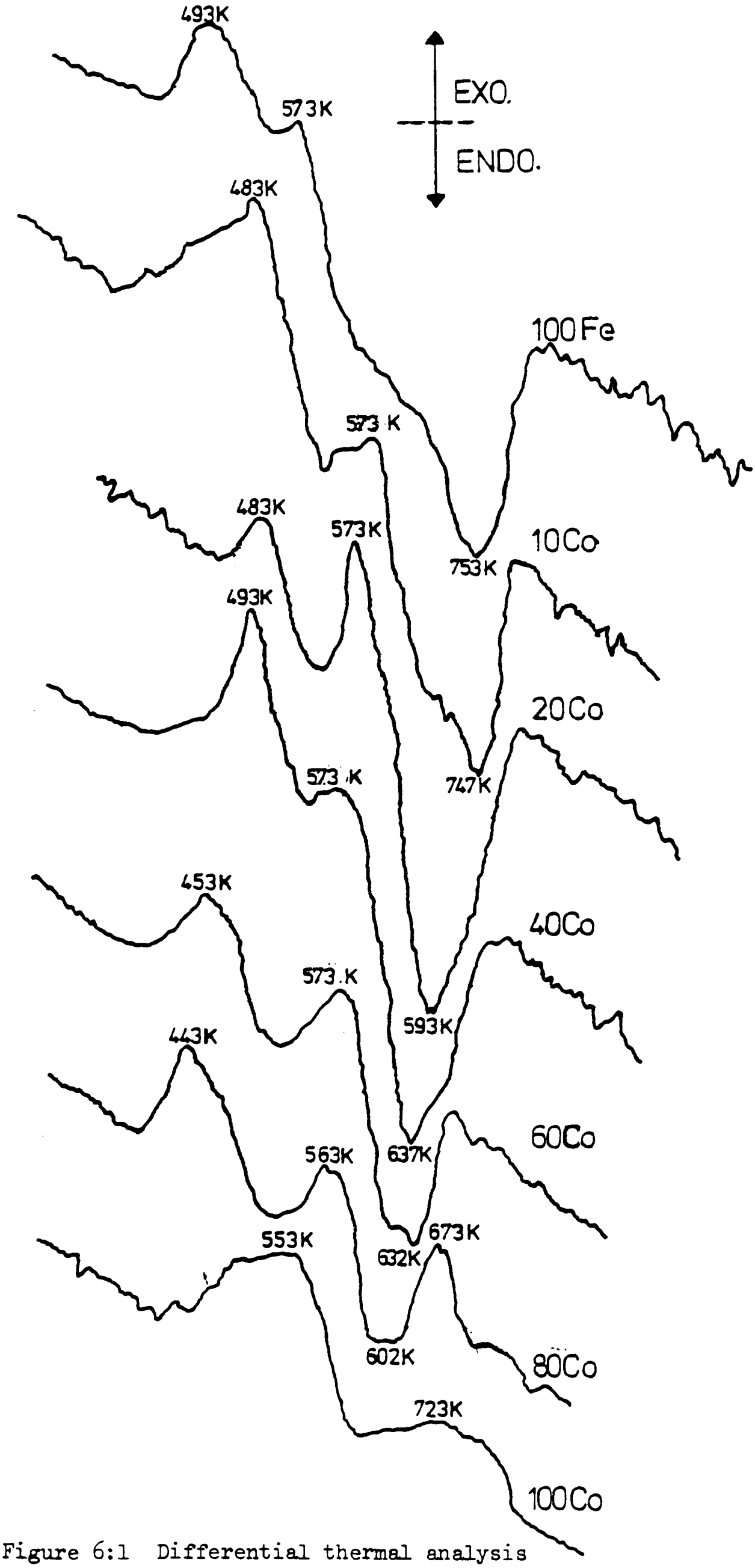

Figure 6:1 Differential thermal analysis thermograms for iron-cobalt catalysts

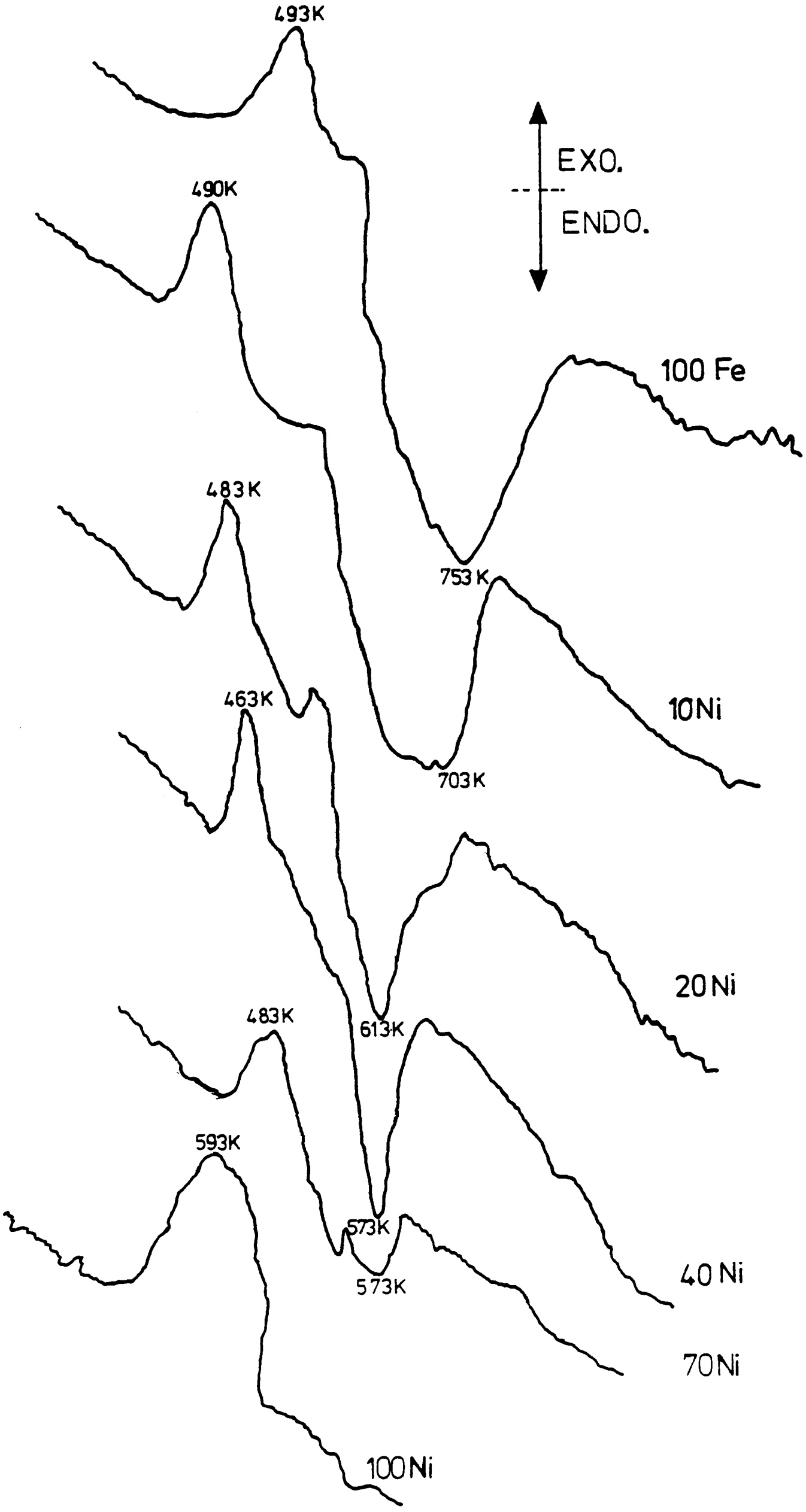

Figure 6:2 Differential thermal analysis thermograms for iron-nickel catalysts.

6:1:3 X-ray diffractometry examination

Catalysts were examined by X-ray diffractometry before and after reduction to determine phase composition, mean crystallite size and lattice parameter. Details of the X-ray analyses of the unreduced iron/cobalt and iron/nickel catalysts are given in Table 6:2 and those of the reduced (at 853 K) catalysts are given in Table 6:3.

The unreduced iron, cobalt and nickel catalysts were highly crystalline and all major phases were identified. In the case of the mixed metal oxides the samples were not highly crystalline and broad overlapping bands were obtained which hindered the identification of phases present. Thus, alumina may have been present in solid solution but was never detected as such.

Diffraction patterns of the reduced catalysts (except Fe(20)Co(80)) confirmed that complete alloy formation occurred on reduction. The origin and identification of the trace phase present in the reduced iron and some of the iron rich alloys is discussed in chapter seven.

6:1:4 Catalyst surface areas

The total metal area of reduced (at 853 K) iron/cobalt and iron/nickel catalysts, determined by room temperature chemisorption of carbon monoxide (5:2:4), are presented in Table 6:4.

Table 6:2

X-ray analysis of unreduced iron/cobalt and iron/nickel catalysts

Sample	Phase Composition	Lattice Parameter/ A°	Mean Crystallite Size/ A°
Co	Cobalt (II and III) oxide with 3% Al_2O_3 in solid solution	8.080	198
Fe(20)Co(80)	mixed iron/cobalt spinels	8.120	107
Fe(40)Co(60)	mixed iron/cobalt spinels	8.390	100
Fe(60)Co(40)	mixed iron/cobalt spinels	8.160	60
Fe(80)Co(20)	mixed iron/cobalt spinels - major αFe_2O_3 minor	8.300	130
Fe(90)Co(10)	αFe_2O_3 - major mixed iron/cobalt spinels - minor	5.024	134
Fe(95)Co(5)	αFe_2O_3 - major mixed iron/cobalt spinels - minor	5.024	200
Fe	haematite with 3% Al_2O_3 in solid solution	5.024	450
Fe(95)Ni(5)	αFe_2O_3 major mixed iron/nickel spinel - minor	*	400
Fe(90)Ni(10)	αFe_2O_3 major - mixed iron/nickel spinel - minor	*	180
Fe(85)Ni(15)	αFe_2O_3 major - mixed iron/nickel spinel - minor	*	50
Fe(80)Ni(20)	αFe_2O_3 - major - mixed iron/nickel spinels - minor	8.210	40
Fe(60)Ni(40)	poorly crystalline material - major $NiFe_2O_4$ spinel - minor	8.350	40
Fe(30)Ni(70)	probably mixed iron/nickel oxides - major amorphous material - minor	-	52
Ni	bunsenite with 3% Al_2O_3 in solid solution	8.080	159

* value not determined

Table 6:3

X-ray analysis of reduced (at 853 K) iron/cobalt and iron/nickel catalysts

Sample	Phase Composition	Lattice Parameter[(a)]/A°
Co	mixture of α and β cobalt	*
Fe(20)Co(80)	b.c.c. iron/cobalt alloy - major mixture of α and β cobalt - minor	2.839
Fe(40)Co(60)	b.c.c. iron/cobalt alloy	2.8500
Fe(60)Co(40)	b.c.c. iron/cobalt alloy	2.8621
Fe(80)Co(20)	b.c.c. iron/cobalt alloy	2.8690
Fe(90)Co(10)	b.c.c. iron/cobalt alloy - major unidentified - minor	2.8672
Fe(95)Co(5)	b.c.c. iron/cobalt alloy - major unidentified - minor	2.8680
Fe	b.c.c. iron - major unidentified - minor	2.8666
Fe(95)Ni(5)	b.c.c. iron/nickel alloy	*
Fe(90)Ni(10)	b.c.c. iron/nickel alloy - major unidentified - minor	2.8698
Fe(85)Ni(15)	b.c.c. iron/nickel alloy - major unidentified - minor	2.8703
Fe(80)Ni(20)	b.c.c. iron/nickel alloy - major f.c.c. nickel/iron alloy - minor unidentified - trace	2.8705 *
Fe(30)Ni(70)	f.c.c. nickel/iron alloy	*
Ni	f.c.c. nickel metal	3.523

(a) Experimental values accurate to ±0.0008 A°.

* Value not determined.

Note: All samples have a mean crystallite size of about 600 A°.

Table 6:4

Total metal area of reduced (at 853 K) iron/cobalt and iron/nickel catalysts

Sample	Area[(a)] / $m^2\ g^{-1}$	Sample	Area[(a)] / $m^2\ g^{-1}$
Fe	3.7	Fe	3.7
Fe(95)Co(5)	3.7	Fe(95)Ni(5)	2.8
Fe(90)Co(10)	4.3	Fe(90)Ni(10)	2.0
Fe(80)Co(20)	4.3	Fe(85)Ni(15)	1.7
Fe(60)Co(40)	3.5	Fe(80)Ni(20)	2.7
Fe(40)Co(60)	5.7	Fe(60)Ni(40)	1.5
Fe(20)Co(80)	4.8	Fe(30)Ni(70)	1.5
Co	8.5	Ni	8.1

(a) expressed per gram of unreduced catalyst and assuming an area of 1.3×10^{-19} m^2 for each CO molecule.

Repeat measurements of the metal areas of seven of the samples indicates that the reproducibility is subject to an average error of ±8%.

6:2 Nitrogen isotope equilibration on iron/cobalt and iron/nickel alloys

6:2:1 Kinetic parameters

The rate of nitrogen isotope equilibration on iron/cobalt and iron/nickel alloy catalysts was investigated (using a 4/1 mixture of nitrogen-14/nitrogen-15 at 50 torr total pressure) in the temperature

range 723-853 K. Measured rates of reaction were calculated by the method described in 5:3:5 and are reported both in terms of observed rate (activity per unit mass of catalyst) and in terms of intrinsic rate (activity per unit area). Activation energies and frequency factors were calculated from "best fit" least square lines and all reported rates were found by interpolation of "best fit" Arrhenius plots.

The catalytic activity of a virgin catalyst was found to be identical to that of a used catalyst which had been reactivated as described in 5:3:4 i.e. treated with flowing hydrogen at 843 K for one hour. Consequently, this enabled a single charge of catalyst to be used for several different experiments.

Kinetic parameters for iron/cobalt alloys are presented in Table 6:5 and those for iron/nickel alloys in Table 6:6. For many of the samples, repeat experiments were performed (indicated by an asterisk in Tables 6:5 and 6:6) which all gave good agreement with the original data. In these cases the values in Table 6:5 and Table 6:6 were obtained from a combination of both original and repeat experiments.

The major feature to note in Tables 6:5 and 6:6 is that the intrinsic rate of the nitrogen equilibration reaction passes through a maximum value as a function of alloy composition for the samples Fe(95)Co(5) and Fe(95)Ni(5).

6:2:2 The order of nitrogen isotope equilibration on unpromoted and promoted iron, cobalt and nickel

The dependence of reaction rate on total nitrogen pressure (between nitrogen pressures of 10 to 200 torr and temperature 723-843 K) was determined from slopes of graphs of log (reaction rate)/ molecules s^{-1} m^{-2} against log (nitrogen pressure)/torr. In all cases,

Table 6:5

Kinetic parameters for nitrogen isotope equilibration on reduced (at 853 K) iron/cobalt catalysts between 773 and 853 K

Sample	Observed Reaction Rate[(a)] / 10^{15} molecules s^{-1} g^{-1}	Intrinsic Reaction Rate[(a)] / 10^{15} molecules s^{-1} m^{-2}	log(A/ molecules s^{-1} m^{-2})	Activation Energy/ kJ mol^{-1}
Fe*	60.3	16.3	27.1	177±13
Fe(95)Co(5)*	92.9	25.1	26.0	157±16
Fe(90)Co(10)*	73.9	17.2	27.9	191±12
Fe(80)Co(20)*	74.8	17.4	26.9	175±20
Fe(60)Co(40)	28.4	8.1	27.2	184±50
Fe(20)Co(80)	42.2	8.8	26.42	151±12
Co	104.6	12.3	24.48	137±10

(a) Reaction rate at 823 K and 4/1 nitrogen-14/nitrogen-15 at total pressure of 50 torr.

* Average result of more than one experiment.

Table 6:6

Kinetic parameters for nitrogen isotope equilibration on reduced (at 853 K) iron/nickel catalysts between 773 and 853 K

Sample	Observed Reaction Rate[(a)] / 10^{15} molecules s^{-1} g^{-1}	Intrinsic Reaction Rate[(a)] / 10^{15} molecules s^{-1} m^{-2}	log(A/ molecules s^{-1} m^{-2}	Activation Energy/ kJ mol^{-1}
Fe*	60.3	16.3	27.1	177±13
Fe(95)Ni(5)*	103.4	36.8	28.8	188±17
Fe(90)Ni(10)*	33.8	16.9	25.6	153±24
Fe(85)Ni(15)*	44.9	26.4	25.8	153±25
Fe(80)Ni(20)*	51.6	19.1	28.4	198±31
Fe(60)Ni(40)	7.6	5.1	26.9	182±10
Fe(30)Ni(70)	6.9	4.6	26.1	170±59
Ni	19.4	2.4	21.9	107±10

(a) Reaction rate at 853 K and 4/1 nitrogen-14/nitrogen-15 at total pressure 50 torr.

* Average result of more than one experiment.

good straight lines (which were analysed by the method of least squares) were obtained and experimental orders of reaction are shown in Table 6:7.

Table 6:7

Order of reaction on unpromoted and promoted iron, cobalt and nickel

Sample	Order of Reaction[(a)]	Sample	Order of Reaction[(a)]
Fe	0.7	Fe+0.9% K_2O	1.0
Co	0.6	Co+0.6% K_2O	1.0
Ni	0.8	Ni+0.6% K_2O	1.0

(a) experimental values accurate to ±10%.

6:2:3 The influence of hydrogen on the rate of nitrogen isotope equilibration

The effect of carrying out nitrogen isotope equilibration in the presence of increasing partial pressures of hydrogen, using a 4/1 mixture of nitrogen-14/nitrogen-15 at a total pressure (nitrogen and hydrogen) of 50 torr was investigated. The rates of reaction, interpolated from "best fit" Arrhenius plots, and apparent activation energies for reaction occurring in different partial pressures of hydrogen are given in Table 6:8.

6:2:4 Nitrogen isotope equilibration on promoted catalysts

Nitrogen isotope equilibration on promoted (K_2O) iron, cobalt and nickel was investigated using a standard 4/1 nitrogen isotope mixture at 50 torr total pressure in the temperature range 723-843 K. The results of this investigation, along with results referring to a commercial ammonia synthesis catalyst, are summarised in Table 6:9.

Table 6:8

Influence of hydrogen on rate of nitrogen isotope exchange on iron/cobalt and iron/nickel catalysts

Sample	NO	Hydrogen	N_2/H_2 2/1		N_2/H_2 1/3	
	(a)	(b)	(c)	(b)	(d)	(b)
Co	12.3	137	10	150	9	160
Fe(20)Co(80)	8.8	151	*	*	*	*
Fe(60)Co(40)	8.1	184	*	*	*	*
Fe(80)Co(20)	17.4	175	16	165	18	160
Fe(90)Co(10)	17.2	191	18	180	17	182
Fe(95)Co(5)	25.1	157	30	175	21	173
Fe	16.3	171	17	165	20	177
Fe(95)Ni(5)	36.8	188	28	173	40	182
Fe(90)Ni(10)	16.9	153	20	160	21	157
Fe(85)Ni(15)	26.4	153	17	160	25	140
Fe(80)Ni(20)	19.1	198	*	*	*	*
Fe(60)Ni(40)	5.1	182	*	*	*	*
Fe(30)Ni(70)	4.6	170	*	*	*	*
Ni	2.4	107	1	136	3	115

(a) Intrinsic reaction rate (at 823 K and 4/1, nitrogen-14/nitrogen-15 at 50 torr total pressure)/10^{15} molecules s^{-1} m^{-2}

(b) Activation energy in kJ mol^{-1}

(c) Intrinsic reaction rate (at 823 K with 1/2 H_2/total N_2 mixture at 50 torr pressure and rate corrected to a nitrogen pressure of 50 torr)/10^{15} molecules s^{-1} m^{-2}.

(d) Intrinsic reaction rate (at 823 K with 3/1 H_2/total N_2 mixture at 50 torr pressure and rates corrected to a nitrogen pressure of 50 torr)/10^{15} molecules s^{-1} m^{-2}.

* Value not measured.

Table 6:9

Summary of activities of alkali promoted catalysts in the temperature range

773 K - 853 K

Sample	Observed rate[(a)] / 10^{15} molecules s^{-1} g^{-1}	Intrinsic rate[(a)] / 10^{15} molecules s^{-1} m^{-2}	log A (molecules s^{-1} g^{-1})	Activation Energy/kJ mol^{-1}
Fe + 0.9% K_2O	8	23	26.1	160±7
Co + 0.6% K_2O	83	*	23.3	101±10
Ni + 0.6% K_2O	31	*	23.3	108±9
Commercial ammonia synthesis catalyst[(b)]	34	63	30.3	217±20

(a) reaction rate at 823 K and 4/1 nitrogen-14/nitrogen-15 mixture at total pressure 50 torr.

(b) I.C.I. 35-40 catalyst.

* metal area not measured.

6:3 Nitrogen chemisorption and ammonia synthesis on iron/cobalt and iron/nickel alloys reduced at 853 K

6:3:1 Nitrogen chemisorption

Nitrogen chemisorptions were done volumetrically in the system previously described (5:2:4).

The adsorption of nitrogen on iron at 673 K, 773 K and 833 K is shown in Figure 6:3 as a plot of surface coverage (defined as the number of nitrogen molecules adsorbed as a fraction of the number of carbon monoxide molecules adsorbed at complete coverage) against nitrogen exposure. Following adsorptions at 673 K and 773 K the samples were evacuated to better than 10^{-5} torr for fifteen hours at the adsorption temperature to remove reversibly adsorbed nitrogen. The results of the readsorption of nitrogen on the surface carrying strongly adsorbed nitrogen are also presented in Figure 6:3.

Several points emerge from an examination of Figure 6:3 :-

(i) The chemisorption at 673 K is slow, requiring an exposure of 10^{10} Langmuirs (equivalent to about five hours under the experimental conditions) before reaching a constant value. At 773 K and above the rate of adsorption is much faster and reaches a constant value after ninety minutes.

(ii) Although the amount adsorbed appears to reach a constant value it is unlikely that this corresponds to thermodynamic equilibrium since the amount adsorbed increases with increasing adsorption temperature, the latter observation, if it corresponded to adsorption equilibrium, would imply an endothermic sorption, which is unlikely.

(iii) Evacuating the sample overnight at the adsorption temperature, followed by readsorption of nitrogen, gives a measure of the amount of nitrogen which is reversibly adsorbed. As the adsorption temperature is increased the fraction of the total adsorption

which is reversible also increases (by 773 K this fraction represents about 90% of the total adsorption). It seems likely that the fraction of nitrogen that is reversibly adsorbed varies continuously with adsorption temperature although a closer examination of the adsorption might show that more than one type of adsorption is involved.

Nitrogen adsorption on the alloy catalysts is exemplified by two iron/nickel alloys in Figure 6:4. The major difference (other than the amounts adsorbed) between these samples and the iron sample is that the sample Fe(90)Ni(10) adsorbs less at 773 K than at 673 K in accord with an exothermal adsorption process. In consequence, the results for all samples are summarised, in Table 6:10, in terms of two parameters, namely the initial rate of adsorption (expressed in molecules L^{-1} m^{-2} to allow for differences in initial nitrogen pressure and in metal surface areas of the various samples) and the surface coverage after an exposure of 10^{10} Langmuirs (at which the coverage has reached a constant value even if this does not correspond to adsorption equilibrium).

Adsorption of nitrogen on cobalt and nickel showed a different character to that over iron and the alloys. Over cobalt the surface coverage increased linearly with exposure for the duration of the experiment whereas on nickel it was not detectable at 673 K but as 773 K proceeded to its final (presumably equilibrium) value within three minutes (see also Table 6:10). A number of additional features are evident from Table 6:10:-

(i) The observation for iron that the nitrogen adsorption is almost completely reversible at 773 K is even more marked in the case of the two iron/nickel alloys.

(ii) Except for the Fe(95)Co(5) sample the initial rate of adsorption is generally faster at 773 K than 673 K.

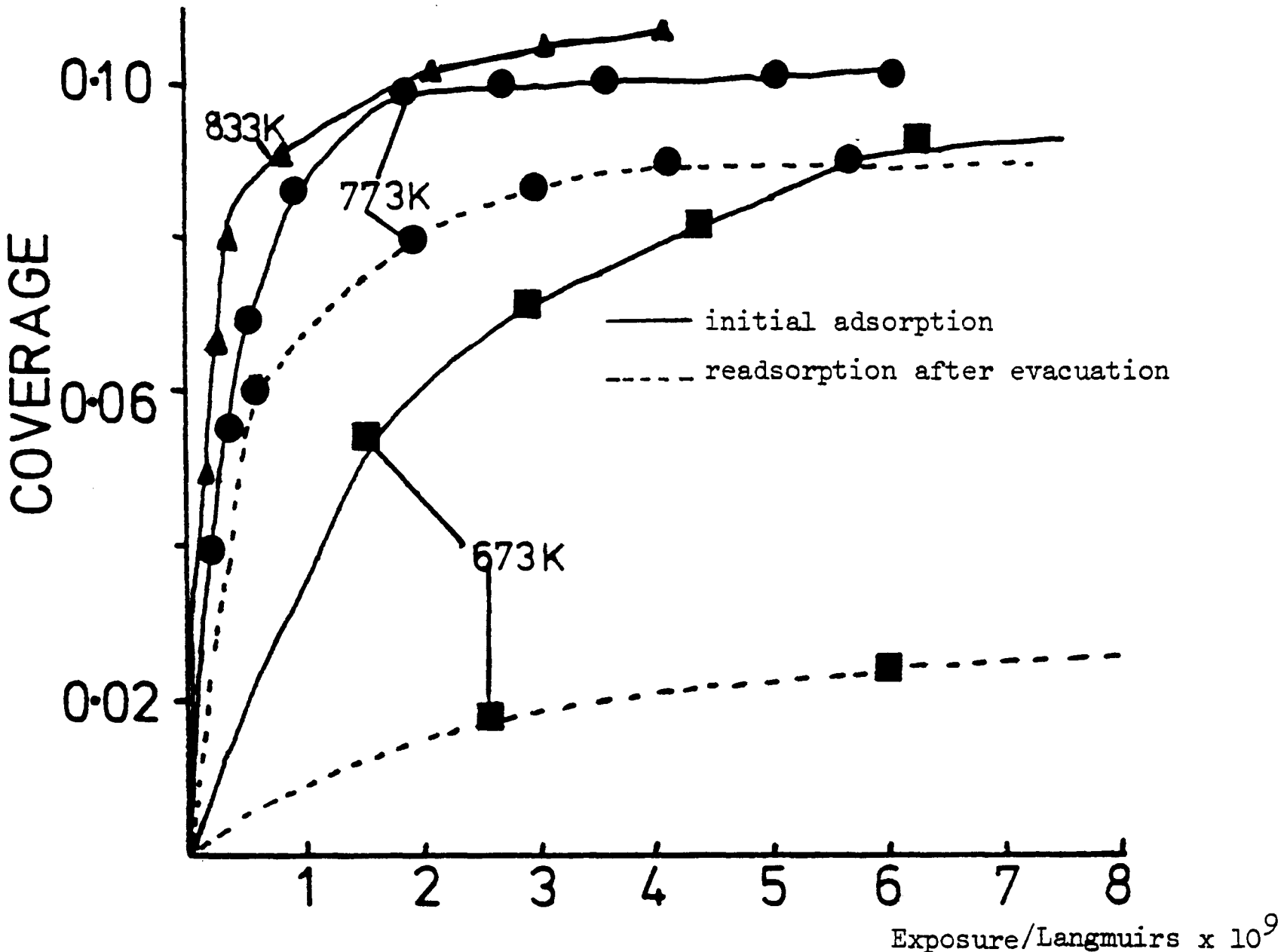

Figure 6:3 Nitrogen chemisorption on iron.

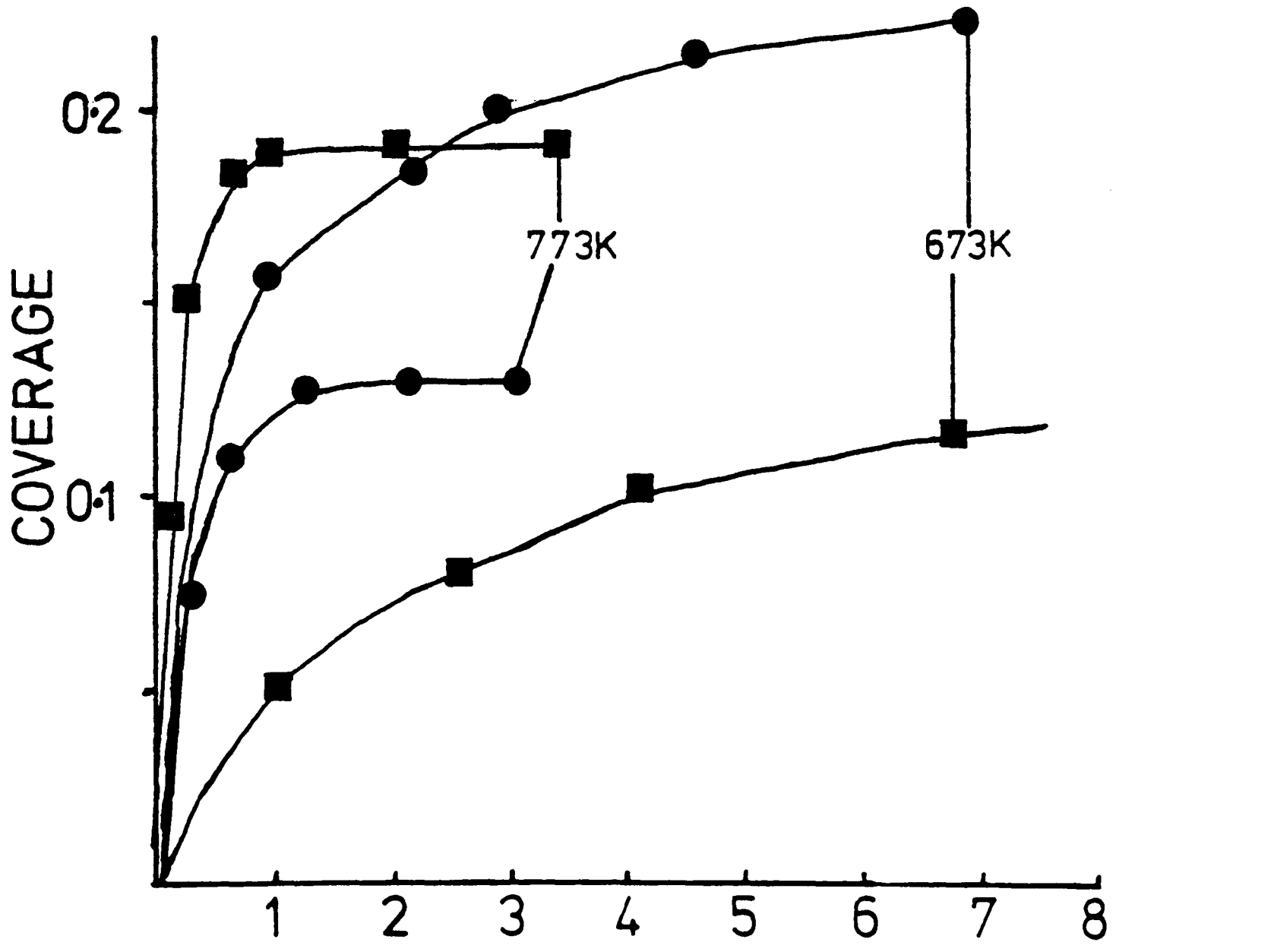

Figure 6:4 Chemisorption of nitrogen on Fe(90)Ni(10) (●) and Fe(80)Ni(20) (■).

Table 6:10

Summary of nitrogen chemisorption experiments at 673 and 773 K

Sample	Initial Adsorption Rate/ 10^{18} molecules L^{-1} m^{-2}		Coverage 10^{10} L Exposure[a]	
	673 K	773K	673 K	773 K
Fe	6(0.64)[b]	30(38)[b]	0.095(0.031)[b]	0.100(0.089)[b]
Fe(95)Co(5)	211	84	>0.190[c]	0.104
Fe(90)Co(10)	14	42	0.140	0.082
Co	0.2	1	0.024	(d)
Fe(90)Ni(10)	21(2)	43(36)	0.234(0.136)	0.142(0.138)
Fe(80)Ni(20)	6(0.8)	440(440)	0.132(0.025)	0.190(0.185)
Ni	<0.05	86	<0.002	0.05

(a) expressed as the number of nitrogen molecules adsorbed as a fraction of the number of carbon monoxide molecules adsorbed at complete coverage.

(b) readsorption after evacuation of the sample at the adsorption temperature.

(c) the value corresponds to that after an exposure to $5x10^8$ L at which point virtually all of the dose of nitrogen had been adsorbed.

(d) insufficient data.

(iii) The capacity to adsorb nitrogen (both as initial rates and coverage after an exposure of 10^{10} Langmuirs) passes through a maximum with alloy composition for the samples Fe(95)Co(5) and Fe(90)Ni(10) (the iron/nickel system at 773 K is an exception to this). Only for the samples Fe(95)Co(5) and Fe(90)Ni(10) is adsorption equilibrium possibly obtained since the coverage after 10^{10} L exposure is greater at 673 K than at 773 K.

6:3:2 Ammonia synthesis

Rates of ammonia synthesis were measured in a closed pyrex circulating system similar to that described by Ozaki, Taylor and Boudart[118], in which ammonia was removed by liquid nitrogen traps and net synthesis rates were calculated from the resultant decrease in volume at constant pressure.

In Figure 6:5 are Arrhenius plots for the synthesis of ammonia over two different catalysts using 700 torr of a 3/1, hydrogen/nitrogen mixture and a fixed flow rate of 6 $cm^3\ s^{-1}$. The units of the ordinate are percentage of ammonia in the gas leaving the catalyst bed, which is directly proportional to the observed reaction rate at a fixed flow rate. This illustrates clearly that as reaction temperature is increased above a certain temperature the observed rate of synthesis decreases due to equilibrium constraints imposed on the exit gas composition. All the other catalysts display this general behaviour, with differences in catalytic activity apparent only in region B (Figure 6:5) while in region A the data is superimposable.

Since the purpose of the study was to investigate the effect of alloying and not to make a detailed kinetic analysis, all catalysts were examined under a standard set of conditions viz. a flow rate of 6 $cm^3\ s^{-1}$ and total pressure of 700 torr. A summary of the kinetic

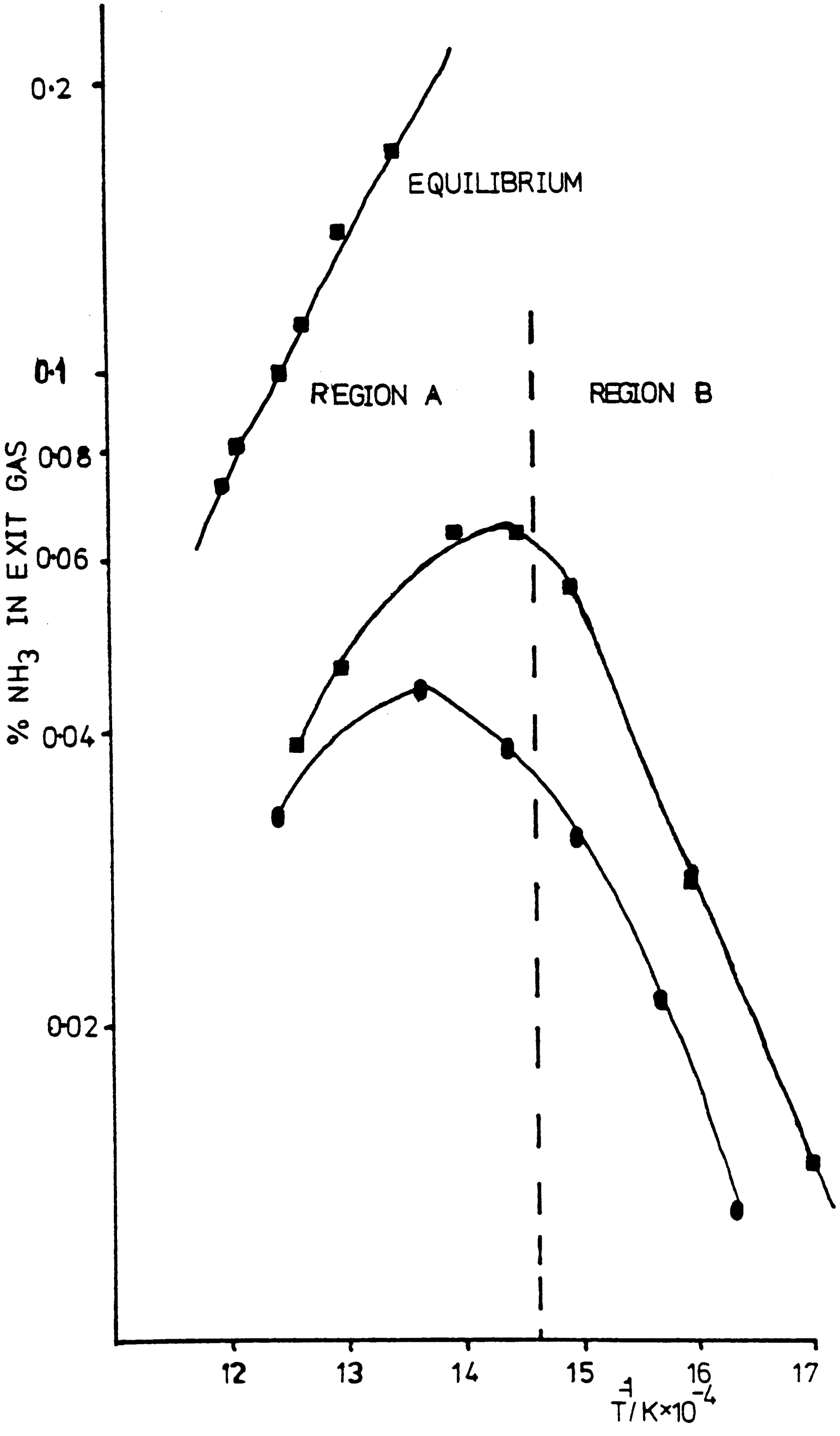

Figure 6:5 Arrhenius plots for ammonia synthesis on two different catalysts.

Table 6:11

Summary of ammonia synthesis experiments

Sample	Intrinsic Reaction Rate at 673 K/ molecules s^{-1} m^{-2} x 10^{15}	Activation Energy/ kJ mol^{-1}	log (A/molecules s^{-1} m^{-2})
Co	0.5	115±20	23.6
Fe(20)Co(80)	2.8	97±19	23.0
Fe(40)Co(60)	3.6	77±9	21.5
Fe(60)Co(40)	22.4	68±7	21.6
Fe(80)Co(20)*	22.9	79±5	22.5
Fe(90)Co(10)*	28.7	68±9	21.7
Fe(95)Co(5)*	36.1	65±5	21.6
Fe*	18.9	56±8	20.6
Fe(95)Ni(5)	27.8	63±10	21.3
Fe(90)Ni(10)	23.3	65±6	21.4
Fe(85)Ni(15)	32.9	62±9	21.3
Fe(80)Ni(20)	17.7	61±6	21.0
Fe(60)Ni(40)	11.2	84±5	22.6
Fe(30)Ni(70)	16.7	60±4	20.9
Ni	0.5	50±5	18.6

*Results of more than one experiment

parameters obtained from studies of all the catalysts is given in Table 6:11. As previously mentioned the data corresponds to that measured in region B.

6:4 Discussion of results

6:4:1 The relationship between nitrogen isotope equilibration nitrogen chemisorption and ammonia synthesis

It has already been pointed out that the slow step of both ammonia synthesis and nitrogen isotope equilibration is the chemisorption of nitrogen. Consequently, numerous comparisons of the rates of these reactions have been made, but with little agreement between different authors. The rate of nitrogen isotope equilibration has been found to be comparable with, slower than and possibly faster than the rate of ammonia synthesis. The variety of results probably arises from the widely differing experimental conditions employed to measure ammonia synthesis and nitrogen isotope equilibration.

The major differences lie in the pressures employed and the use of circulating or static systems. Ammonia synthesis is studied in a flow system at or above atmospheric pressure on account of the low equilibrium concentration of ammonia and the adverse effect on this of lowering the pressure. Nitrogen isotope equilibration, which requires a mass spectrometer and an expensive reactant, is studied at low pressures in a static system. Similarly, nitrogen chemisorption is investigated at or below one atmosphere pressure. Although corrections to allow for these differences can be made by the application of suitable kinetic expressions (where available) the extrapolations are long and corrections unreliable. The nitrogen pressures used in this research (0.5-1, 50 and 175 torr for nitrogen chemisorption, nitrogen isotope equilibration and ammonia synthesis), which are similar to those used by other investigators, illustrate the problem.

The allowance for the use of a flow system in ammonia synthesis is still more difficult since increasing the synthesis gas flow rate increases the reaction rate[118] by decreasing the inhibitory effect of ammonia, a situation which has no parallel in the other two processes. The use of a circulating system to measure nitrogen isotope equilibration is not a complete solution, nor is the effect of ammonia on nitrogen chemisorption or equilibration readily determined since ammonia would rapidly decompose to immeasurably low levels unless high nitrogen pressures were used.

The difference in reaction temperature necessary to avoid the close approach to equilibrium in ammonia synthesis at higher temperatures, (ca. >773 K), and that required to measure rates of nitrogen isotope equilibration are more easily corrected for via. the Arrhenius equation. However, large differences in the apparent activation energies (the values of 171 and 56 kJ mol^{-1} found in this study over iron are comparable with literature values[75]) can result in different comparisons at different temperatures.

In addition to variations in the experimental parameters, a number of other factors inherent to the processes themselves must be taken into consideration before drawing conclusions from the comparisons. Firstly, although all three processes involve the chemisorption of nitrogen, the nature of the surface on which adsorption occurs is different in each case. During nitrogen chemisorption the surface is initially bare but builds up a layer of surface adsorbent with time. Evidence indicates that as the surface coverage of nitrogen increases the heat of adsorption decreases and the activation energy of adsorption increases. The rate of adsorption decreases as adsorption progresses (Figure 6:3) and this also accords with the fact that for some samples adsorption becomes immeasurably slow before equilibrium is reached, an observation also made by Ertl[77] for the individual crystal faces of iron. Ammonia

synthesis and nitrogen isotope equilibration, are, such that, under a given set of conditions, the surface coverage with nitrogen reaches a constant steady state value. Since the rate of adsorption varies with surface coverage and is the slow step for both reactions, differences in the steady state surface coverage will be reflected by differences in reaction rate under otherwise similar experimental conditions.

Such differences in nitrogen coverage could occur if the subsequent hydrogenation and desorption steps of ammonia synthesis were much faster than the recombination and desorption steps of nitrogen equilibration or if different types of adsorbed nitrogen were involved (e.g. if ammonia synthesis proceeded mainly by the hydrogenation of adsorbed nitrogen molecules while adsorbed atoms were the required intermediate for equilibration). The dependence of adsorption rate upon surface coverage provides an explanation for the large observed differences in the temperature dependences of ammonia synthesis and nitrogen isotope equilibration already noted.

Secondly while all three processes involve nitrogen, ammonia synthesis also requires the presence of hydrogen. The influence of hydrogen on the chemisorption of nitrogen has not been carefully studied but it appears[39] that the presence of hydrogen accelerates the rate of adsorption on iron catalysts promoted by K_2O, presumably due to the formation of such species as -NH- and $-NH_2$. There is consequently a problem in comparing rates of nitrogen adsorption measured in the absence of hydrogen directly with rates of ammonia synthesis even when similar conditions of temperature and pressure are used.

The effect of hydrogen on the rate of nitrogen isotope equilibration has been a subject of much dispute. Earlier workers[65] found that the presence of hydrogen produced an acceleration in the equilibration rate. Later workers[68] found no such acceleration and suggested that any effect was due to further reduction of initially poorly reduced catalysts.

In this research, involving well reduced catalysts (see chapter seven), hydrogen had no effect on the equilibration rate (Table 6:8) for concentrations up to those found in ammonia synthesis (i.e. 3/1, H_2/N_2), in agreement with the latter view.

The rates of nitrogen chemisorption, nitrogen isotope equilibration and ammonia synthesis measured in this research over the single metals, iron, cobalt and nickel are compared in Table 6:12. In view of the many complications, as outlined above, involved in making such comparisons the similarity in the rates of the three processes over cobalt and nickel is surprisingly good, in agreement with the precept that nitrogen adsorption is indeed the slow step in all three reactions. The results over iron are marked by a considerably higher rate (whether corrected or uncorrected for pressure differences) for ammonia synthesis than nitrogen isotope equilibration. While this may be linked with the steady state coverage during reaction (e.g. if the iron surface had a high degree of heterogeneity) the problems inherent in making these comparisons mean that no definite mechanistic conclusions should be drawn.

Nevertheless, despite the difficulties of making quantitative rate comparisons a very good qualitative agreement is found for the pattern of intrinsic reaction rate with alloy composition between the three processes. Consequently, the maximum in intrinsic reaction rate observed for nitrogen isotope equilibration over iron rich alloys containing small concentrations of cobalt or nickel is also reflected in ammonia synthesis (Figure 6:6 and Figure 6:7) and nitrogen chemisorption measurements (Table 6:10).

The occurrence of this maximum is significant even though the increase in activity is slight (being about a factor of two) for nitrogen isotope equilibration and ammonia synthesis. It could, for example, be argued that such increases might be specific to the reaction conditions employed and result from changes in the kinetic equations for nitrogen

Table 6:12

Comparison of the rates of nitrogen chemisorption, nitrogen isotope equilibration and ammonia synthesis at 673 K and 773 K

		Rates measured under experimental conditions/ 10^{14} molecules s^{-1} m^{-2}		Rates corrected to a standard nitrogen pressure of 175 torr[(a)]/10^{14} molecules s^{-1} m^{-2}		
SAMPLE	TEMPERATURE/ K	NITROGEN ADSORPTION - INITIAL RATE	NITROGEN EQUILIBRATION	AMMONIA SYNTHESIS	NITROGEN EQUILIBRATION	AMMONIA SYNTHESIS
Fe	673	7.6	0.6*	200	1.4	200
	773	25	32	690*	77	690
Co	673	0.2	1.1*	4.1	2.4	4.1
	773	1.4	30	69*	72	69
Ni	673	-[(b)]	0.8*	5.1	1.9	5.1
	773	20	8.9	17*	22	17

* these are extrapolated values, the remainder are as measured.

(a) nitrogen equilibration rates are converted using the measured pressure dependences

(b) no sensible assessment of these values can be made since the total amount adsorbed is at the limit of detection of the apparatus.

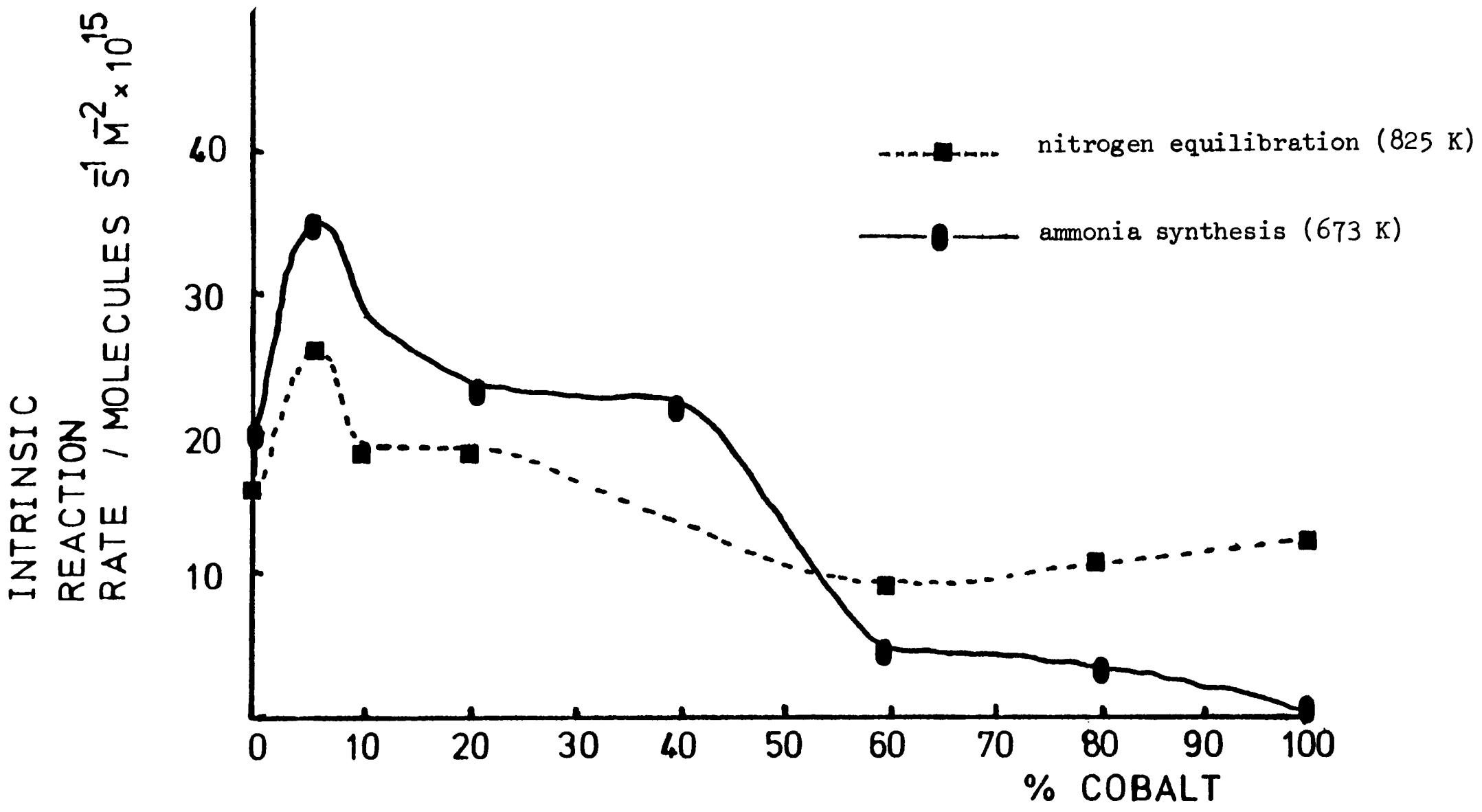

Figure 6:6 Variation of ammonia synthesis activity at 673 K and nitrogen equilibration activity at 825 K with alloy composition for iron-cobalt alloys.

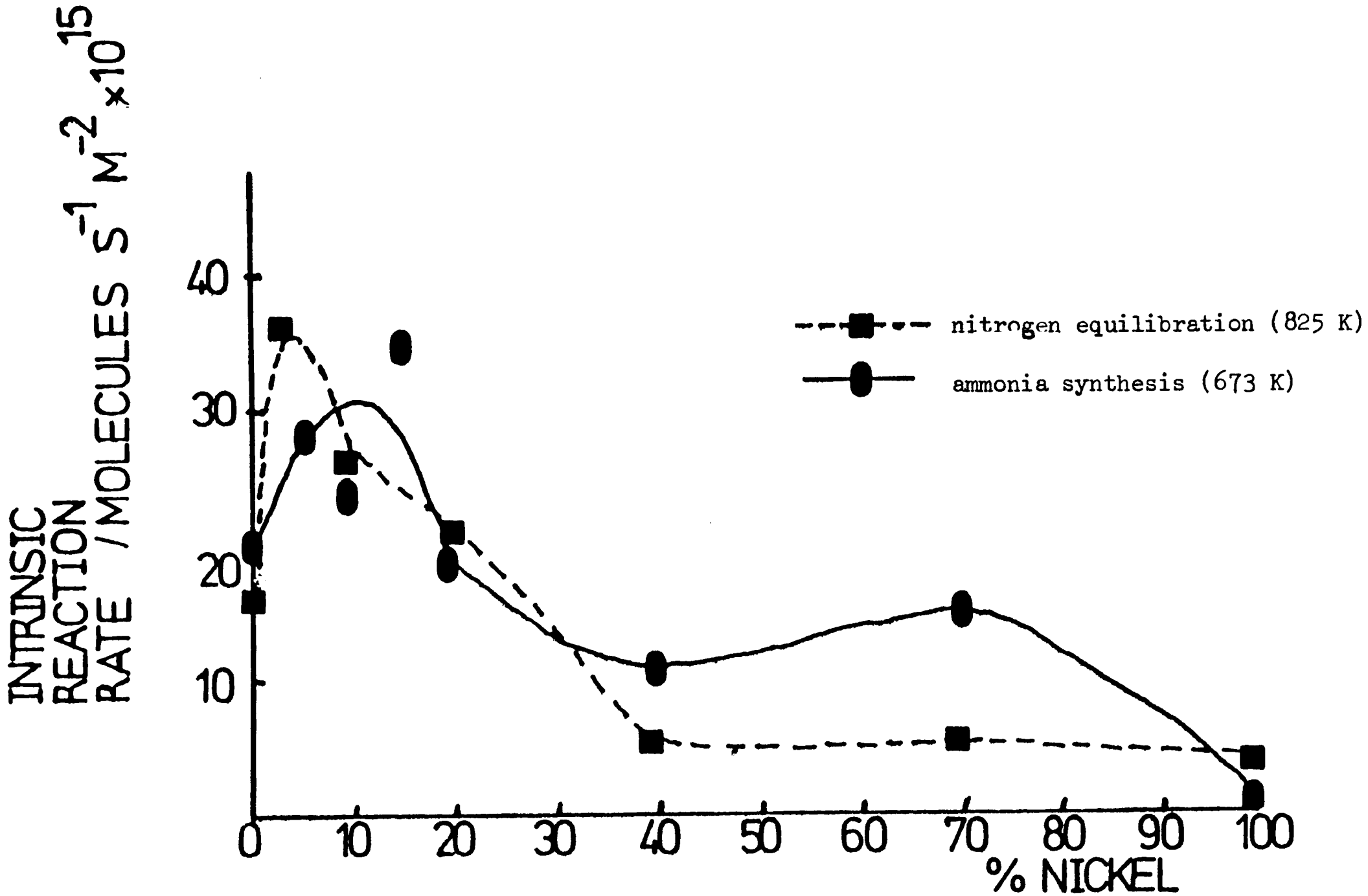

Figure 6:7 Variation of ammonia synthesis activity at 673 K and nitrogen equilibration activity at 823 K with alloy composition for iron-nickel alloys.

isotope equilibration and ammonia synthesis (the complexity of the factors governing the rates of these reactions have been discussed previously). However, it is not possible to dismiss the maximum observed for nitrogen chemisorption in this way and the qualitative agreement between the three techniques serves to establish its validity.

6:4:2 Significance of maxima in intrinsic reaction rate

The occurrence of this maxima is beyond doubt but it is not readily explained in terms of a simple electronic effect since additions of nickel do not have twice the effect of cobalt as expected from considerations of the average electron/atom ratio. In fact the positions of the two maxima in the case of ammonia synthesis imply that the opposite is true.

It is known (Figure 1:1) that an ordered (CsCl) phase, centred on the composition Fe(50)Co(50), has a boundary extending to Fe(75)Co(25) at 673 K. However, if the increased catalytic activity of iron-cobalt alloys is to be associated with this phase boundary then it must be markedly different in small catalyst particles either because of size effects or because of surface enrichment. In the iron-nickel alloys a body centred cubic phase extends to about 5% nickel at 853 K and this phase boundary is quite close to the activity maxima in that catalyst series. With the present alloys X-ray diffraction indicates that this phase boundary is not reached until 0.20 atomic fraction nickel and consequently it is unlikely to be the cause of the enhanced activity.

Cobalt and nickel oxides reduce at a lower temperature than haematite (6:1:2) and it is conceivable that this accelerates and eases the αFe_2O_3 reduction. If this is so, a cleaner iron surface may be formed but the lower activity of cobalt and nickel would dominate at higher concentrations. As the intrinsic activity is based on the measured area of the reduced metal this explanation seems unlikely.

The addition of cobalt or nickel to iron may affect the crystallisation of iron in such a way as to expose more specific crystal planes or some still more active centre in the iron crystallites. This possibility affords a particularly attractive explanation, since there is strong evidence that specific sites present only on the (111) face of iron are those principally involved both in nitrogen chemisorption[28] and ammonia synthesis[49]. This site, called a C_7 site, is an arrangement of seven iron atoms in the form of an "open pot". The presence of small amounts of cobalt or nickel may affect the surface structure of the iron such that a greater proportion of the surface area occurs as (111) faces than would otherwise be the case. Increasing levels of cobalt or nickel addition would produce an ultimate decrease in catalytic activity due to dilution of the iron content of the surface. The mechanism by which this might occur is speculative.

It is also possible to explain the maximum in activity by considering ensembles containing more than one type of atom in an essentially multifunctional approach. There are several possible situations:-

(i) If the catalytic activity is associated with iron ensembles alone it is unlikely that the maximum in intrinsic reaction rate (in a random alloy) can be accounted for by an increasing concentration of an active site containing a specific number of iron atoms.[12] A simple dilution of an active metal with a less active metal would result in a linear variation in reaction rate, between the values for the single metals (i.e. it is assumed that each metal atom acts as an independent active site and that surface and bulk compositions are identical). However, if activity does depend on the size of the ensemble there might be an optimum size, not too small not too large, which exhibits increased activity. This seems very

unlikely but it is possible that the strength of nitrogen chemisorption does depend on ensemble size.

(ii) Cobalt and nickel are known to chemisorb nitrogen very weakly (2:3) but it is possible that nitrogen weakly adsorbed on cobalt or nickel can accelerate the chemisorption of nitrogen on iron. The energetics of this situation are shown in Figure 6:8.

Figure 6:8

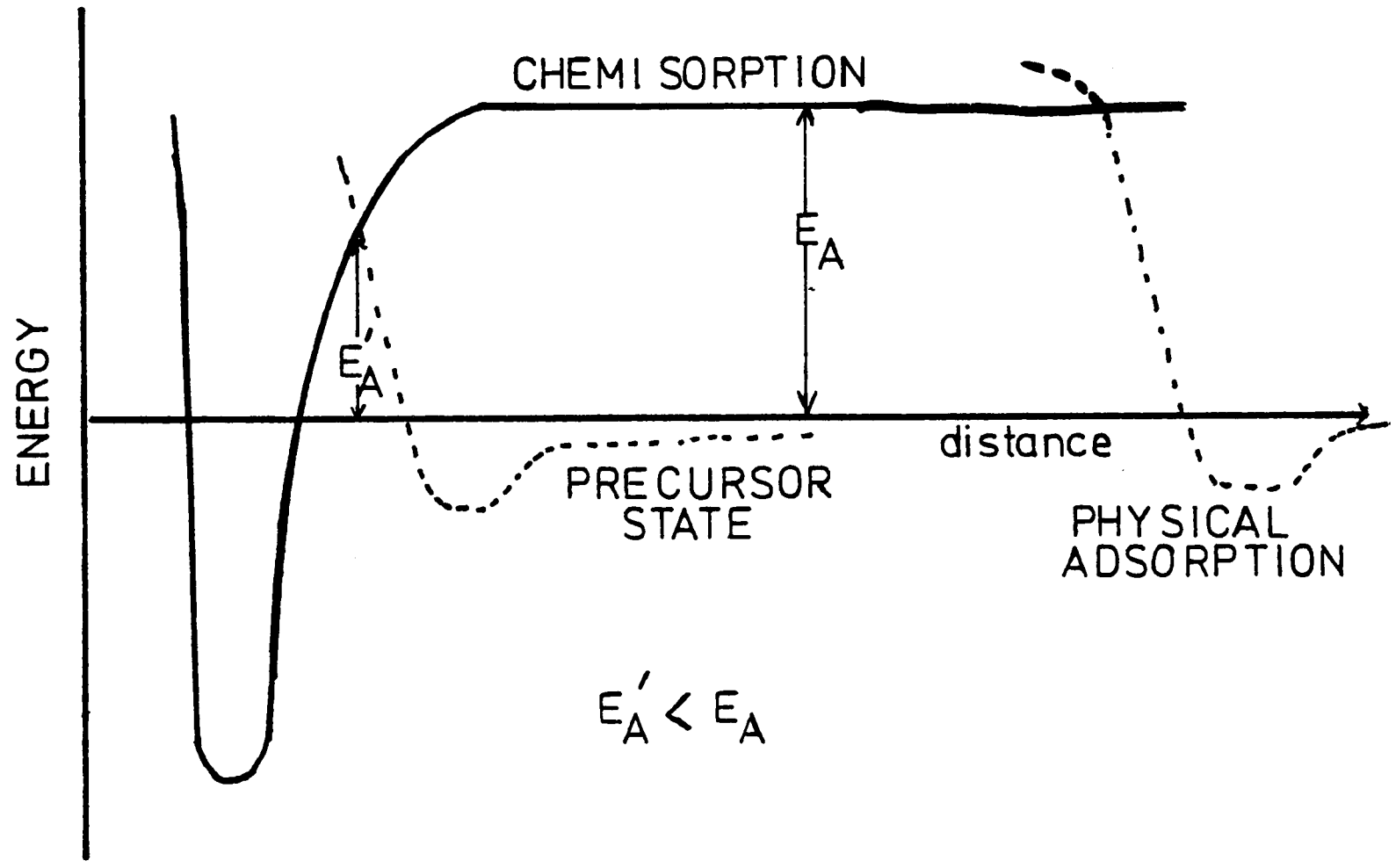

The use of a weakly bound precursor state fits the observed facts concerning nitrogen chemisorption on iron, cobalt and nickel and agrees with the current view that adsorption of nitrogen is rate controlling in ammonia synthesis.

In the case of ammonia synthesis it is possible to postulate other mechanisms to explain the enhanced activity.

(iii) Nitrogen is chemisorbed more efficiently by iron than cobalt or nickel whereas the reverse is true for hydrogen adsorption.

In the alloys of maximum activity nitrogen may be held in some suitable form on iron (perhaps N≡N, -N=N- or =N-N=) and hydrogen adatoms, needed for subsequent hydrogenation reactions, are provided by spill-over from nickel or cobalt. If this were so it would mean that the rate determining step in ammonia synthesis is not nitrogen chemisorption but the hydrogenation of adsorbed nitrogen species. Hydrogenation of adsorbed nitrogen has been suggested to be rate controlling in ammonia synthesis over reduced molybdenum dioxide[118].

(iv) The reverse of (iii) i.e. ready chemisorption of nitrogen on nickel or cobalt and spill-over of hydrogen from iron is not in accord with facts for unalloyed elements and consequently cannot explain enhanced activity.

(v) When considering conventional multifunctional catalysis only reaction intermediates which have a finite lifetime can be deployed. In the present situation these intermediates are di-imide (NH=NH) and hydrazine (NH_2-NH_2). It is possible that di-imide might form on iron ensembles and diffuse via the gas phase, to a cobalt or nickel ensemble where it is hydrogenated and hydrogenolysed to ammonia.

The reaction schemes outlined in (iii), (iv) and (v) require a large interface between the alloy components (maximum boundaries are at 50/50 composition) to have maximum efficiency. However, if allowance is made for the different efficiencies of iron and cobalt andnickel in their respective roles it is possible to rationalise why the observed enhancement does not occur with an alloy of equal composition.

These mechanistic considerations are continued in chapter seven in relation to variations of catalyst reduction temperature.

Chapter Seven

Nitrogen Isotope Equilibration and Related Processes on Iron/Cobalt and Iron/Nickel Alloys: Catalysts Reduced at Temperatures Above 853 K

The present chapter reports the results of an examination of the effect of variations of reduction temperature, in the range 853-1273 K, on the three processes of nitrogen isotope equilibration, ammonia synthesis and nitrogen chemisorption.

7:1 Characterisation of iron/cobalt and iron/nickel catalysts

7:1:1 Catalyst surface areas

The total metal surface areas of reduced (at 1073 K) iron/cobalt and iron/nickel catalysts, determined by room temperature chemisorption of carbon monoxide, are shown in Table 7:1.

Table 7:1

Total metal area of reduced catalysts

Iron Reduction Temperature/K	Metal Area[(a)(b)] / $m^2\ g^{-1}$	Alloy Reduced at 1073 K	Metal Area[(a)(b)] / $m^2\ g^{-1}$
853	4.2	Fe(95)Co(5)	0.3
923	4.7	Fe(90)Co(10)	0.2
973	3.5	Fe(80)Co(20)	0.2
1023	1.7	Fe(60)Co(40)	0.3
1073	0.7	Fe(90)Ni(10)	0.2
1173	0.3	Fe(80)Ni(20)	0.1
1273	0.1		

(a) expressed per gram of unreduced catalyst and assuming an area of $1.3 \times 10^{-19}\ m^2$ for each CO molecule

(b) the reproducibility of the area measurement is $\pm 8\%$ subject to an absolute uncertainty of $\pm 0.1\ m^2\ g^{-1}$.

The metal surface area of the iron sample decreases in a regular manner with increasing reduction temperature above 923 K and there is no evidence for any sudden discontinuity in the measured area values. The metal areas of the alloy samples are essentially equal as all measurements are subject to an absolute uncertainty of $\pm 0.1\ m^2\ g^{-1}$.

7:1:2 Thermogravimetric analysis

The reduction characteristics of iron and iron containing alloys were investigated by thermogravimetric analysis, using reduction temperatures as high as 1273 K. An experimental thermogram (plotted as the rate of mass loss against reduction temperature) for the iron catalyst is shown in Figure 7:1. Three major reduction processes, labelled A, B and C, are evident from examination of Figure 7:1. Process A, which occurs at approximately 500 K, corresponds to the transformation $\alpha Fe_2O_3 \rightarrow Fe_3O_4$ whereas Process B, which begins at about 700 K, is due to the main reduction i.e. $Fe_3O_4 \rightarrow FeO \rightarrow \alpha Fe$. Process C is very much smaller than either process A or B and only occurs after the reduction temperature is greater than 1000 K.

Process C, which is equivalent to a mass loss of 0.3 wt. % cannot be brought about by simply heating in a non reducing atmosphere: heating in nitrogen, after hydrogen reduction at 853 K, produced no mass loss. Consequently, it must be considered that process C is a discreet phenomenon arising from the reduction or partial reduction of a trace component of the sample.

Investigation of this discreet high temperature reduction (Process C) was extended to alloy catalysts. The occurrence of Process C is characterised by two parameters, namely the temperature

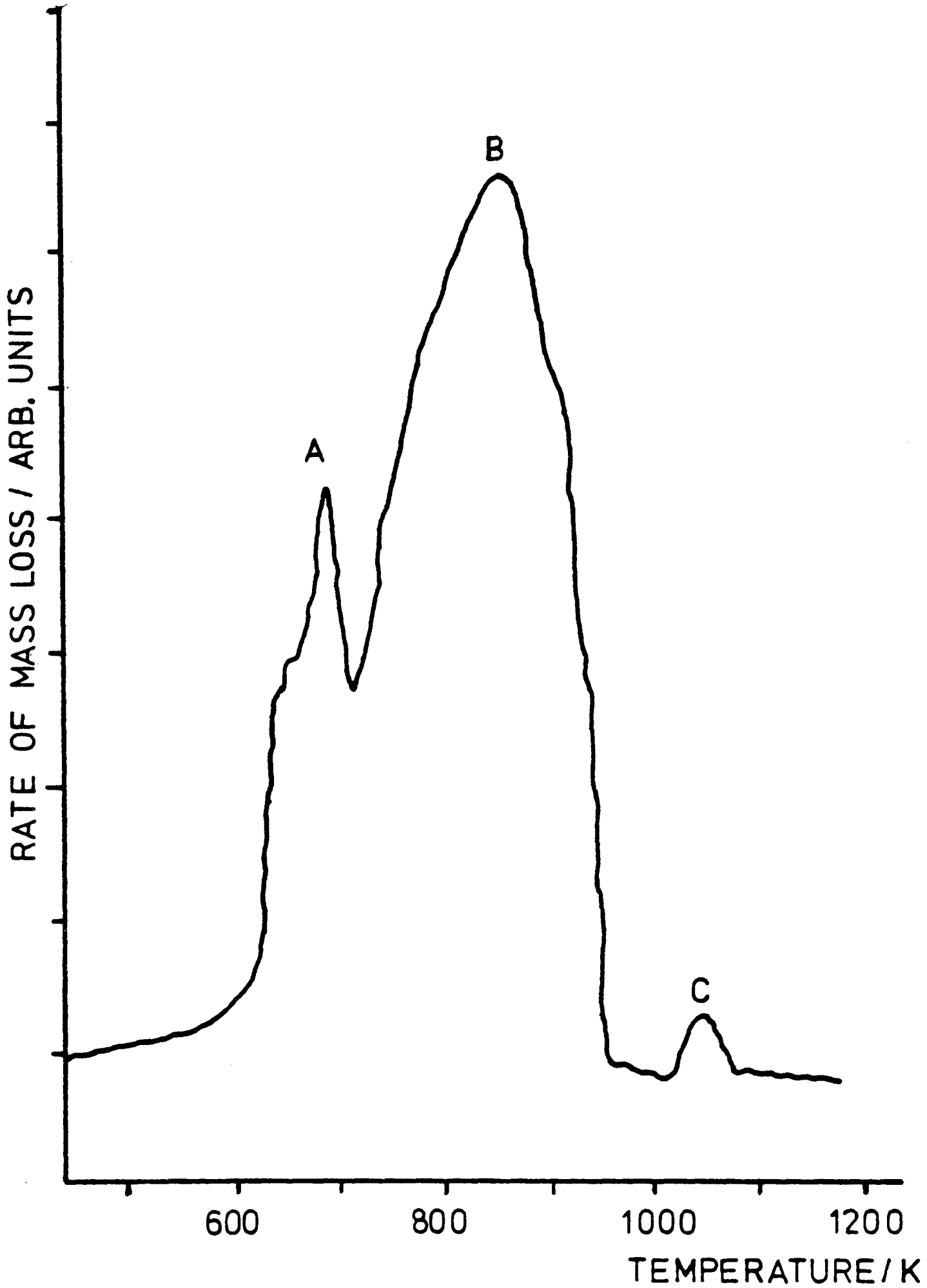

Figure 7:1 Reduction thermogram for iron.

at which it occurs and the magnitude of the mass loss. The results of investigations on alloy catalysts are summarised in Table 7:2.

Table 7:2

High temperature reduction processes in iron-cobalt-nickel catalysts

Sample	Temperature of Mass Loss/K	Magnitude of Mass Loss/ wt. % of initial mass
Ni	*	*
Fe(80)Ni(20)	*	*
Fe(90)Ni(10)	997	0.13
Fe(95)Ni(5)	1013	0.24
Fe	1038	0.31
Fe(90)Co(10)	1123	0.30
Fe(80)Co(20)	1163	0.30
Fe(60)Co(40)	1233	0.35

* no observable effect.

Increasing the nickel content of the alloy reduces the amount of material involved in Process C and decreases the temperature at which it occurs. Whereas for iron/cobalt alloys the amount of material involved in Process C remains approximately constant and the reduction temperature increases with increasing cobalt content.

7:1:3 X-ray diffractometry examination

Details of the X-ray analysis of alloys formed by reduction at 1073 K are given in Table 7:3.

Table 7:3

X-ray analysis of reduced (at 1073 K) iron/cobalt and iron/nickel catalysts

Sample	Phase Composition	Lattice Parameter[(a)]/A°
Fe(30)Ni(70)	b.c.c. iron-nickel alloy	*
	f.c.c. nickel-iron alloy	*
Fe(80)Ni(20)	b.c.c. iron-nickel alloy	2.8705
	trace of f.c.c. nickel-iron alloy	*
Fe(85)Ni(15)	b.c.c. iron-nickel alloy	2.8703
Fe(90)Ni(10)	b.c.c. iron-nickel alloy	2.8702
Fe	b.c.c. iron	2.8708
Fe(95)Co(5)	b.c.c. iron-cobalt alloy	2.8668
Fe(90)Co(10)	b.c.c. iron-cobalt alloy	2.8677

(a) experimental values accurate to ±0.0009 A°.

* value not determined.

Note: All samples have mean crystallite size greater than 800 A°.

It is valuable to compare the results presented in Table 7:3 with those for catalysts reduced at 853 K (6:1:3). Except for iron, increasing reduction temperature has no influence on the measured lattice parameter and both reduction temperatures result in complete alloy formation. However, higher reduction temperature does result in the disappearance of the unidentified trace phase observed for iron and iron rich alloys reduced at 853 K. The disappearance of this phase can be associated with the small component which is reduced at temperatures above 1000 K i.e. Process C of 7:1:1. Although insufficient information is available for an unequivocal identification of this phase, observed

diffraction peaks are consistent (but do not prove) with the presence of ferrous aluminate i.e. $FeAl_2O_4$.

7:2 Nitrogen isotope equilibration on catalysts reduced above 853 K

7:2:1 Activity versus reduction temperature for iron

The effect of varying the reduction temperature (in the range 853-1273 K) on the intrinsic activity of iron for nitrogen isotope equilibration catalysis was investigated. The results of this investigation, using a 4/1 mixture of nitrogen-14/nitrogen-15 at 50 torr total pressure in the temperature range 823-923 K, are presented in Table 7:4.

Table 7:4

Kinetic parameters for nitrogen isotope equilibration in the temperature range 823-923 K on iron catalysts reduced at temperatures greater than 853 K

Reduction Temperature /K	Intrinsic Rate[(a)] / 10^{15} molecules s^{-1} m^{-2}	log(A/ molecules s^{-1} m^{-2})	Activation Energy/ kJ mol^{-1}
853	16	27.1	171±12
973	21	26.7	164±10
1073	91	26.3	148±20
1173	90	27.9	173±9
1275	105	27.4	164±15

(a) At 823 K and a 4/1, nitrogen-14/nitrogen-15 mixture at 50 torr total pressure.

The major feature to note in Table 7:4 is that the intrinsic rate of reaction remains essentially constant up until a reduction temperature of 973 K whereafter a step change in the intrinsic reaction rate occurs. As intrinsic activity reverts to a constant value with reduction temperatures above 1073 K it would appear that the dramatic enhancement in activity results from a discreet phenomenon occurring in the temperature range 973-1073 K. rather than a continuous process. It is not possible to explain the increase in intrinsic activity by variations in metal surface area: metal surface area declines continuously whereas catalytic activity changes in a stepwise manner.

An iron catalyst which was reduced at 853 K and then heated <u>in vacuo</u> ($<10^{-5}$ torr for 18 hours) at 1075 K showed no such increase in intrinsic activity. The 1075 K evacuated catalyst had a comparable intrinsic activity to that of the 853 K reduced catalyst and consequently it is suggested that the enhanced activity is associated with the discreet reduction process occurring in the temperature range 1023-1073 K (7:1:2).

7:2:2 <u>Nitrogen isotope equilibration on alloys reduced at 1073 K</u>

The activities of iron rich alloys, reduced at 1073 K for 18 hours, were investigated using a standard 4/1 nitrogen-14/nitrogen-15 mixture at 50 torr total pressure in the temperature range 823-923 K. The results of this study are summarised in Table 7:5.

Table 7:5

Summary of catalytic activities of alloy catalysts reduced at 1073 K in the temperature range 823-923 K

Sample	Observed Rate (a)(b) / 10^{15} molecules s^{-1} g^{-1}	Intrinsic Rate (a) / 10^{15} molecules s^{-1} g^{-1}	$\log_{10}$ A/ molecules s^{-1} g^{-1}	Activation Energy/ kJ mol^{-1}
Fe(80)Ni(20)	0.4	3.6	24.3	138±13
Fe(90)Ni(10)	2	8.4	25.4	150±7
Fe	155	91	26.3	148±20
Fe(90)Co(10)	102	511	29.5	185±20
Fe(80)Co(20)	14	70.8	27.3	165±10
Fe(60)Co(40)	1	3.6	26.5	172±20

(a) reaction rate at 823 K and 4/1, nitrogen-14/nitrogen-15 mixture at 50 torr pressure.

(b) expressed per gram of unreduced catalyst.

It is useful to compare the results presented in Table 7:5 with those for the corresponding alloys formed by reduction at 853 K (6:2:1). As was noted for the 853 K reduced catalysts the apparent activation energy does not vary significantly with catalyst composition and is independent of reduction temperature. The intrinsic rate of reaction for iron and iron alloys containing up to 20% cobalt is increased by 1073 K reduction whereas the intrinsic activity of other catalysts does not vary appreciably with reduction temperature. The maximum in intrinsic activity observed for the 853 K reduced iron/cobalt alloys persists in the 1073 K reduced samples but that found with the 853 K reduced iron/nickel alloys does not.

7:3 Nitrogen chemisorption and ammonia synthesis on catalysts reduced at temperatures above 853 K

7:3:1 Nitrogen chemisorption

Isotherms for the adsorption of nitrogen, on iron reduced at 1073 K, are shown in Figure 7:2. The adsorption temperature was varied between 673 K and 973 K and the catalysts were evacuated to $<10^{-5}$ torr for 18 hours at 773 K or the adsorption temperature (whichever was higher) after reduction but prior to making adsorption measurements. At the lower adsorption temperatures (below 825 K) adsorption was very slow, taking three to four hours to achieve equilibrium. At the higher temperatures equilibrium was attained much more rapidly, taking only ten to fifteen minutes at 973 K.

A comparison of nitrogen adsorption at 673 K and 773 K (evacuation temperature 773 K) on iron catalysts reduced at 853 K and 1073 K (Figure 7:3) reveals that the catalyst reduced at 1073 K adsorbs nitrogen faster initially and to a greater surface coverage.

7:3:2 Ammonia synthesis

The results of an investigation of the influence of reduction temperature on the intrinsic rate of ammonia synthesis on iron are given in Table 7:6.

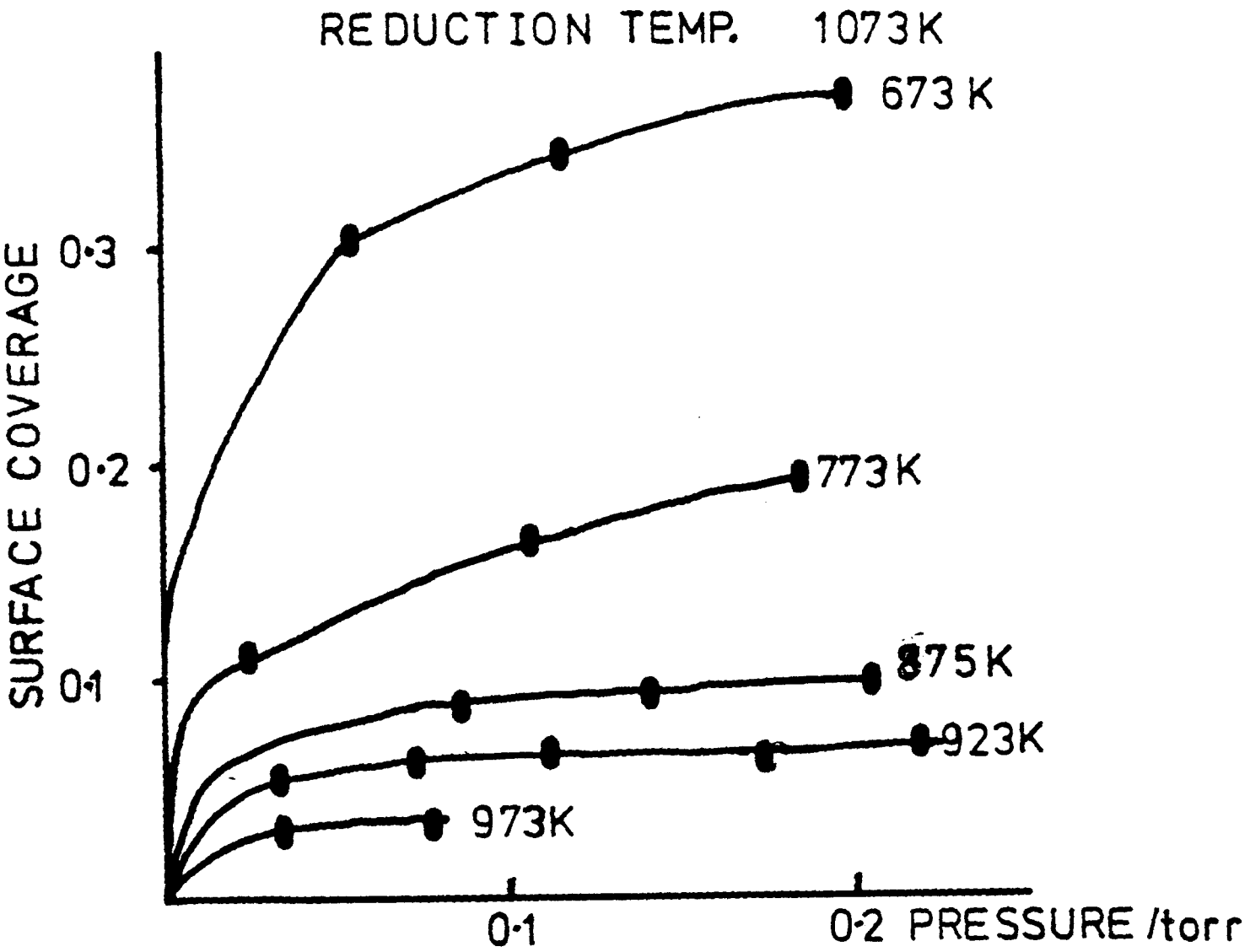

Figure 7:2 Isotherms for the adsorption of nitrogen on iron at various temperatures.

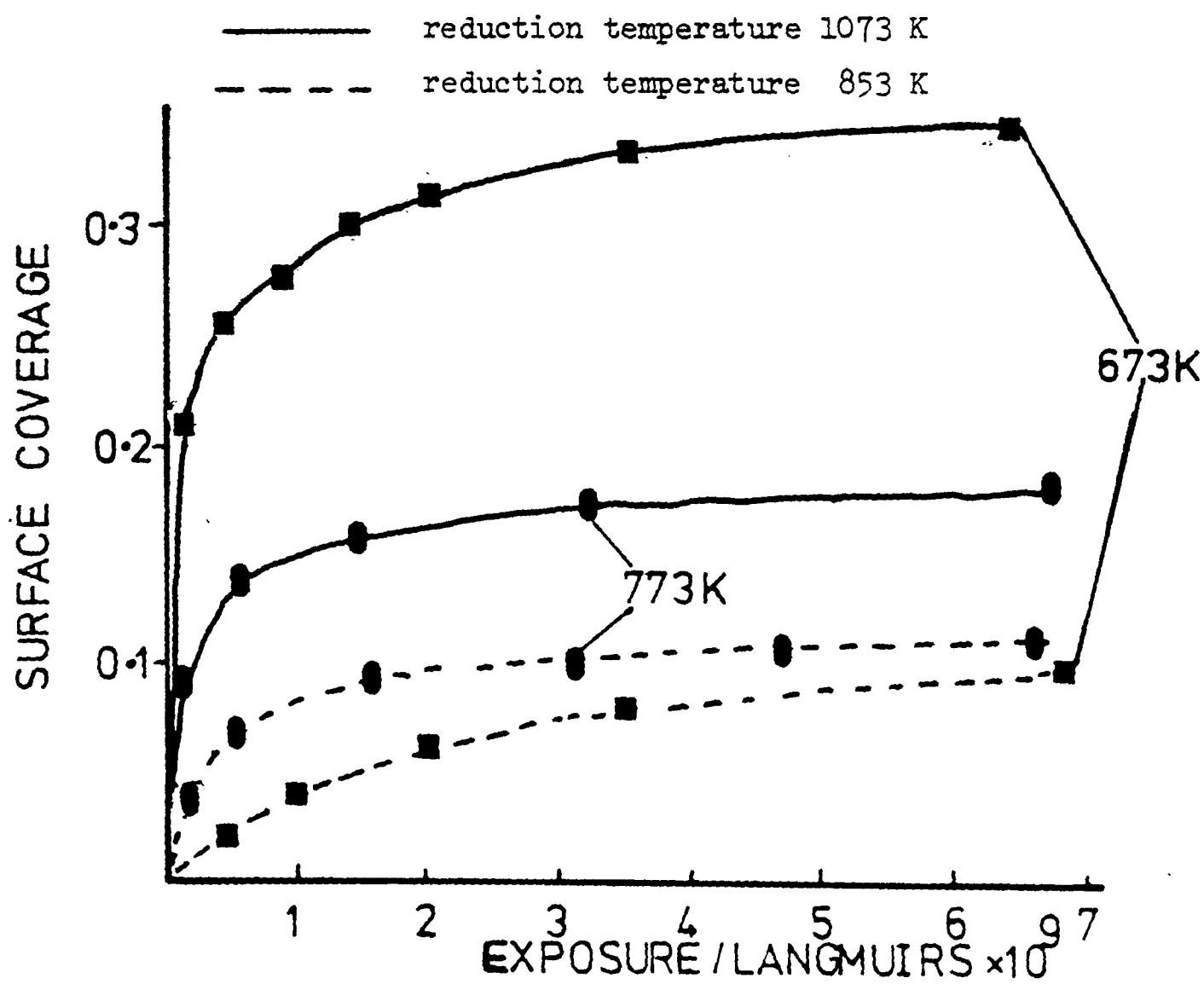

Figure 7:3 Adsorption of nitrogen on iron reduced at 1073 K and 853 K.

Table 7:6

Summary of ammonia synthesis data over the iron catalyst reduced at 853 K and above

Reduction Temperature / K	Intrinsic Rate[(a)] / 10^{16} molecules s^{-1} m^{-2}	$\log_{10}$(A / molecules s^{-1} m^{-2}	Activation Energy / kJ mol^{-1}
853	1.9	20.6	56±8
923	0.9	21.5	72±14
973	1.0	20.8	62±18
1023	1.7	20.5	54±15
1073	5.1	22.2	71±22
1173	22.4	22.6	68±13
1275	17.9	*	*

(a) reaction rate at 673 K and 3/1, hydrogen/nitrogen mixture at 700 torr total pressure and synthesis gas flow rate of 6 cm^3 s^{-1}.

* insufficient data.

As for nitrogen isotope equilibration, the intrinsic rate of ammonia synthesis undergoes a sudden step change as reduction temperature increases above 1023 K.

A summary of the results concerning ammonia synthesis on alloy catalysts reduced at 1073 K is presented in Table 7:7.

Table 7:7

Ammonia synthesis data for alloy catalysts reduced at 1073 K

Sample	Intrinsic Rate[(a)] / 10^{16} molecules s^{-1} m^{-2}	$\log_{10}$(A/ molecules s^{-1} m^{-2}	Activation Energy/ kJ mol^{-1}
Fe(80)Ni(20)	3.2	*	*
Fe(90)Ni(10)	10.7	22.1	64±9
Fe	5.1	22.2	71±22
Fe(95)Co(5)	14.4	21.7	59±11
Fe(90)Co(10)	16.8	22.8	72±7
Fe(80)Co(20)	14.1	21.1	50±14
Fe(60)Co(40)	0.7	*	*

(a) reaction rate at 673 K and 3/1, hydrogen/nitrogen mixture at 700 torr pressure and synthesis gas flow rate of 6 cm^3 s^{-1}.

* insufficient data.

Several features emerge from a comparison of the results given in Table 7:7 with those for 853 K reduced catalysts (6:3:2).

(i) The intrinsic activity of iron and iron alloys containing less than 40% nickel or cobalt is increased by reduction at 1073 K.

(ii) The intrinsic activities of alloys containing less than 40% iron are not affected by increasing reduction temperature.

(iii) The maxima in intrinsic rate observed for iron/cobalt and iron/nickel alloys reduced at 853 K is also evident in catalysts reduced at 1073 K.

7:4 Discussion

The variations in intrinsic activity with reduction temperature for nitrogen isotope equilibration and ammonia synthesis on iron are compared in Figure 7:4. For both reactions the constant intrinsic activity found for the reduction temperature range 853-1025 K confirms that the lower reduction temperature (853 K) used for investigations reported in chapter six is adequate for complete reduction of the iron oxide. At reduction temperatures above 1025 K the intrinsic activity increases dramatically for both reactions (and also for nitrogen chemisorption) and maintains an approximately constant value for reduction temperatures above 1150 K. This step change in activity coincides both with the occurrence of an additional, but minor, reduction process and the disappearance of weak lines from the X-ray diffraction patterns. The link between increased catalytic activity and this high temperature reduction (Process C, 7:1:2) is reinforced by the observation that simply heating the iron sample in vacuo (to 1025 K), after reduction at 853 K, does not produce an increase in catalytic activity.

In Figure 7:5 the intrinsic activities of iron-cobalt alloys reduced at 1073 K are compared with the activities of the corresponding alloys reduced at 853 K. The enhanced activity observed for iron is also evident for those alloy catalysts, reduced at 1073 K, containing less than 40% cobalt. For the catalyst containing about 40% cobalt the intrinsic activity has the same value as the corresponding sample reduced at 853 K. These observations are in agreement with the correlation between the enhanced activity and the occurrence of a high temperature reduction process. The temperature at which the latter occurs rises progressively with increasing cobalt content to 1233 K for a 40% cobalt concentration, a temperature well above the

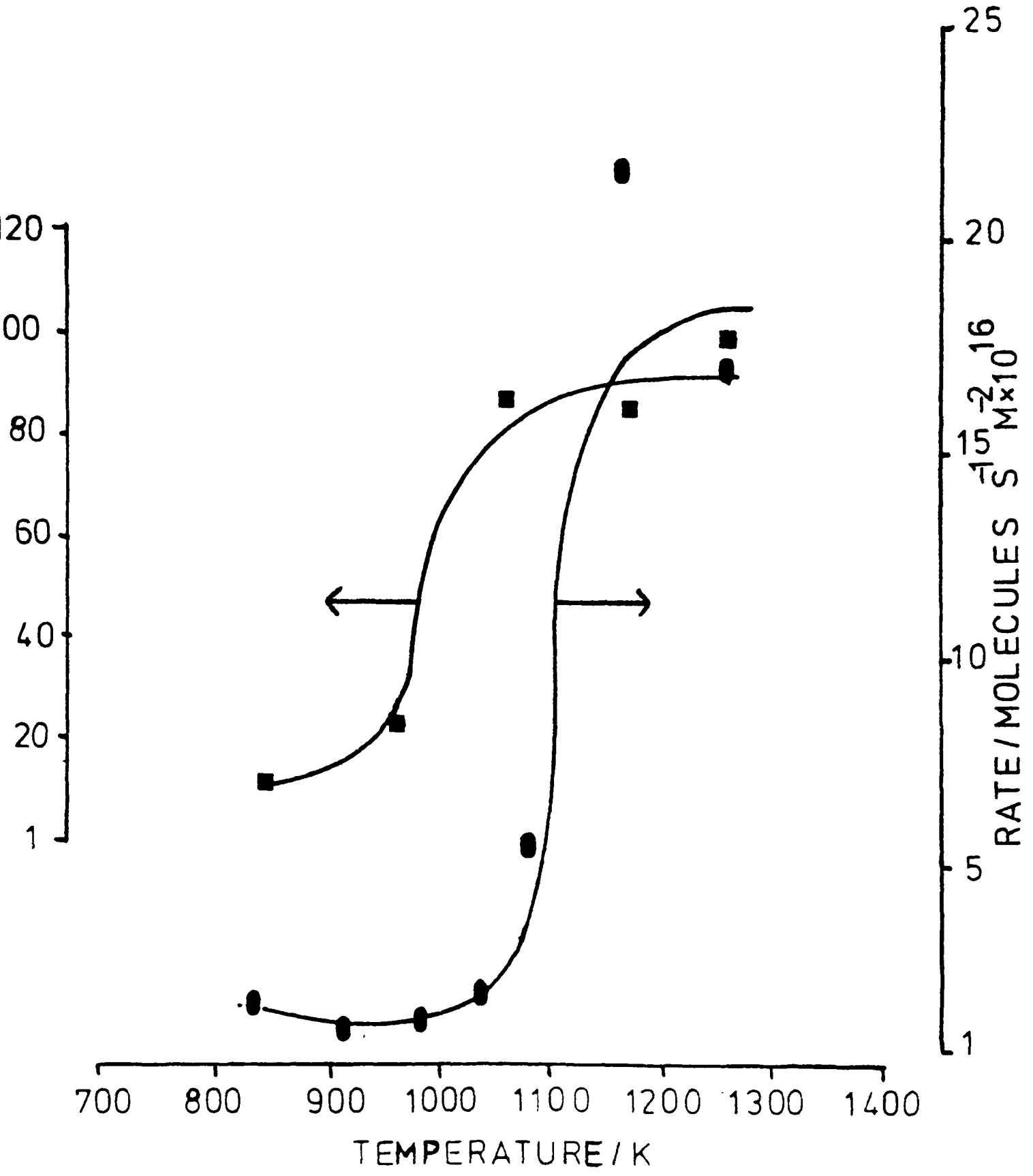

Figure 7:4 Variation of ammonia synthesis (●) activity at 673 K and nitrogen equilibration activity (■) at 823 K with reduction temperature for iron.

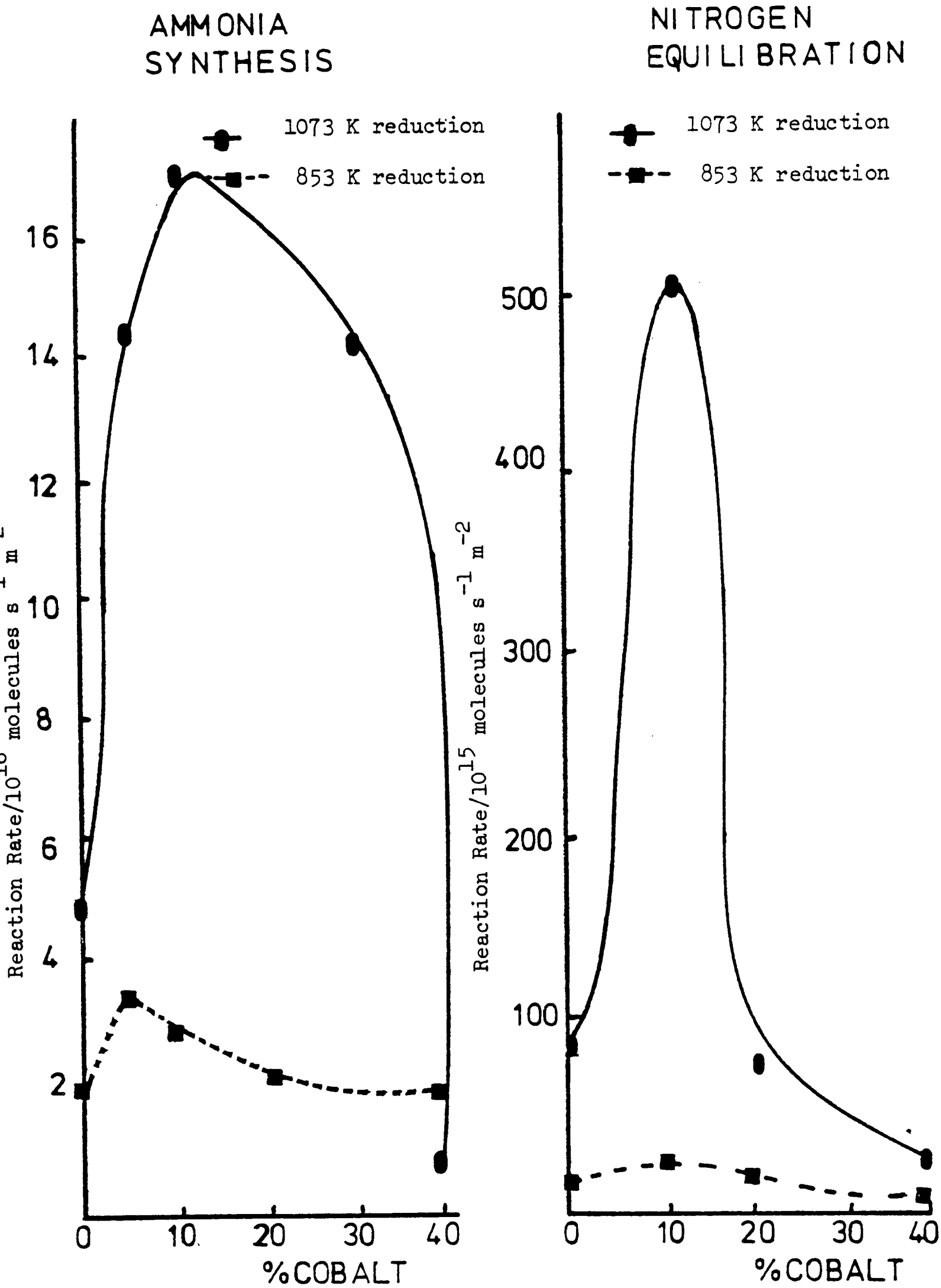

Figure 7:5 Variation of ammonia synthesis activity at 673 K and nitrogen isotope equilibration activity at 825 K with alloy composition for iron-cobalt alloys reduced at 853 K and 1073 K.

1073 K used to reduce the catalyst.

It is not obvious why the magnitude of the high temperature reduction process remains constant and the temperature at which it occurs increases with cobalt content. The experimental thermograms give no evidence for two species being present and the suggestion is that both iron and cobalt are involved in the species being reduced (e.g. a mixed aluminate $Fe_xCo_{1-x}Al_2O_4$?) with the cobalt making the material more resistant to reduction. The only relevant information found in the literature is that cobalt aluminate is more stable towards its formation from the oxides than either the iron or nickel analogues which are about the same[119].

A quantitative correlation between increased activity and high temperature reduction is not exact, since from Table 7:2 a reduction temperature of 1073 K would not be expected to result in a higher activity for alloys containing more than about 5% cobalt. In addition, the size of the increase in activity varies considerably for each catalyst although the mass loss associated with the high temperature reduction changes little. Such discrepancies can possibly be accounted for by the nature of the experimental measurements:

(a) the temperatures quoted in Table 7:2 were inferred from thermogravimetric measurements which involved a programmed temperature change whereas catalytic experiments followed a constant reduction temperature maintained for 18 hours.

(b) the metal surface areas of the alloys reduced at 1073 K are small (much smaller than for iron, Table 7:1) and consequently subject to a proportionally larger error. Although the errors are not large enough to nullify the observed increase in intrinsic activity for the alloys they can account for the greater part of the fluctuation in the magnitude of the increase.

In Figure 7:6 the intrinsic activities of iron-nickel alloys after reduction at 1073 K are compared with the corresponding alloys reduced at 853 K. The maximum in the intrinsic rate of nitrogen isotope equilibration observed for the 853 K reduced alloys does not persist in the 1073 K reduced catalysts. However, the maximum found for ammonia synthesis with 853 K reduced catalysts is also evident in 1073 K reduced samples. Only those alloys which display a high temperature mass loss (i.e. those containing less 20% nickel) exhibit enhanced ammonia synthesis activity.

Increasing concentrations of nickel decrease the magnitude of the high temperature mass loss without appreciably effecting the temperature at which it occurs. The decrease in the amount of reducible material on adding nickel suggests that if the high temperature reduction processes does involve the reduction of an aluminate that nickel aluminate, $NiAl_2O_4$, is not associated with the high temperature reduction process. Either nickel aluminate is irreducible up to 1233 K or it is reduced at much lower temperatures during the main oxide reduction. The suggestion that a $NiAl_2O_4$ species is not involved with the high temperature reduction process is supported by the constancy of the reduction temperature on adding nickel to the catalyst. That no $FeAl_2O_4$ is present with nickel contents of 20% or more further suggests that the $NiAl_2O_4$ species is more readily formed than $FeAl_2O_4$.

In view of the previous discussion it is therefore likely that the small (in total weight terms) reduction step occurring at temperatures above 1023 K is the direct cause of the observed increase in catalytic activity. The positive identification of the chemical species involved, in the reduction, is not easy although X-ray diffraction suggests that it may be ferrous aluminate. The presence of such a compound in the samples (which contain transition metal oxide

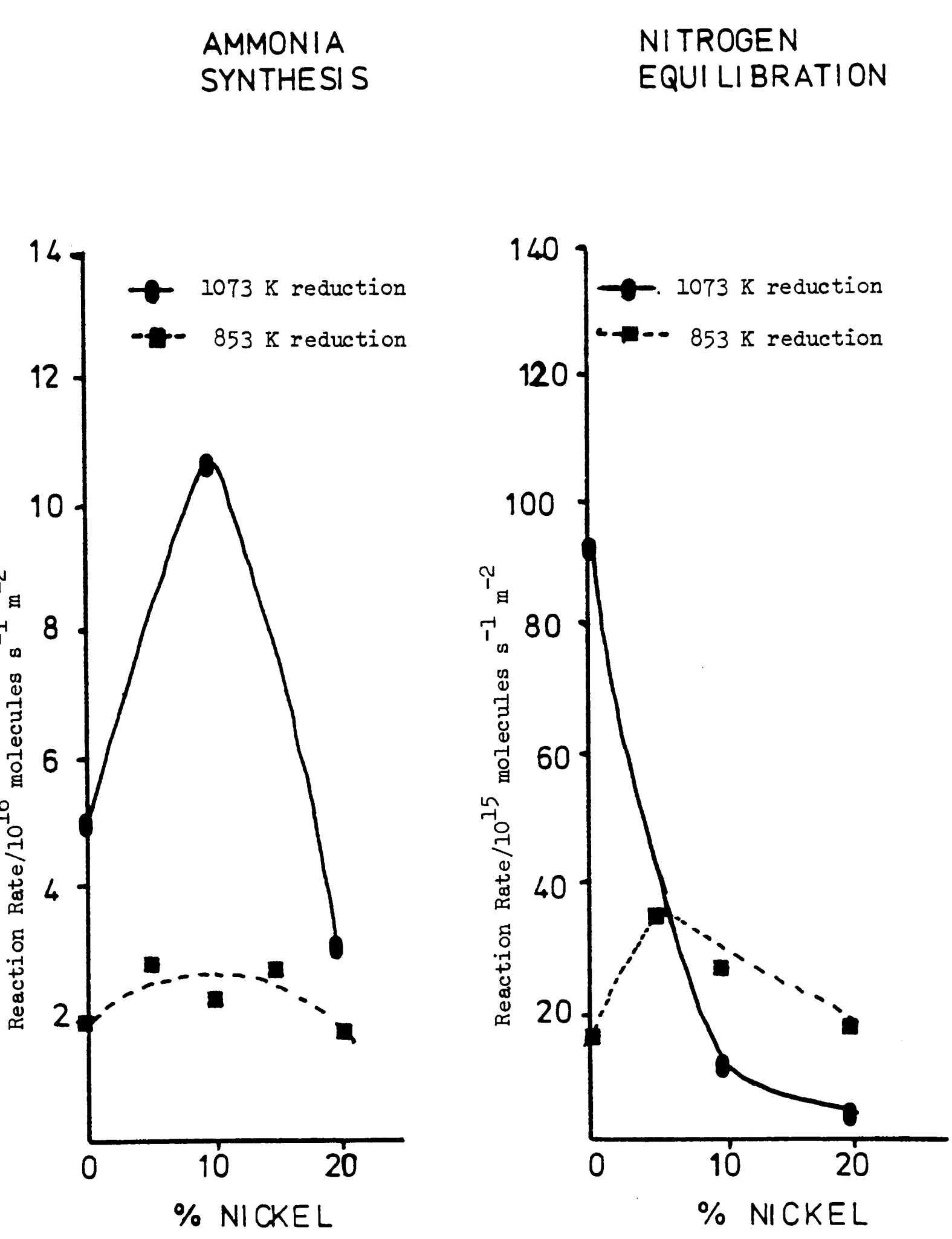

Figure 7:6 Variation of ammonia synthesis activity at 673 K and nitrogen isotope equilibration activity at 825 K with alloy composition for iron-nickel alloys reduced at 853 K and 1073 K.

and alumina before reduction) is likely and has been the subject of earlier investigations concerning ammonia synthesis catalysts[120,121].

Quantitatively the size of the mass losses (ca. 0.3% Table 7:2) are consistent with the amount of alumina present (if all the alumina were present as $FeAl_2O_4$ the mass loss corresponding to the process $FeAl_2O_4 \rightarrow Fe + Al_2O_3$ would be about 0.6%) in the catalysts. The different behaviours displayed by the two alloy systems may then be associated with differences in the thermodynamics of formation or the reducibilities of the corresponding cobalt and nickel aluminates. An unequivocal identification of the species involved must nevertheless await a more detailed investigation of the catalyst surface.

In seeking to explain the enhanced catalytic activity resulting from the high temperature reduction process, the small mass losses involved lead one to consider the formation of a catalyst promoter. It is known that small amounts of alkali act as a chemical promoter for nitrogen isotope equilibration (6:2:4) and ammonia synthesis reactions[122]. The mechanism is believed to involve donation of electrons from the more electronegative alkali metal into the iron and thence into the antibonding orbitals of the nitrogen molecule[117] which facilitates its dissociation and adsorption on the iron surface. A promotional explanation involving aluminium can be envisaged if one considers the high temperature reduction process important here not to be the reduction of ferrous aluminate to iron but the further reduction of alumina to aluminium metal. The partial reduction of alumina may result in the formation of a few chemisorbed aluminium atoms or of an iron/aluminium alloy which, since aluminium is more electronegative than iron, could facilitate the adsorption of nitrogen by a similar mechanism to that proposed for alkali metal. The reduction of alumina and the formation of a platinum/aluminium alloy under similar conditions

has been reported for a Pt/Al_2O_3 catalyst[123]. A major drawback to this explanation is that it is difficult to explain the dependence of the high temperature process on alloy composition. However, this dependence may be associated with the thermodynamics and kinetics of the reduction of individual aluminate species.

An alternative explanation is that the high temperature reduction produces a form of iron that is especially active for the catalytic reactions. It is difficult to reconcile this with the small mass losses involved. However, for iron the weight loss of 0.3% corresponds to the production of about $3x10^{20}$ iron atoms g^{-1} by the process $FeAl_2O_4 \rightarrow Fe + Al_2O_3$. This is equivalent to about fifty times the number of carbon monoxide molecules needed to form a monolayer on the metal surface of the iron catalyst reduced at 1073 K and is therefore sufficient to account for the considerable increase in activity without the requirement for a promotional effect.

In the previous chapter the high activity of a particular type of site (the C_7 site) present on the (111) crystal face of iron was discussed in detail. Such a surface resulting preferentially from the reduction of ferrous aluminate could also be the especially active form of iron required here, particularly since the spinel structure is pseudomorphic with Fe(111). Magnetite, Fe_3O_4, which also has a spinel structure is the preferred starting material for preparing industrial ammonia synthesis catalyst[48]. This explanation is very attractive not only because it links the effects of alloying and high temperature reduction observed in this research, but also it raises the possibility that all the adsorption and catalytic properties of the group VIII transition metals towards the nitrogen molecule are dominated by the occurrence of this one particular type of surface site.

Chapter Eight

Nitrogen Isotope Equilibration on Ruthenium/Rhodium Catalysts Reduced at 973 K

The results of an investigation of nitrogen isotope equilibration on ruthenium/rhodium catalysts are given in the present chapter.

8:1 Catalyst characterisation

The physical properties of ruthenium/rhodium catalysts, reduced at 973 K, are shown in Table 8:1.

Table 8:1

Physical properties of ruthenium/rhodium catalysts reduced at 973 K

Sample	Actual Composition[(a)] / % Ruthenium	X-ray Diffraction Analysis
Ru	100	ruthenium metal (300 A^{o})
Ru(90)Rh(10)	92	poorly crystalline hexagonal phase near ruthenium - major rhodium metal (200 A^{o}) - minor
Ru(80)Rh(20)	82	as for Ru(90)Rh(10)
Ru(70)Rh(30)	73	as for Ru(90)Rh(10)
Ru(60)Rh(40)	61	as for Ru(90)Rh(10)
Rh	0	rhodium metal (200 A^{o})

(a) ruthenium expressed as a percentage of total metal content and value accurate to $\pm 1\%$.

The X-ray diffraction analysis of the reduced catalysts gave no direct evidence for either ruthenium metal or ruthenium/rhodium solid solution. The hexagonal phase near ruthenium metal may contain some ruthenium/rhodium solid solution as less than three percent ruthenium/rhodium would have very little effect on the observed diffraction pattern. The low metal loading and the strong X-ray reflections from the α alumina support prohibited further characterisation of the metallic phase.

The metal areas of the reduced catalysts were found to be very small (in the case of ruthenium less than 0.1 $m^2\ g^{-1}$) and consequently near the limit of detection of the apparatus. As the measured metal areas are so small they are subject to a gross proportional error and because of this all catalytic activities are reported as observed activities (i.e. per unit mass of catalyst) and not as intrinsic activities (i.e. per unit metal area).

8:2 Catalytic results

The results of nitrogen isotope equilibration experiments in the temperature range 873-973 K using a 4/1, nitrogen-14/nitrogen-15 mixture at a total pressure of 50 torr are summarised in Table 8:2. Rates of reaction and activation energies were determined as described previously (5:3:5).

Table 8:2

Kinetic parameters for nitrogen isotope equilibration on ruthenium/rhodium catalysts in the temperature range 873-973 K

Sample	Observed Rate[(a)] / 10^{15} molecules s^{-1} g^{-1}	log(A/ molecules s^{-1} g^{-1})	Activation Energy/ kJ mol^{-1}
Ru	50.5 (600)[(b)]	25.0	146±18 (162)
Ru(90)Rh(10)	20.1	22.0	100±12
Ru(80)Rh(20)	8.7	22.8	121±6
Ru(70)Rh(30)	2.4	21.5	109±11
Ru(60)Rh(40)	<0.1	*	*
Rh	<0.01	*	*

(a) reaction rate at 923 K with 4/1, nitrogen-14/nitrogen-15 mixture at 50 torr total pressure and expressed per gram of catalyst used.

(b) ruthenium catalyst promoted by 0.3% sodium salt.

* insufficient data for accurate assignment.

The major features to notice in Table 8:2 are that the observed rate of nitrogen isotope equilibration rapidly declines with increasing rhodium concentration and that the observed activity and apparent activation energy for nitrogen isotope equilibration on ruthenium are increased by alkali promotion.

8:3 Discussion

Due to the high level of uncertainty associated with the accuracy of the measured catalyst total metal areas only the rates of nitrogen

isotope equilibration per unit mass of catalyst are considered. This means that observed differences in activity between catalyst samples may be partially due to individual catalysts having different surface areas. However, it is unlikely that total metal area varies by more than a factor of two between catalyst samples (see iron/cobalt/nickel system) and as the observed differences in catalytic activity between samples are larger than this it is probably the case that the observed activity (activity per unit mass of catalyst) reflects the intrinsic activity (activity per unit metal area). If this is so, comments made concerning the observed activity against catalyst composition pattern will be valid for the intrinsic activity against catalyst composition pattern.

The measured relative activities of ruthenium and rhodium are comparable to those which have been reported for potassium promoted ruthenium and rhodium supported on active carbon[81]. In both situations the catalytic efficiency of ruthenium is at least two orders of magnitude greater than that of rhodium. The large difference in activity between ruthenium and rhodium can be rationalised in terms of the metals ability to chemisorb nitrogen as atoms. Ruthenium is a Group $VIII_1$ element and is known to readily chemisorb nitrogen as atoms whereas rhodium, which is a Group $VIII_2$ element, does not readily chemisorb nitrogen.

The large increase in ruthenium catalytic efficiency after alkali promotion has been explained by previous workers in terms of electron transfer from alkali metal to ruthenium and thence into the antibonding orbitals of the nitrogen molecule. As the purpose of the present research was to investigate the influence of alloying the study of alkali promoted catalysts was limited to ruthenium.

The decline in catalytic activity for nitrogen isotope

equilibration (shown in Figure 8:1) for those catalysts containing increasing quantities of rhodium is significant as it cannot be explained by a simple dilution of an active metal (ruthenium) with a less active metal (rhodium). If dilution were responsible for the decline in activity a linear variation of reaction rate, between the values of the end members, would be expected (i.e. it is assumed that each metal atom acts as an independent active site and that no segregation occurs). It is more likely that the decline in activity is associated with a decrease in the number and type of a particular surface ensemble (see 1:1:3). Without knowledge of particular surface compositions and surface geometries it is impossible to identify which particular type of surface ensemble may be involved in the catalysis but the rapid fall off in catalytic activity suggests that it is a grouping of several ruthenium atoms.

Simple probability calculations concerning the number of groupings of n atoms of type A present in a random alloy AB indicate that the decrease in catalytic activity is consistent with the active equilibration site containing at least two and possibly as many as five ruthenium atoms. However, this analysis cannot be extended as the nature and extent of alloy formation is unknown.

As ruthenium and rhodium lie directly below iron and cobalt in the Periodic Table it is of interest to qualitatively compare the activity patterns obtained for the respective alloys. The shape of the two activity patterns is different: iron/cobalt alloys display a maximum but ruthenium/rhodium catalysts do not. Another difference between the two catalyst series is that iron/cobalt activities only vary by an order of magnitude whereas ruthenium is at least two orders of magnitude more active than rhodium. The latter observation is

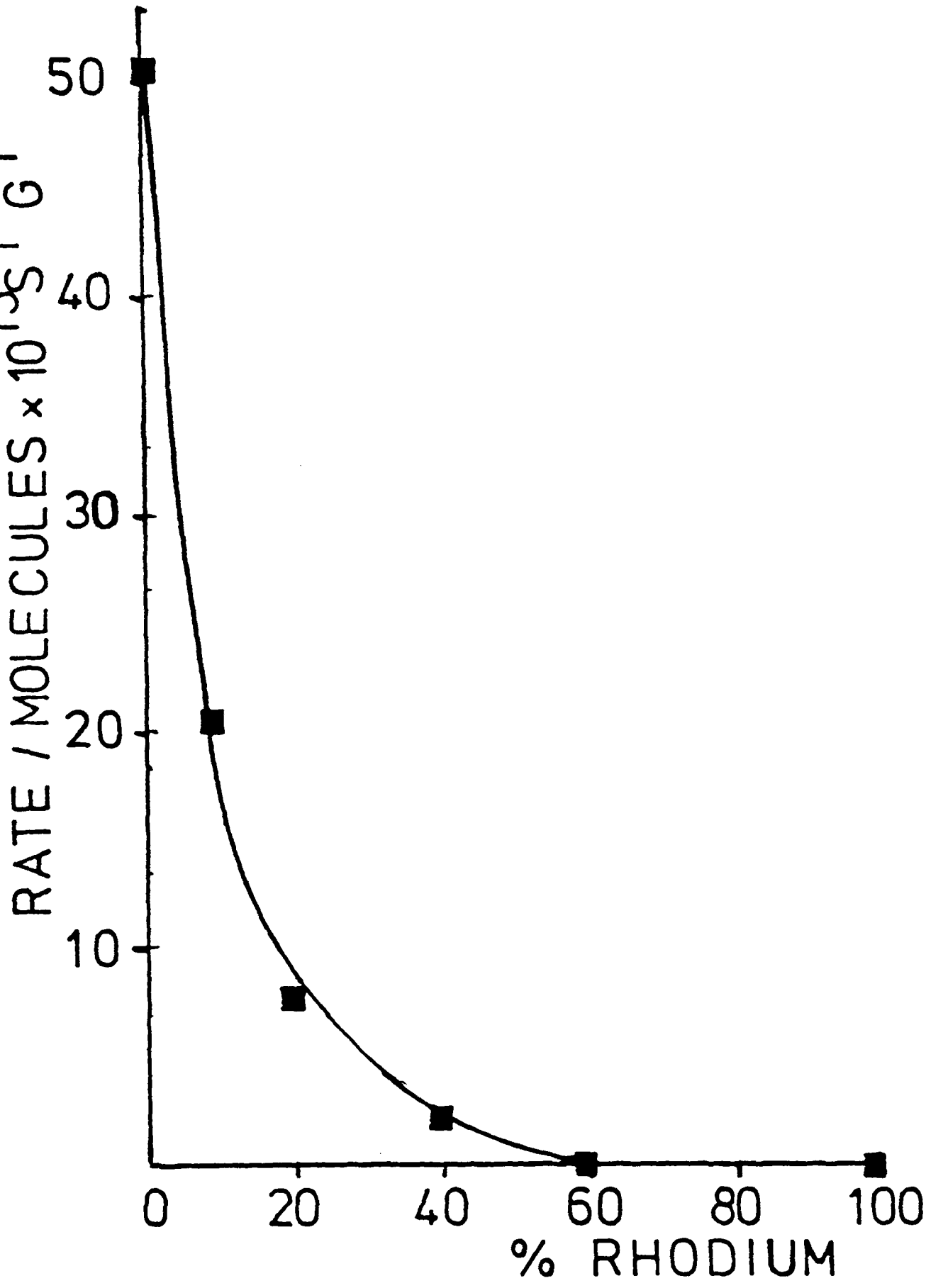

Figure 8:1 Variation of nitrogen isotope equilibration activity at 923 K with catalyst composition for ruthenium-rhodium catalysts.

probably the cause of the different activity patterns. Any possible beneficial influence of rhodium on the reaction rate (e.g. by mechanisms similar to those discussed in 6:4:2) is most likely counteracted by a very dramatic dilution of the active ruthenium phase. Nevertheless, it is possible that if catalysts containing very small additions of rhodium, perhaps ½ wt. %, were examined then an increase in activity corresponding to that found in the iron/cobalt system would occur.

Chapter Nine

Hydrogenation of Carbon Monoxide Over Group VIII Base Metal Alloys

The present chapter reviews the results of an investigation of the carbon monoxide hydrogenation reaction over iron-cobalt, iron-nickel and cobalt-nickel alloy catalysts. Explanations of the observed results are considered and a comparison is made between methanation and ammonia synthesis.

9:1 Catalyst characterisation

Details of the characterisation of the reduced (at 853 K) catalysts have been given previously (6:1) except those for cobalt-nickel catalysts which are given in Table 9:1.

Table 9:1

Physical properties of reduced (at 853 K) cobalt-nickel alloy catalysts

Sample	Actual Composition/ % Cobalt + 0.05	X-Ray Diffraction Analysis	Metal Area (a) $/m^2\ g^{-1}$
Co	100	α and β cobalt	8.5
Co(67)Ni(33)	65.3	f.c.c. Ni-Co alloy - major Co type phase - minor	12.3
Co(33)Ni(67)	32.7	f.c.c. Ni-Co alloy	10.0
Ni	0	f.c.c. nickel	8.1

(a) expressed per gram of unreduced catalyst and assuming an area of $1.3 \times 10^{-19}\ m^2$ for each CO molecule.

9:2 Carbon monoxide hydrogenation

As the purpose of the present research was to investigate the influence of alloying on catalytic processes, carbon monoxide hydrogenation experiments were carried out under a standard set of conditions i.e. a 3/1 mixture of hydrogen/carbon monoxide at 80 torr total pressure and a fixed reaction temperature of 473 K. Carbon monoxide cannot be detected by a flame ionisation detector and because of this reactant (i.e. CO) conversions are reported as amount of carbon monoxide converted to gas phase products and no allowance is made for carbon monoxide deposited on the catalyst surface.

9:2:1 Reaction character

(a) Single metals

The course of the carbon monoxide hydrogenation reaction on iron, cobalt and nickel is illustrated in Figures 9:1, 9:2 and 9:3 respectively. The main features to notice are:

(i) All catalysts produce methane as the major product (>70%) with smaller amounts of ethane, propane and n-butane.

(ii) With the iron catalyst reaction is limited to approximately 25% carbon monoxide converted to gaseous products during the time course of the experiment and there is no evidence for subsequent hydrogenolysis of the reaction products.

(iii) Cobalt gives complete carbon monoxide conversion to gaseous products within 100 minutes after which the reaction products are not subject to hydrogenolysis.

(iv) Nickel also gives complete reactant conversion to gaseous products within 100 minutes after which hydrogenolysis of the larger hydrocarbons converts all the products to methane.

(v) Repeat reactions on cobalt and nickel, after evacuation of the first reaction mixture, indicate no change in the activity of the catalysts.

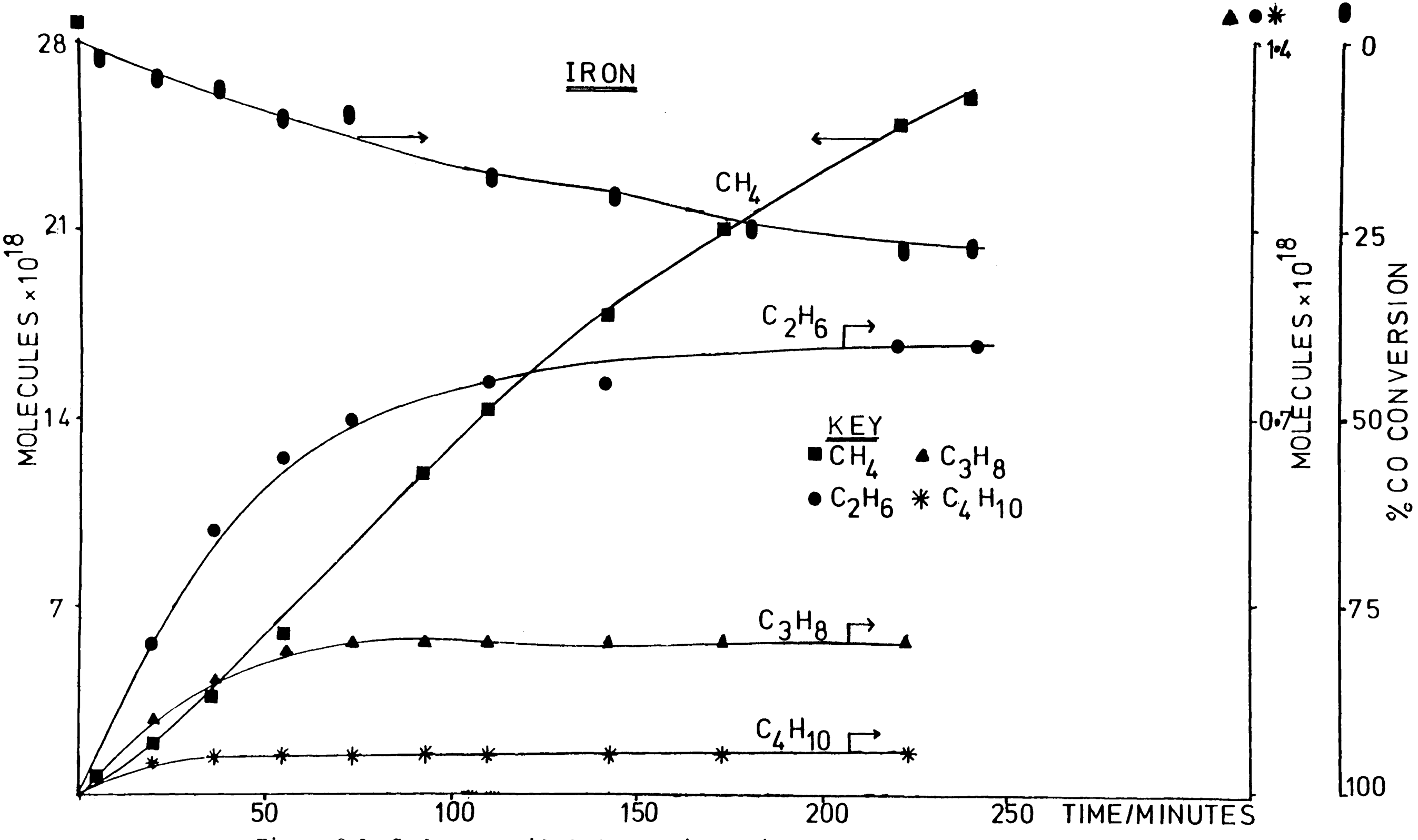

Figure 9:1 Carbon monoxide hydrogenation on iron.

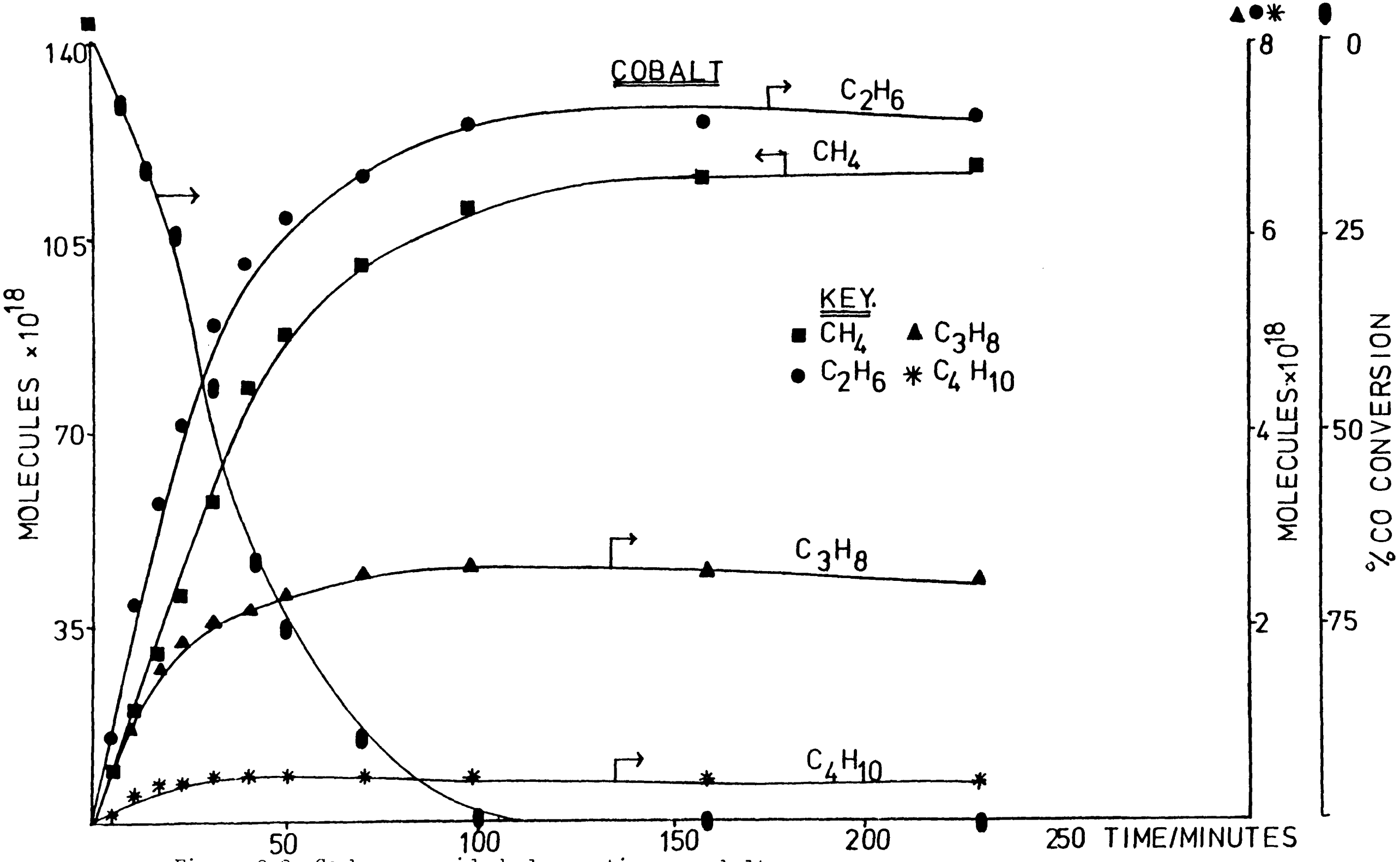

Figure 9:2 Carbon monoxide hydrogenation on cobalt.

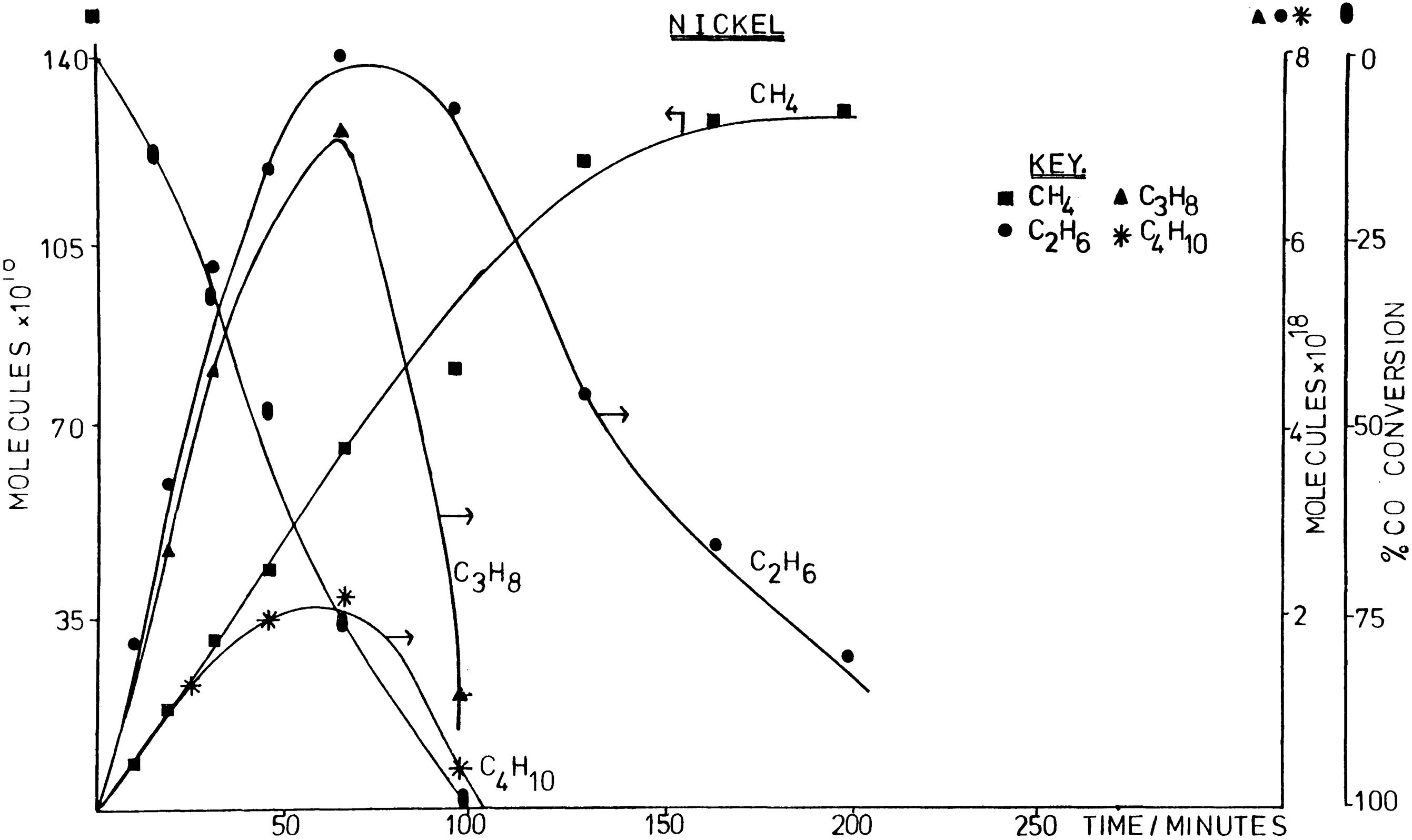

Figure 9:3 Carbon monoxide hydrogenation on nickel.

(b) Alloys

The general characteristics of the reaction over the alloy catalysts can be summarised as follows:-

(i) All alloys produce methane as the major product (>60%) with lesser amounts of ethane, propane and n-butane.

(ii) All iron-nickel alloys (except Fe(30)Ni(70)) give complete conversion of carbon monoxide to gas phase products and these products are then stable to secondary hydrogenolysis reactions.

(iii) Iron-cobalt alloys containing more than 50% iron display small (<30%) conversions of carbon monoxide to gas phase products after which reaction ceases and there is no evidence for secondary hydrogenolysis reactions. For iron-cobalt alloys containing less than 50% iron the reactant conversion to gas phase products increases to 40-60% before the reaction stops. Again the final products are stable towards hydrogenolysis reactions.

(iv) Cobalt-nickel alloys give complete carbon monoxide conversion to gas phase products followed by hydrogenolysis of the products to methane as observed for the nickel sample.

9:2:2 Initial reaction rates and initial product distributions

It is evident from 9:2:1 that the later stages of the reaction are severely influenced by hydrogenolysis and poisoning effects. In view of this, measured reaction rates are restricted to the initial stages of the reaction. For about the first 20-30 minutes of reaction approximately linear reaction rates (i.e. the rate of appearance) are observed for all products. It is therefore possible to classify the reaction by an initial overall rate and an initial product distribution (found by expressing individual product reaction rates as a percentage of the total). However, care must be taken when interpreting such rates due to problems associated with surface carbon laydown.

Iron-cobalt alloys

The total and individual initial intrinsic rates of reaction on iron-cobalt alloys are presented along with initial product distributions in Table 9:2. Reaction rates are expressed per unit metal area and refer to a temperature of 473 K with a 3/1 hydrogen/carbon monoxide reactant mixture at 80 torr total pressure and were determined as described in 5:4:4. The major features to note in Table 9:2 are that the total initial rate of reaction (i.e. total rate of appearance of gas phase products per unit time per unit area) decreases with increasing iron content and that there is a maximum in selectivity towards higher hydrocarbon production which occurs with an alloy containing approximately 40% iron.

Iron-nickel alloys

Initial rates of reaction and initial product distributions for iron-nickel alloys are given in Table 9:3. The results concerning the Fe(30)Ni(70) sample are the average results of three separate measurements. The initial product distribution shows a slight tendency towards methane production on iron rich alloys but the overall variation is small (±10%) if compared with that of iron-cobalt alloys (27%). The total intrinsic rate of reaction (i.e. total rate of appearance of gas phase products per unit time per unit area) exhibits a maximum for an alloy containing approximately 70% nickel.

Cobalt-nickel alloys

The initial rates of reaction and the initial product distributions for cobalt-nickel alloys are summarised in Table 9:4. There is a modest (15%) increase in selectivity towards methane production with increasing cobalt content but this is less than that observed

Table 9:2

IRON - COBALT ALLOYS

Summary of initial rates of reaction[a]

Sample	CH_4	C_2H_6	C_3H_8	nC_4H_{10}	Total
Fe	0.9	0.1	0.06	0.03	1.1
Fe(80)Co(20)	0.6	0.1	0.1	0.03	0.8
Fe(60)Co(40)	1.8	0.4	0.4	0.2	2.8
Fe(40)Co(60)	2.4	0.6	0.6	0.4	4.0
Fe(20)Co(80)	2.1	0.5	0.5	0.4	3.5
Fe(5)Co(95)	10.0	1.5	1.7	1.1	14.3
Co	16.0	1.5	0.7	0.2	18.4

[a] expressed in 10^{15} molecules s^{-1} m^{-2} at 473 K with a 3/1 mixture of H_2/CO at 80 torr total pressure

Summary of initial product distributions[b]

Sample	CH_4	C_2H_6	C_3H_8	nC_4H_{10}
Fe	81.8	9.1	5.5	2.7
Fe(80)	72.3	12.0	12.0	3.6
Fe(60)	64.3	14.3	14.3	7.2
Fe(40)	60.0	15.0	15.0	10.0
Fe(20)	60.0	14.3	14.3	11.4
Fe(5)	70.0	10.5	11.8	7.8
Co	87.0	8.1	3.8	1.1

[b] at 473 K with a 3/1 H_2/CO mixture at 80 torr total pressure

Table 9:3

IRON - NICKEL ALLOYS

Summary of initial rates of reaction[(a)]

Sample	CH_4	C_2H_6	C_3H_8	nC_4H_{10}	Total
Fe	0.90	0.10	0.06	0.03	1.10
Fe(90)Ni(10)	5.11	0.6	0.26	0.26	6.23
Fe(60)Ni(40)	6.36	0.88	0.35	0.35	7.94
Fe(45)Ni(55)	3.20	0.57	0.21	0.03	4.01
Fe(30)Ni(70)	26.7	5.60	1.95	0.42	34.67
Fe(15)Ni(85)	9.64	2.40	1.28	0.21	13.53
Ni	9.08	1.50	1.50	0.54	12.62

[(a)] expressed as 10^{15} molecules s^{-1} m^{-2} at 473 K with a 3/1 H_2/CO mixture at 80 torr total pressure

Summary of initial product distributions[(b)]

Sample	CH_4	C_2H_6	C_3H_8	nC_4H_{10}
Fe	81.8	9.1	5.5	2.7
Fe(90)Ni(10)	82.0	9.6	4.2	4.2
Fe(60)Ni(40)	80.1	11.1	4.4	4.4
Fe(45)Ni(55)	79.8	14.2	5.2	0.7
Fe(30)Ni(70)	77.1	16.1	5.6	1.2
Fe(15)Ni(85)	71.2	17.7	9.5	1.3
Ni	71.9	11.9	11.9	4.3

[(b)] at 473 K with a 3/1 H_2/CO mixture at 80 torr total pressure

Table 9:4

COBALT - NICKEL ALLOYS

Summary of initial rates of reaction[(a)]

Sample	CH_4	C_2H_6	C_3H_8	nC_4H_{10}	Total
Co	16.0	1.5	0.7	0.2	18.4
Co(67)Ni(33)	23.7	1.9	0.9	0.1	26.6
Co(33)Ni(67)	15.6	1.6	3.8	0.3	21.3
Ni	9.1	1.5	1.5	0.5	12.6

(a) expressed in 10^{15} molecules s^{-1} m^{-2} at 473 K with a 3/1 mixture of H_2/CO at 80 torr total pressure

Summary of initial product distributions[(b)]

Sample	CH_4	C_2H_6	C_3H_8	nC_4H_{10}
Co	87.0	8.1	3.8	1.1
Co(67)Ni(33)	89.1	7.1	3.4	3.8
Co(33)Ni(67)	73.2	7.5	0.8	1.4
Ni	71.9	11.9	11.9	4.3

(b) at 473 K with a 3/1 H_2/CO mixture at 80 torr total pressure

for the iron-cobalt system. The intrinsic initial reaction rate (i.e. total rate of appearance of gas phase products per unit time per unit area) shows a broad shallow maximum in activity centred around catalysts containing approximately equal proportions of cobalt and nickel.

9:2:3 High temperature reduction

The initial product distributions and initial intrinsic reaction rates of carbon monoxide hydrogenation on the iron catalyst reduced at 1073 K are compared with the corresponding rates found for 853 K reduced iron in Table 9:5.

Table 9:5

Effect of reduction temperature on the iron catalyst

	Initial product distributions[(a)]			
Reduction Temperature/K	CH_4	C_2H_6	C_3H_8	nC_4H_{10}
853	81.8	9.1	5.5	2.7
1073	76.9	11.0	11.0	1.1

	Initial intrinsic reaction rates[(a)]			
Reduction Temperature/K	CH_4	C_2H_6	C_3H_8	nC_4H_{10}
853	0.9	0.1	0.06	0.03
1073	0.7	0.1	0.1	0.01

(a) determined at 473 K with 3/1 H_2/CO mixture at 80 torr total pressure and reaction rate expressed as 10^{15} molecules s^{-1} m^{-2}.

As can be seen from Table 9:5 reducing the iron catalyst at a higher temperature (1073 K) has no significant influence on either the intrinsic rates of reaction or on the initial product distribution.

9:4 Carbon retention

The propensity of catalysts to retain surface carbon at both small and large carbon monoxide conversions was investigated following evacuation ($<10^{-5}$ torr for 2 min. at 473 K) of the reaction mixture, by reacting the surface with 80 torr of hydrogen at 473 K. Table 9:6 shows the amounts of carbon removable from catalysts at different carbon monoxide conversions. The major features of Table 9:6 are:-

(i) Iron retains a very large concentration (equivalent to 50% of the carbon monoxide initially present) of carbon on the surface. On hydrogenation, in addition to methane small quantities of ethane are also formed.

(ii) Cobalt retains very little surface carbon after complete reactant conversion but it maintains an appreciable quantity during the early stages of the reaction some of which can be hydrogenated to ethane as well as methane.

(iii) On nickel a significant amount of removable carbon is present on the surface during the early stages of the reaction whereas at complete carbon monoxide conversion it is either completely removed or converted to irremovable species.

(iv) Cobalt-nickel alloys behave similarly to nickel.

(v) Iron containing alloys over which the reaction stops at low carbon monoxide conversions (i.e. iron-cobalt alloys with greater than 50% iron) are characterised by low levels of removable carbon after cessation of reaction. However, the quantity of removable carbon does increase with increasing temperature (e.g. by 673 K 20% can be removed from the Co(20)Fe(80) sample).

(vi) Significant amounts of ethane and propane are removable from iron-cobalt alloys. These alloys also show an increased selectivity towards higher hydrocarbon production during reaction.

Table 9:6

Summary of carbon retention data

Sample	Total amount of hydrocarbon removed at 473 K as % of CO in reaction mixture	Amount of hydrocarbon removed as ethane or propane at 475 K as % of CO in reaction mixture
After 1% conversion[(a)]		
Fe	50	5 (ethane)
After 7.5% conversion		
Co(20)Fe(80)	7 → 20 (at 673 K)	12 (at 673 K)
Co(95)Fe(5)	9	6
Co	12	2
Ni	7	*
Ni(55)Fe(45)	5	*
Co(67)Ni(33)	5	*
After 35% conversion		
Co(95)Fe(5)	1 → 3 (at 673 K)	*
After 100% conversion		
Co(67)Ni(33)	0.4	*
Ni	*	*
Co	0.5	*

(a) conversion defined as percentage of initial carbon monoxide converted to gas phase products

* none observed

9:5 Discussion

In 4:2 various reaction mechanisms for the direct hydrogenation of carbon monoxide were discussed. The results of the present investigation, concerning carbon monoxide hydrogenation on alloys, can be rationalised by considering the reaction scheme outlined by Ponec and associates[110]. Before illustrating how this can be done it is worthwhile restating the basic postulates on which Ponec's mechanism is based:

(i) Carbon monoxide dissociates and is partially hydrogenated to CH_X.

(ii) CH_X grows into a longer chain by repeated CO insertion and partial hydrogenolysis (C_MH_N).

(iii) Chain growth is terminated by hydrogenation.

9:5:1 Fischer-Tropsch synthesis

Iron-cobalt alloys

The selectivity towards higher hydrocarbon production exhibits a maximum for those alloys containing approximately equal proportions of cobalt and iron (Figure 9:4).The occurrence of this maximum in higher hydrocarbon selectivity is quite reasonable and is what might be expected according to Ponec's mechanism for Fischer-Tropsch synthesis.

The heat of adsorption of carbon monoxide decreases[124] in the order iron>cobalt>nickel and consequently it can be assumed that there is an initial higher concentration of adsorbed carbide species, whether adsorbed CO or carbon, on iron than cobalt. The data in Table 9:6 also indicate this. Addition of cobalt to the catalyst provides a metal which is a well known carbon monoxide insertion catalyst e.g. in the use of cobalt in the OXO process[125]. Consequently,

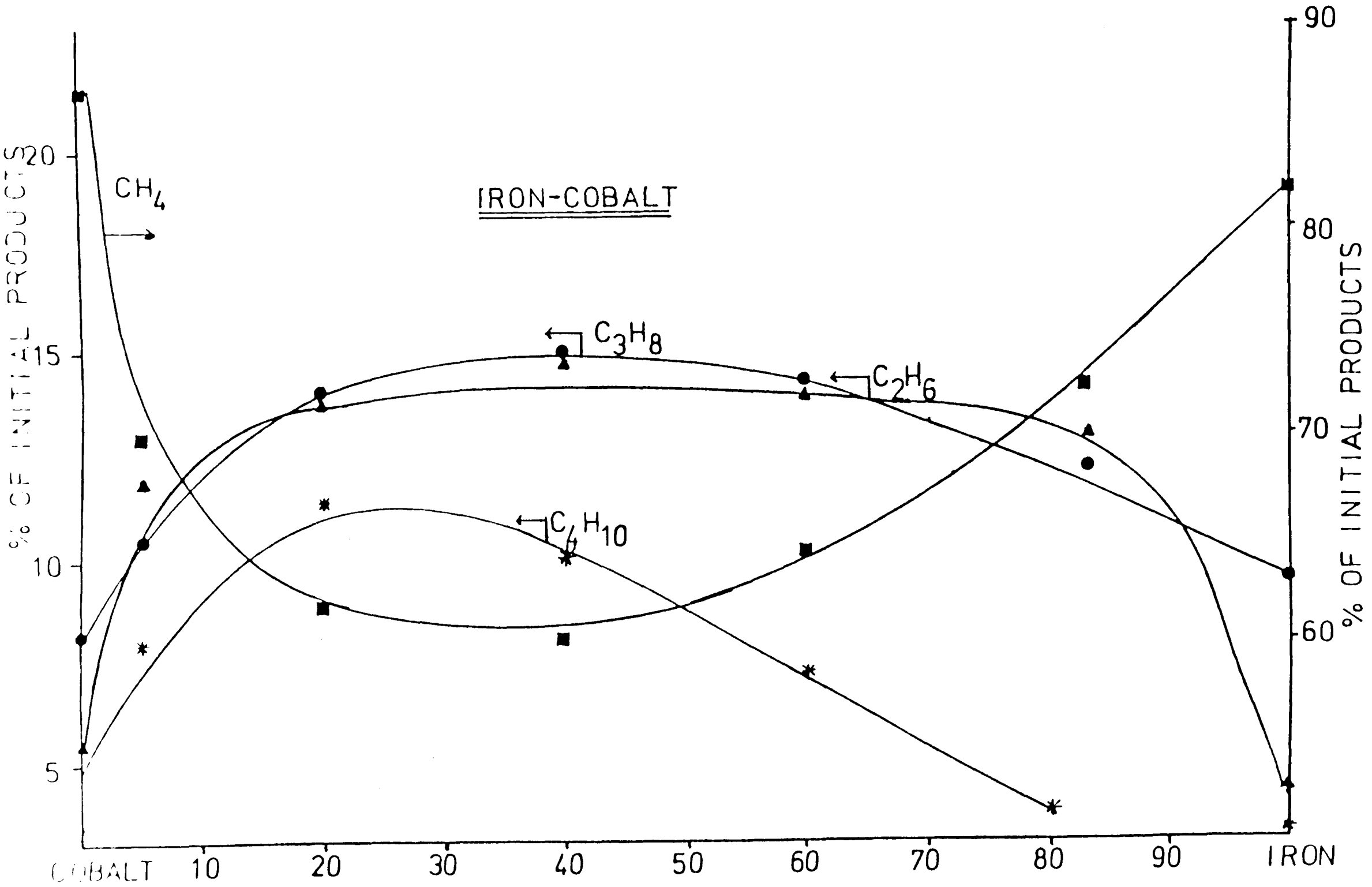

Figure 9:4 Initial product distributions on iron-cobalt alloys.

if Fischer-Tropsch synthesis does proceed by carbon monoxide insertion it would be expected that the selectivity towards higher hydrocarbons will increase with cobalt addition.

The selectivity towards higher hydrocarbons increases up until a catalyst composition of Fe(50)Co(50) and then declines. The decline in selectivity for those alloys containing more than 50% cobalt is explained by a decreasing concentration of surface CO species which are required for chain propagation. In line with this explanation the maximum in selectivity occurs at the equiatomic concentration i.e. where the maximum number of iron/cobalt boundaries occur.

Further support for the suggestion that Fischer-Tropsch synthesis proceeds by CO insertion and that iron-cobalt catalysts operate in a bi-functional manner is given by consideration of the quantities of removable carbon species present at different extents of reaction.

Iron has large quantities of removable carbon present at small (1%) reactant conversion to gas phase products and reaction proceeds relatively slowly. Alloys which contain more than 50% iron proceed to about 20% carbon monoxide conversion and then reaction ceases completely. Hydrogenation of surface carbon indicates that there is little removable carbon at the end of the reaction but the quantity which is removed does increase with temperature. Therefore, it is likely that any surface carbon is strongly bound and perhaps is polymeric in nature. It is likely that polymeric carbon will form readily on iron rich alloy catalysts as there will be a high concentration of surface carbon due to the iron and this may be readily polymerised by cobalt. Alloys which contain less than 50% iron proceed to a conversion of 60% carbon monoxide then stop. This

is in agreement with a lower surface carbon concentration and a consequently longer time required for a build up of a polymeric layer and cessation of reaction.

The presence of polymeric or large carbon number species on iron-cobalt alloys during reaction is shown by the observation that significant amounts of C_2 and C_3 hydrocarbons desorb on hydrogen treatment (see Table 9:6).

Cobalt-nickel alloys

Cobalt-nickel alloys show a slight increase in selectivity towards higher hydrocarbon production with increasing nickel content (Figure 9:5). This small increase may be associated with the relative hydrogenation activities of cobalt and nickel. Although cobalt would be expected to generate more higher hydrocarbons than nickel the overall rate of reaction will depend on final hydrogenation step (part (iii) of Ponec's mechanism) and if this is faster on nickel than cobalt it can explain why more higher hydrocarbons are formed on nickel.

Cobalt-nickel alloys have an appreciable coverage of removable surface carbon at low reactant conversions but negligible surface carbon remains after complete conversion of carbon monoxide to gas phase products. This observation is consistent with the requirement that iron is needed to form stable polymeric carbon and if iron is replaced by nickel surface carbon is rapidly removed by subsequent hydrogenation reactions. However, the possibility that polymeric species are formed by nickel and are then rapidly the subject of hydrogenolysis reactions cannot be discounted as this would also account for the absence of polymeric residues.

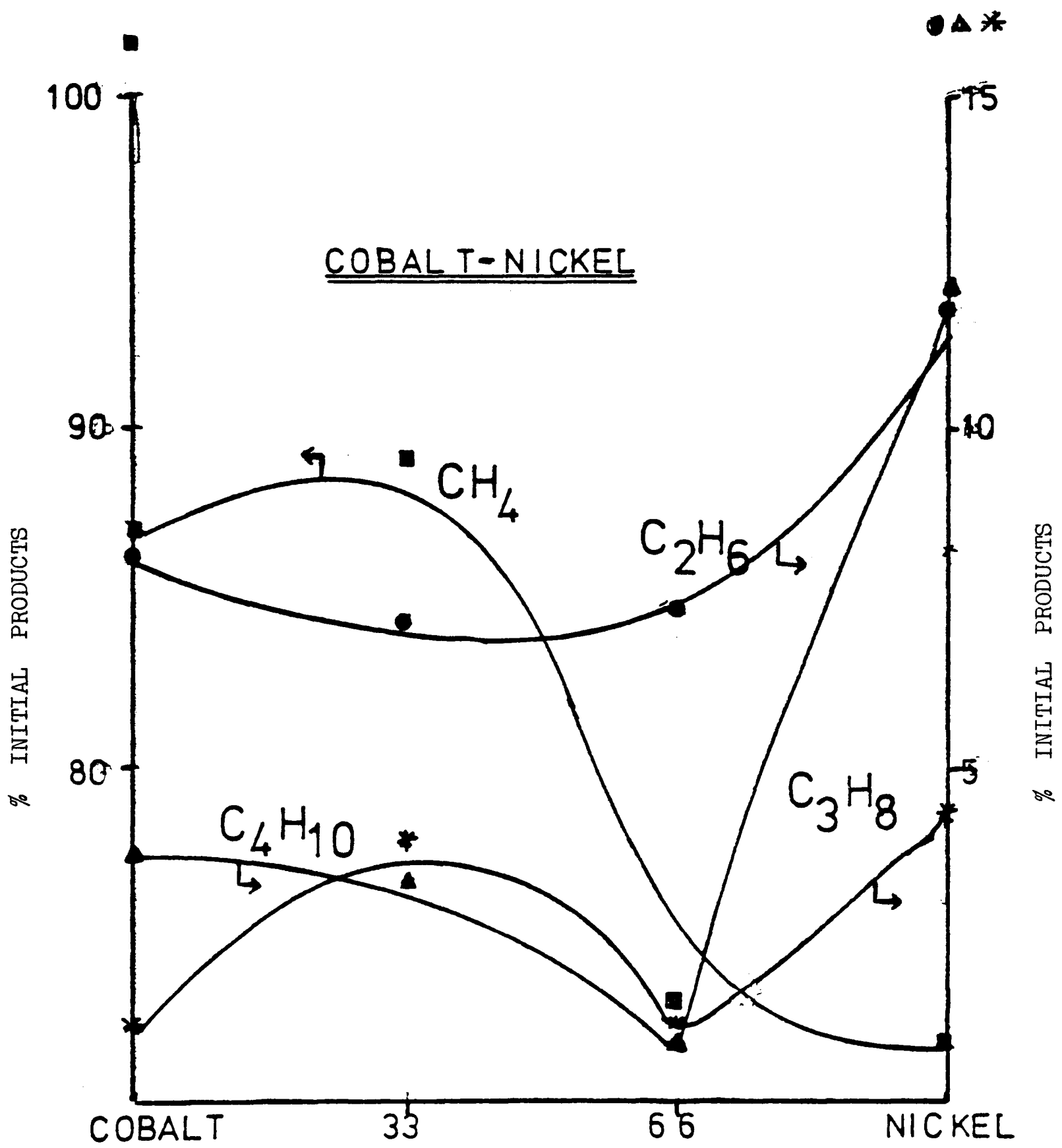

Figure 9:5 Initial product distributions on cobalt-nickel alloys.

Iron-nickel alloys

As was observed for cobalt-nickel alloys selectivity towards higher hydrocarbon production shows a modest increase with increasing nickel concentrations (Figure 9:6). Again this increase is most probably associated with the relative hydrogenation activities of iron and nickel. It has been shown that iron retains a high concentration of carbon and any higher hydrocarbons which are formed will probably remain on the surface. The lower affinity of nickel for retaining carbon and its larger hydrogenation activity ensures that the surface never fully covers with carbon residues and that reaction proceeds to completion.

9:5:2 Methanation activity

Single metals

The intrinsic activities (i.e. carbon monoxide converted to methane per unit time per unit area) of iron, cobalt and nickel for methanation increase in the order iron<<nickel<cobalt. This order is similar to that of the activities per unit mass of catalyst reported by Fischer[126] in 1925 but is different to the specific activities reported by Vannice[127] who observed that the methanation activity increased as nickel<cobalt<iron. The differences in relative intrinsic activity between this investigation and that of Vannice are almost certainly associated with the different experimental conditions. Vannice conducted his experiments at atmospheric pressure in a flow system and the present research involved pressures of 80 torr in a static system. When the spent iron catalyst used by Vannice was analysed for carbon none was found and consequently it was assumed that the measured methanation rate referred to a carbon free surface. In the present research the iron

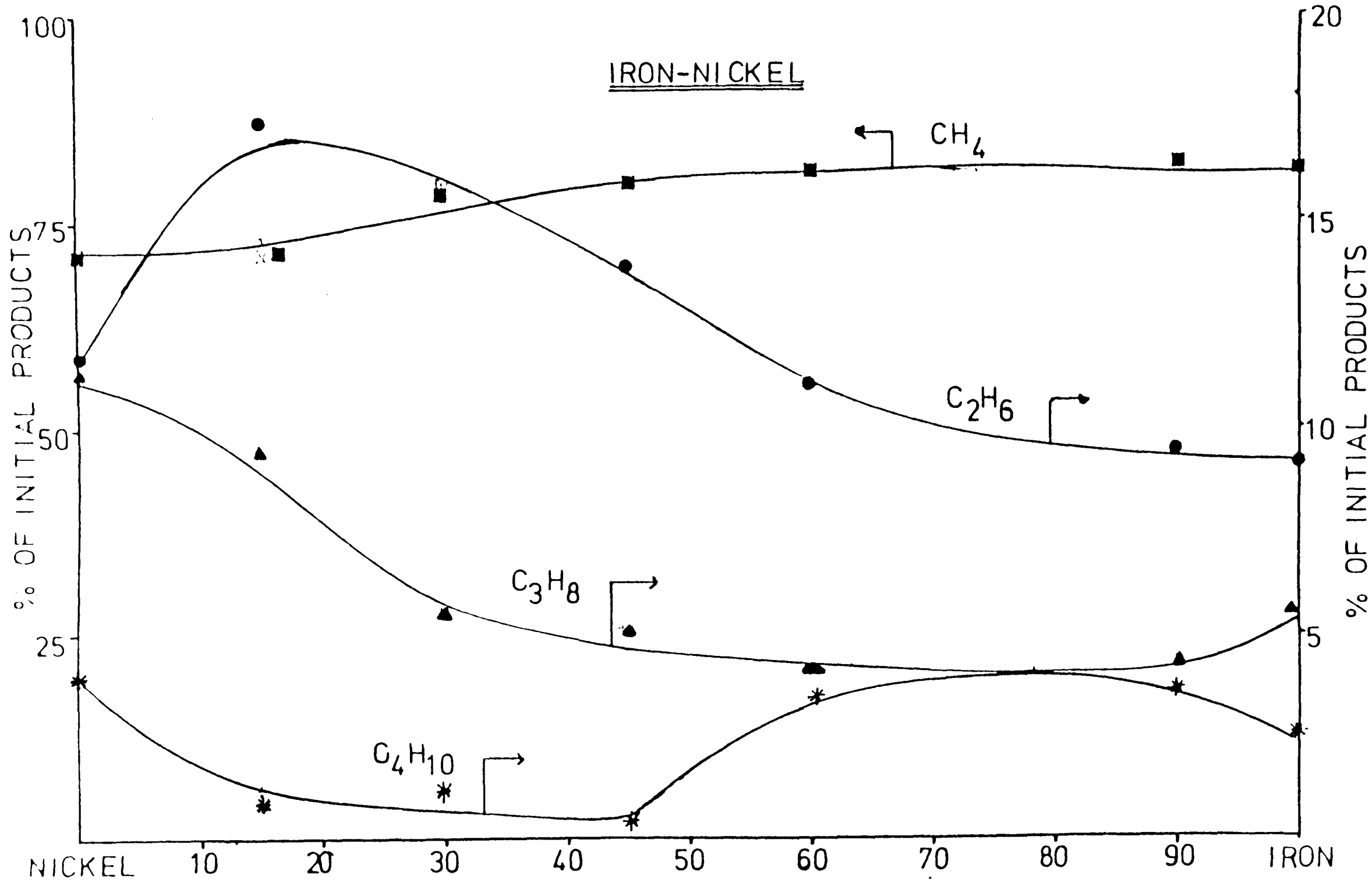

Figure 9:6 Initial product distributions for iron-nickel alloys.

catalyst very rapidly covers with a carbonaceous layer and it is possible that initial methanation rates refer to a partially carbon covered surface. If this is indeed so, the observed reaction rate will be slower than the intrinsic rate of a clean iron surface.

In view of this difficulty great care is needed when considering initial rates of methanation on iron and iron rich alloys. In an attempt to minimise the influence of carbon laydown initial reaction rates on such catalysts were determined after only 5-10 minutes reaction.

Alloy catalysts

If it is assumed that carbon laydown is not affecting the observed methanation rate on iron and iron rich alloys, to a significant extent, the methanation activity against composition curves for the alloy series can be explained by postulating that the optimum electron/atom ratio required for methanation catalysis is midway between that of cobalt and nickel.

The intrinsic methanation rate of cobalt-nickel alloys is larger than that of the single metals (Figure 9:7). This observation is similar to a recent patent which indicates that small additions of cobalt to nickel bring about an increase in methanation activity[128]. The observed maximum in activity occurs for an alloy of approximately 67% cobalt and may result from an "optimisation" of the average electron/atom ratio required for methanation catalysis (it is assumed that carbon laydown is not influencing methanation rate).

There is also a maximum in intrinsic methanation rate with iron-nickel alloys (Figure 9:8).However, this maximum no longer occurs at approximately 33% nickel but with an alloy containing about 70% nickel. This is an interesting observation as iron has one less

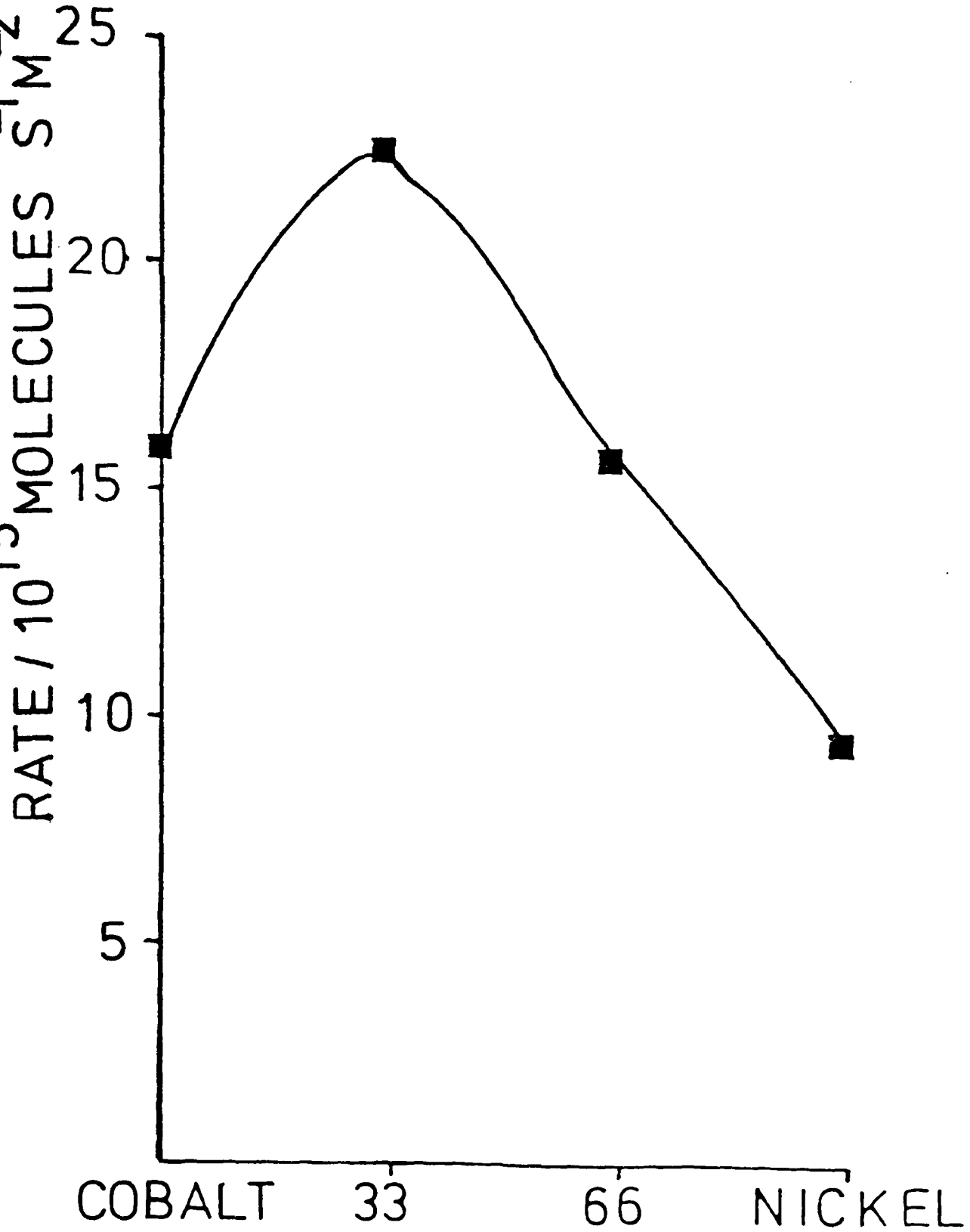

Figure 9:7 Variation of intrinsic methanation rate with alloy composition for cobalt-nickel alloy.

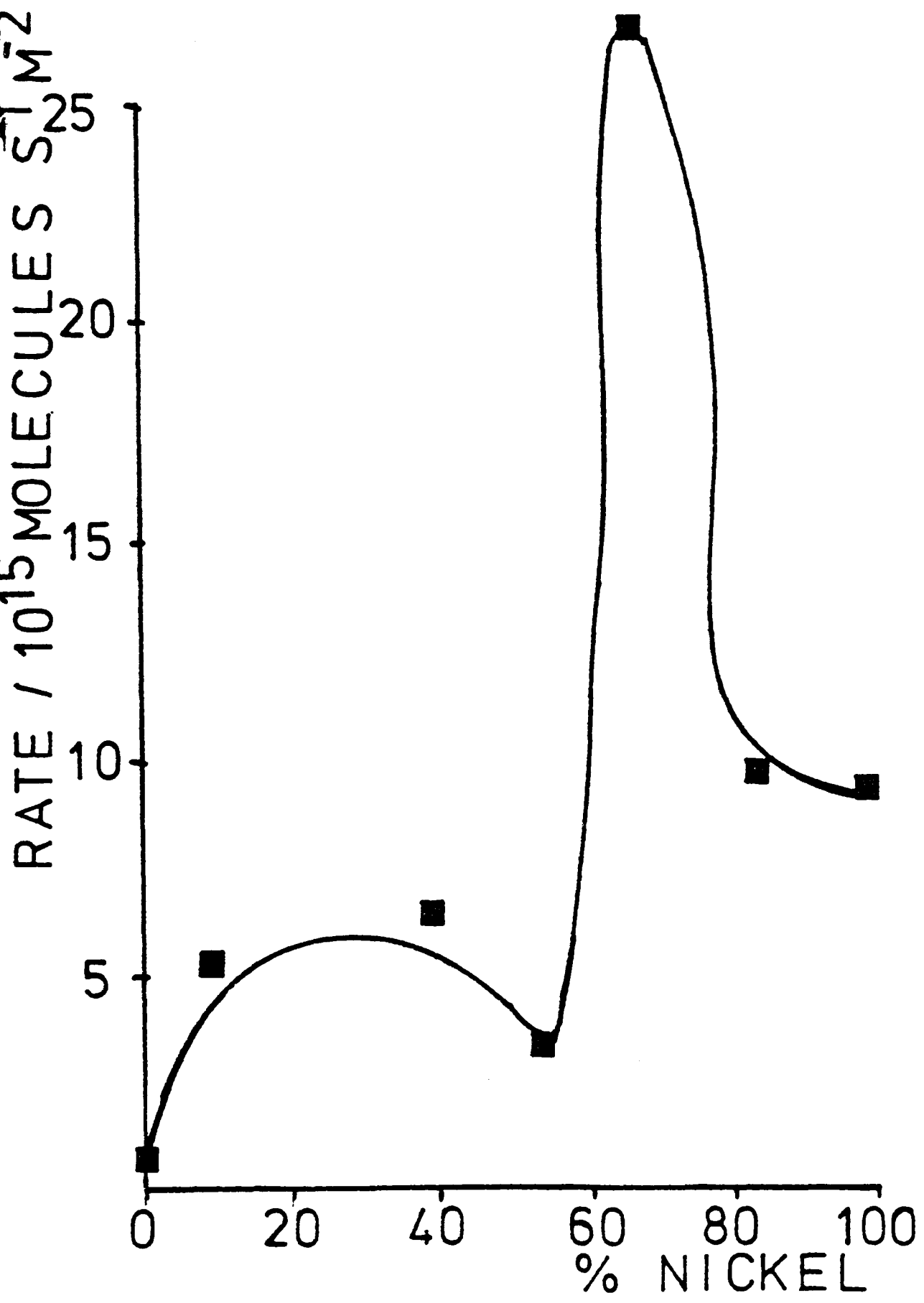

Figure 9:8 Variation of intrinsic methanation rate at 473 K with alloy composition for iron-nickel alloys.

d electron than cobalt and by a simple electronic approximation would be expected to have twice the influence of cobalt. That such an effect is observed serves to strengthen the suggestion that addition of cobalt or iron to nickel varys the electronic structure in such a manner as to yield a more active methanation catalyst.

Examination of reduced catalysts by X-ray diffraction showed that ordering or the generation of a new phase e.g. $FeNi_3$ had not occurred in the catalyst of optimum methanation activity.

Whereas both iron-nickel and cobalt-nickel alloys display a maximum in intrinsic methanation rate with alloy composition iron-cobalt alloys do not (Figure 9:9). The absence of this maximum is in accord with the axiom that increased methanation activity results from the optimisation of nickel's electronic structure and that it is not purely due to the measured methanation rates being influenced by carbon deposition.

The intrinsic methanation rate of iron-cobalt alloys decreases sharply with increasing iron concentrations. The decrease in activity cannot be explained by a simple dilution of active cobalt by inactive iron as a linear variation, between the values of the single metals, would result from this situation (i.e. it is assumed that each metal atom acts as an independent active site and no segregation occurs). Assuming that methanation activity is restricted to the cobalt component of the alloy (a reasonable assumption since iron is about eighteen times less active towards methanation) the decrease in activity would be much more rapid, with increasing iron contents, if the active site involved two or more cobalt atoms. The actual shape of a plot of activity against alloy composition will vary with the size of the ensemble required and can be calculated statistically for a random alloy[12]. It is readily seen that the more cobalt atoms present in the active methanation

site the more rapidly will the methanation activity decrease as the iron content of the alloy is increased. The activity pattern found in this study (Figure 9:9) therefore corresponds to the active site being an ensemble of at least two cobalt atoms and perhaps as many as four or five atoms as has been suggested for methanation on ruthenium[13] and nickel[111] when combined with copper in a bi-metallic catalyst.

9:5:3 Comparison of methanation and ammonia synthesis

McNicol and Jones[129] have commented on the many similarities between methanation and ammonia synthesis. Both reactions involve the hydrogenation of isoelectronic molecules and both occur on group VIII metal catalysts. There is also some similarity in the behaviour towards alkali promoter and in the nature of the rate limiting steps. The influence of alkali on the rates of ammonia synthesis and methanation reactions has been associated with electron transfer from the more electronegative alkali metal into the transition metal and thence into the antibonding orbitals of either nitrogen or carbon monoxide which facilitates dissociative chemisorption. In view of these similarities it is of interest to compare the results of this present research with results concerning ammonia synthesis on the same group VIII base metal alloys (chapter 6).

The intrinsic activity for ammonia synthesis catalysis (using a 3/1 H_2/N_2 mixture at 673 K in a circulating system) decreases in the order iron>cobalt>>nickel whereas the intrinsic methanation activity (using a 3/1 H_2/CO mixture at 493 K in a static system) shows the order cobalt>nickel>>iron. However, as previously discussed, interpretation of observed methanation rates on iron is complicated by the influence of substantial carbon deposition. When intrinsic methanation rates are measured under conditions where carbon deposition

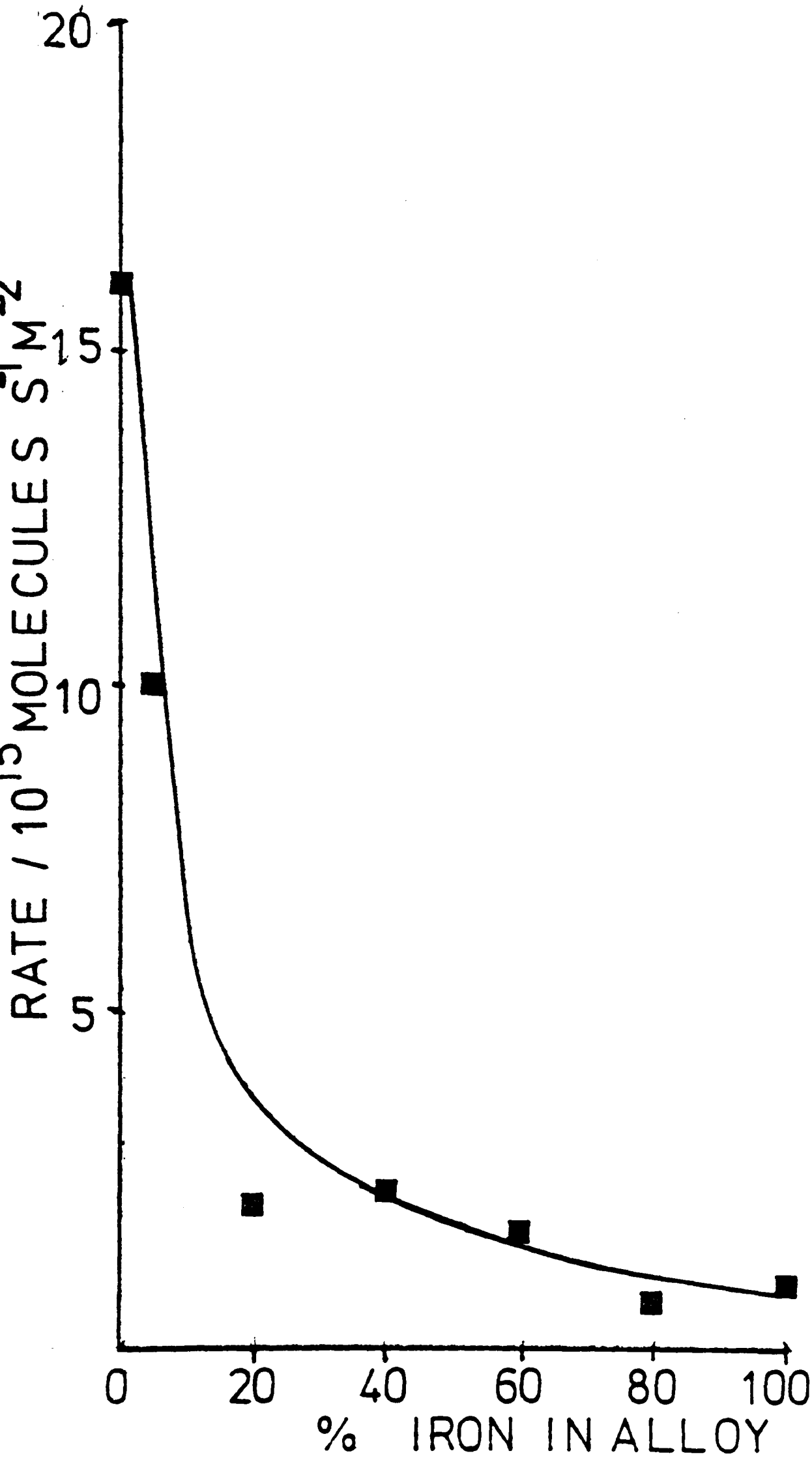

Figure 9:9 Variation of intrinsic methanation rate at 473 K with alloy composition for iron-cobalt alloys.

does not occur[127] the observed intrinsic methanation rate decreases in the order iron>cobalt>nickel i.e. similar to that found for ammonia synthesis catalysis.

The intrinsic rates of ammonia synthesis and methanation (determined in this research) over iron-cobalt and iron-nickel alloys are compared in Figures 9:10 and 9:11 respectively. Examination of Figures 9:10 and 9:11 shows clearly that the respective active patterns have very little resemblance. Iron-cobalt alloys display a maximum for ammonia synthesis whereas there is no corresponding maximum for methanation and the maxima observed in the iron-nickel alloy series occur at different compositions for ammonia synthesis and methanation.

The intrinsic activity of the iron sample for ammonia synthesis catalysis is increased by an order of magnitude by reducing the sample at temperatures above 1073 K (chapter seven). The intrinsic methanation rate of iron is unaffected by reduction temperatures in excess of 1073 K and consequently although there are some similarities in the nature of the rate determining step, the active site for ammonia synthesis is unlikely to be that required in carbon monoxide hydrogenation.

Carbon monoxide hydrogenation is severely influenced by problems of carbon deposition e.g. iron and iron rich alloys may form carbide species and this will reduce the observed methanation rate. Ammonia synthesis has no corresponding problems asscciated with nitride formation and because of this difference it is not possible to directly compare the ammonia synthesis and methanation experiments.
It is possible that if methanation activities were determined under conditions where carbon deposition did not occur that a similar

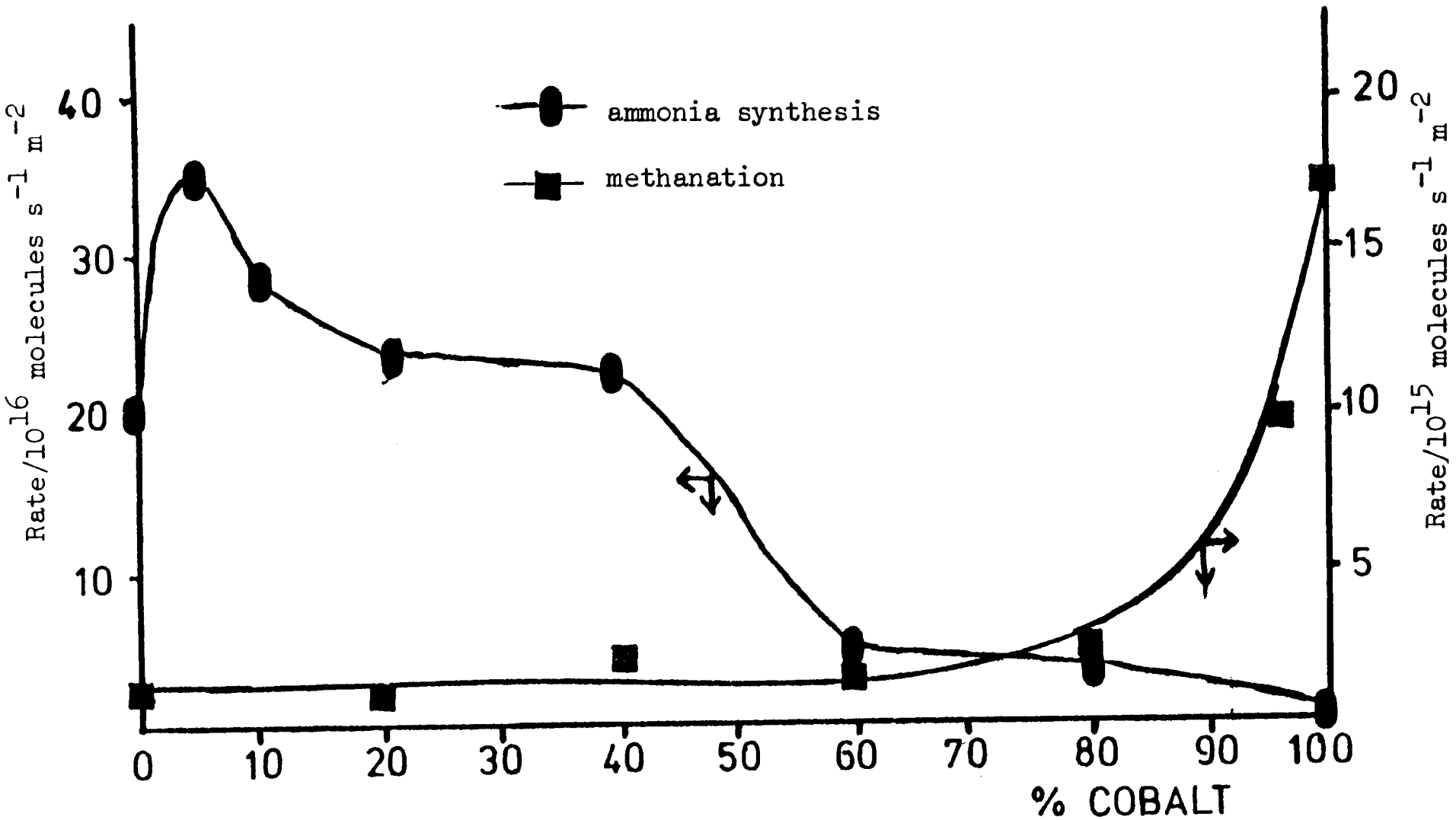

Figure 9:10 Variation of ammonia synthesis rate at 673 K and methanation rate at 473 K with alloy composition on iron-cobalt alloys.

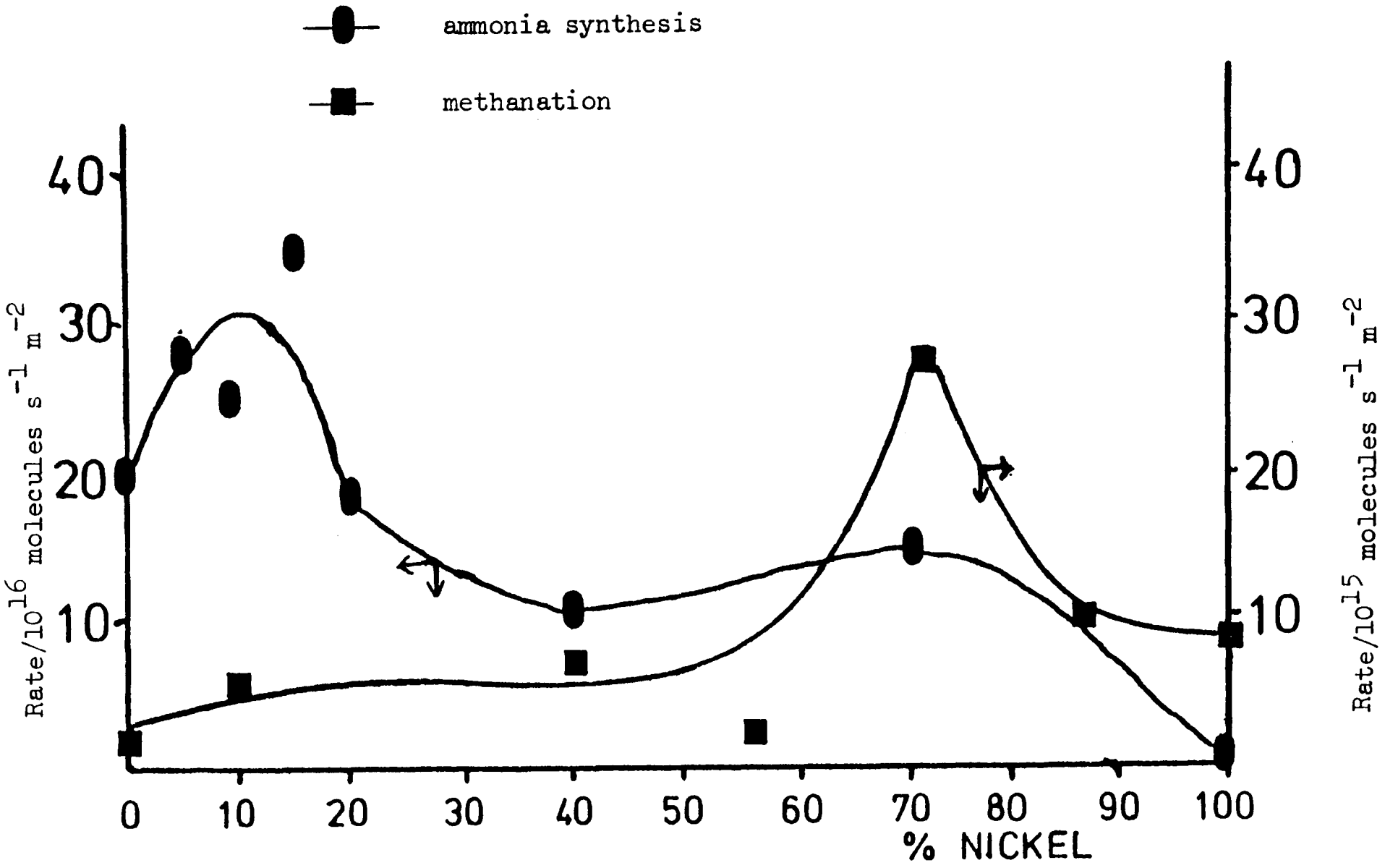

Figure 9:11 Variation of ammonia synthesis activity at 673 K and methanation activity at 473 K with alloy composition for iron-nickel alloys.

activity pattern to that observed with ammonia synthesis might result. However, the present results indicate that this is unlikely and that any resemblance is superficial.

The results concerning ammonia synthesis have been interpreted in terms of surface structural changes optimising the concentration of the active site necessary for the dissociative chemisorption of nitrogen and so facilitating subsequent catalysis. Whereas the results concerning methanation are clouded by the problems of carbon deposition and may be interpreted as involving an optimisation of electronic structure. The results associated with high temperature reduction are in accord with these explanations.

References

1. G.C. Bond, Catalysis by Metals, Academic, London 1962.
2. D.A. Dowden, Ind. Eng. Chem., 44, 977 (1952).
3. W.M.H. Sachtler, J. Vac. Sci. Technol., 9, 828 (1972).
4. E. Bauer, Vacuum, 22, 539 (1972).
5. R.L. Pork, Surface Physics of Crystalline Solids. (J.M. Blakely, ed.), Academic, London 1974.
6. G.V. Raynor, Electron Theory of Metals, Institute of Metals, London 1953.
7. L. Pauling, Nature of the Chemical Bond, Cornell University Press, Ithaca, New York 1948.
8. G.M. Stocks, R.W. Williams and J.S. Faulkner, Phys. Rev., B4, 4390 (1971).
9. B. Velicky, S. Kirkpatrick and H. Ehrenreich, Phys. Rev., 175, 747 (1968).
10. N.I. Kobozev, Acta. Physico. Chem. U.S.S.R., 9, 805 (1938).
11. V. Ponec, Catal. Rev. - Sci. Eng., 11(1), 1 (1975).
12. D.A. Dowden, Proc. Inter. Congr. Catal. 5th, 1972, North Holland 1973.
13. G.C. Bond and B.D. Turnham, J. Catal., 45, 128 (1976).
14. J.M. Beelen, V. Ponec and W.M.H. Sachtler, J. Catal., 28, 376 (1973).
15. M. Hansen, Constitution of Binary Alloys, McGraw-Hill, London 1958.
16. W. Hume-Rothey, Atomic Theory for Students of Metallurgy, Institute of Metals, London 1947.
17. R.W. Floyd, Institute of Metals Annotated Equilibrium Diagrams Series, no. 11, The Institute of Metals, London 1955.

18. R.A. Beeke and N.P. Stevens, J. Amer. Chem. Soc., 62, 2134 (1940).

19. R.J. Kokes and P.H. Emmett, J. Amer. Chem. Soc., 82, 1037 (1960).

20. A. Van Itterbeek and J. Borghs, Z. Physik. Chem., B50, 128 (1942).

21. N.N. Kavtaradze and E.A. Zelyaeva, Izv. Akad. Nauk. S.S.S.R., Ser. Khim., 11, 2618 (1970) (Russ.).

22. R.J. Kokes and P.H. Emmett, J. Amer. Chem. Soc., 80, 2082 (1958).

23. G. Wedler and D. Borgmann, Forschungsber Wehrtech (Bundesminist. Verteidigung) 1976.

24. G. Wedler, D. Borgmann and K.P. Geuss, Surf. Sci., 47, 592 (1975).

25. N.N. Kavtaradze and E.A. Zelyaeva, Izv. Akad. Nauk. S.S.S.R., Ser. Khim., 11, 2618 (1970).

26. S. Brunauer and P.H. Emmett, J. Amer. Chem. Soc., 62, 1732 (1940).

27. C. Bokhoven, C. Van Heerden, R. Westrik and P. Zwiettering, Catalysis, vol. 3 (Ed. Emmett, Reinhold, New York 1955).

28. R. Brill, E.L. Richter and E. Ruch, Angew. Chem. Int. Ed., 6(10), 882 (1967).

29. P.H. Emmett and S. Brunauer, J. Amer. Chem. Soc., 55, 1738 (1933). P.H. Emmett and S. Brunauer, J. Amer. Chem. Soc., 56, 35 (1934).

30. S. Brunauer, K.S. Love and R.G. Keenan, J. Amer. Chem. Soc., 64, 751 (1942).

31. T. Kwan and K. Yamamori, Kagaku, 23, 533 (1953).

32. M.V.C. Sastri and H. Srikant, Current Sci. (India), 19, 343 (1950).

33. J.J.F. Scholten and P. Zwiettering, Trans. Far. Soc., 53, 1363 (1957).

34. N. Kadota and T. Kanagawa, Shokubai (Tokyo), 7(5), 454 (1965) (Japan).

35. Yu. N. Artyukh and V.A. Il'yushonok, Kinet. Katal., 17(4), 1078 (1976) (Russ.).

36. I.R.V. Chesnokova, A.I. Gorbunov, S.S. Lachinov, G.K. Muravskaya and G.A. Erdedi, Kinet. Katal., 6(2), 338 (1965) (Russ.).

37. M.V.C. Sastri and H. Srikant, Current Sci. (India), 20, 15 (1951).

38. K. Tamaru, Trans. Far. Soc., 59, 979 (1963).

39. M.G. Martsenyuk, M.T. Rusov and N.P. Samchenko, Kinet. Katal., 4, 129 (1968) (Russ.).

40. I.R.V. Chesnokova, A.I. Gorbunov, S.S. Lachnivov and G.K. Muravskaya, Kinet. Katal., 11(6), 1486 (1970) (Russ.).

41. H. Koelbel, S. Sridhar and H. Hammer, Z. Phys. Chem. (Frankfurt am Main), 75(5), 225 (1971) (Ger.).

42. M.I. Temkin, V.E. Ostrovskii and E.G. Igranova, Kinet. Katal., 17(5), 1257 (1976) (Russ.).

43. J.J.F. Scholten, J.A. Konvalinka and P. Zwiettering, Trans. Far. Soc., 56, 262 (1960).

44. K. Tamaru, Proc. Inter. Congr. Catal. 3rd, Amsterdam 1964.

45. G. Ertl, M. Grunze and M. Weiss, J. Vac. Sci. Technol., 13(1), 314 (1976).

46. I.D. Gay, M. Textor, R. Mason and Y. Iwasawa, Proc. R. Soc. London, Ser. A (1977), 356 (1684), 25.

47. M. Boudart, J. Vac. Sci. Technol., 12(1), 329 (1975).

48. C. Bokhoven, C. Van Heerden, R. Westrik and P. Zwiettering, Catalysis, vol. 3, (ed. Emmett, Reinhold, New York 1955).

49. J.A. Dumisec and M. Boudart, Catal. Chem. Nitrogen Oxides, Proc. Symp. 1974, Plenum, New York.

50. F. Bozo, M. Grunze, G. Ertl and M. Weiss, J. Catal., 49, 18 (1977).

51. F. Bozo, G. Ertl and M. Weiss, J. Catal., 50, 519 (1977).

52. G. Wedler and D. Borgmann, J. Catal., 44, 139 (1976).

53. H.H. Madden and H.E. Farnsworth, J. Chem. Phys., 34, 1186 (1961).

54. R.P. Eischens and J. Jacknow, Proc. Inter. Congr. Catal. 3rd, Amsterdam 1964.

55. L.M. Roev, S.V. Batgchko and M.T. Rusov, Kinet. Katal., 12(4), 1072 (1971) (Russ.).

56. N. Takezawa, Nippon Kagaku Zasshi, 91(1), 43 (1970) (Jap.).

57. I. Toyoshima, N. Nobutsune and H. Suzuki, J. Chem. Soc. Chem. Commun., 8, 270 (1973).

58. H. Suzuki and I. Toyoshima, Proc. Inter. Congr. Catal. 6th, 1976; Letchworth, Eng.

59. A.I. Krasil'shchikov, L.G. Antonova, Z.M. Biryukova, I.M. Karataeva and T.T. Fil'chenkova, Russ. J. Phys. Chem., 37, 102 (1963).

60. A. Treatise on Dinitrogen Fixation, ed. by R.F. Hardy, F. Bottomley and R.C. Burns, Wiley-Interscience, New York 1979.

61. A. Ozaki, K. Aika and K. Urabe, Catal. Chem. Nitrogen Oxides, Proc. Symp. 1974, Plenum, New York.

62. O. Motomu, A. Ken-ichi, K. Urabe and A. Ozaki, J. Catal., 44, 460 (1976).

63. O. Motomu, K. Urabe and A. Ozaki, J. Catal., 52, 432 (1978).

64. K. Urabe, K. Shiratori and A. Ozaki, J. Catal., 55, 71 (1978).

65. G.G. Jones and H.S. Taylor, J. Chem. Phys., 7, 893 (1939).

66. N.I. Kobozev, Acta. Physico. Chem., U.S.S.R., 9, 805 (1938).

67. J.T. Kummer and P.H. Emmett, J. Chem. Phys., 19, 289 (1951).

68. N. Takezawa and I. Toyoshima, J. Catal., 19, 271 (1970).

69. A. Krylova and S.Z. Roginskii, Bull. Acad. Sci. U.S.S.R. Div. Chem. Sci., 1271 (1957).

70. A.I. Gorbunov, O.L. Masonov and G.K. Boreskov, Proc. Acad. Sci. U.S.S.R. Chem. Sect., 123, 787 (1958).

71. Y. Morikawa and A. Ozaki, J. Catal., 23, 97 (1971).

72. E.E. Rachkovskii, A.V. Khasin, G.K. Boreskov, V.M. Kolchanova and S.N. Filimonova, Dokl. Akad. Nauk. S.S.S.R., 206(6), 1398 (1972) (Russ.).

73. A.I. Gorbunov and G.K. Boreskov, Kinet. Katal., 10, 192 (1960).

74. A. Treatise on Dinitrogen Fixation, ed. by R.W.F. Hardy, F. Bottomley and R.C. Burns, Wiley-Interscience, New York 1979.

75. G.K. Boreskov, V.M. Kolchanova, E.E. Rachkovskii, S.N. Filimonova and A.V. Khasin, Kinet. Katal., 16, 1218 (1975) (Russ.).

76. G. Wedler and D. Borgmann, J. Catal., 44, 139 (1976).

77. F. Bozo, G. Ertl, M. Grunze and M. Weiss, J. Catal., 49, 18 (1977).

78. A. Ozaki, Proc. Inter. Congr. Catal. 5th, 1972, North Holland 1973.

79. K. Urabe, K. Aika and A. Ozaki, J. Catal., 32, 108 (1974).

80. K. Urabe, K. Aika and A. Ozaki, J. Catal., 38, 430 (1975).

81. K. Urabe, A. Oh-ya and A. Ozaki, J. Catal., 54, 436 (1978).

82. K. Tanaka and K. Tamaru, J. Catal., 2, 366 (1963).

83. K. Urabe and A. Ozaki, J. Catal., 52, 542 (1978).

84. W. Guyer, G.G. Jones and H.S. Taylor, J. Chem. Phys., 9, 287 (1941).

85. J.P. McGeer and H.S. Taylor, J. Amer. Chem. Soc., 73, 2743 (1951).

86. T.E. Madey and J.T. Yates, J. Chem. Phys., 44, 1675 (1966).

87. R.P.H. Gasser, C.P. Lawrence and D.G. Newman, Trans. Far. Soc., 61, 1771 (1965).

88. R.P.H. Gasser, A. Hale and C.J. Marsay, Trans. Far. Soc., 63, 1789 (1967).

89. D.D. Eley and S.H. Russel, Proc. R. Soc. London Ser. A. (1974), 341 (1024), 31.

90. A.N. Webb and R.P. Eischens, J. Amer. Chem. Soc., 77, 4710 (1955).

91. R.P. Eischens and W.A. Pliskin, Advances in Catalysis, vol. 10, Academic Press, New York 1958.

92. G. Blyholder and L.D. Neff, J. Phys. Chem., 66, 1464 (1962).

93. F.S. Baker, A. Bradshaw and K.W. Sykes, Surf. Sci., 12, 426 (1968).

94. H.M. Madden, J. Kneppers and G. Ertl, J. Chem. Phys., 58, 3461 (1973).

95. A.M. Bradshaw and J. Pritchard, Proc. R. Soc. London Ser. A. (1970), 316, 69.

96. K. Kiski and M.W. Roberts, Trans. Far. Soc., 70, 1819 (1974).

97. S.J. Gregg and H.F. Leach, J. Catal., 6, 308 (1965).

98. R.W. Joyner and M.W. Roberts, J. Chem. Soc. Far. I, 70, 1819 (1974).

99. S.J. Atkinson, C.R. Brundle and M.W. Roberts, Discuss. Far. Soc., 58, 62 (1974).

100. V. Ponec and R. Merta, Proc. Inter. Congr. Catal. 4th, 1968, Akademiai Kiado Budapest, 1971.

101. O. Boudouard, J. Chem. Soc., 383 (1901).

102. F. Fisher and H. Tropsch, Brennstoff-Chem., 7, 97 (1926).

103. S.R. Craxford and E.K. Rideal, J. Chem. Soc., 1604 (1939).

104. O.C. Elvins and A.W. Nash, Nature, 154, 118 (1926).

105. H. Tropsch, A. Schellenberg and A. Von Philippovich, Ges. Abhondle. Kenntnis, Kahle., 63, 1 (1925).

106. V.M. Vilasenko and G.E. Yuzefovich, Russ. Chem. Rev., 38(9), 1969.

107. H.H. Storch, H. Golumbic and R.B. Anderson, Fischer-Tropsch and Related Synthesis, John Wiley, Chichester 1951.

108. J.H. Le Roux, J. Appl. Chem. Biotechnol., 22, 719 (1972).

109. G. Henrici-Olivé and S. Olivé, Angew. Chem. Int. Ed., 15, 136 (1976).

110. M. Araki and V. Ponec, J. Catal., 44, 439 (1976).

111. V. Ponec, Catal. Rev. - Sci. Eng., 18(1), 151 (1978).

112. M.A. Vannice and R.L. Garten, J. Mol. Catalysis, 1, 201 (1975).

113. C.H. Bartholomew, F.E.-1790-1, Q. Tech. Prof. Rep. to E.R.D.A., April 22 - July 22, 1975.

114. V. Ponec, J.C.M. Harberts, A.F. Bourgonje and J.J. Stephan, J. Catal., 47, 92 (1977).

115. V. Ponec, W.L. Van Dijk and J.A. Groenewegen, J. Catal., 45, 277 (1976).

116. R.J. Kokes and P.H. Emmett, J. Amer. Chem. Soc., 82, 1037 (1960).

117. A. Ozaki, Isotope Studies of Heterogeneous Catalysis, Academic Press, New York 1977.

118. M.R. Hillis, C. Kemball and M.W. Roberts, Trans. Far. Soc., 62, 3570 (1966).

119. A. Navrotsky and O.J. Kleppa, J. Inorg. Nucl. Chem., 30, 479 (1968).

120. R. Hosemann, A. Preisinger and W. Vogel, Ber. Bunsenges. Phys. Chem., 70, 797 (1960).

121. H. Ludwiczek, A. Preisinger, A. Fisher, R. Hosemann, A. Schonfield and W. Vogel, J. Catal., 51, 326 (1978).

122. P.H. Emmett, The Physical Basis of Heterogeneous Catalysis, Plenum Press, New York 1975.

123. G.J. den Otter and F.M. Dautzenberg, J. Catal., 53, 116 (1978).

124. I. Toyoshima and G.A. Somorjai, Catal. Rev. - Sci. Eng., 19(1), 105 (1979).

125. F.A. Cotton and G. Wilkinson, Advanced Inorganic Chemistry, John Wiley, New York 1977.

126. F. Fischer, H. Tropsch and P. Dilthey, Brennst.-Chem., 6, 265 (1925).

127. M.A. Vannice, J. Catal., 37, 449 (1975).

128. U.S. Patent 3,945,944.

129. A. Jones and B. McNicol, J. Catal., 47, 384 (1977).